Modulation of retinal ganglion cell responses by the endocannabinoid system and the involvement of TRPV1 channels

by Xiaohui Lin

Bachelor of Medical Science (Master of Philosophy)

Supervisor: Dr Dario Protti

University of Sydney

School of Medical Sciences

Discipline of Physiology

27th February 2018

THE UNIVERSITY OF SYDNEY

STUDENT PLAGIARISM: COURSE WORK - POLICY AND PROCEDURE COMPLIANCE STATEMENT

INDIVIDUAL

I certify that:

(1) I have read and understood the *University of Sydney Student Plagiarism: Coursework Policy and Procedure*;

(2) I understand that failure to comply with the *Student Plagiarism: Coursework Policy and Procedure* can lead to the University commencing proceedings against me/us for potential student misconduct under Chapter 8 of the *University of Sydney By-Law 1999* (as amended);

(3) this work is substantially my own, and to the extent that any part of this Work is not my own I have indicated that it is not my own by Acknowledging the Source of that part or those parts of the Work.

(4) the word count declared is true and accurate in accordance with conditions stipulated in the course guide.

(5) all printed and submitted versions of the thesis provided to the Discipline of Physiology are identical to the electronic version submitted in accordance with conditions stipulated in the course guide.

Word Count: 21,381

Name: Xiaohui Lin

Signature:

Date: 29th January 2018

Acknowledgements

Firstly, I'd like to express my sincere gratitude towards my supervisor, Dr Dario Protti. Dr. Protti dedicated his time and provided continuously guidance throughout my two year's Master's degree. His knowledge in the visual system, physiology, experimental skills and computer science helped me greatly for this research topic. His patience, encouragements, mentoring and trust in me was crucial in producing my thesis and will be continuously to benefit me in the years to come.

Secondly, I'd like to acknowledge my co-supervisor Dr Jin Huang, who trained us with her expertise in dissection under microscope, patch clamping and staining of the retinal tissues. I am truly grateful for the support and guidance I've received for the past two years, as she is a truly great teacher and provided valuable feedbacks in written work for submission.

Thirdly, I'd like to thank Dr Louise Cole who provided valuable training and support on confocal imaging at the Advanced Microscope Facility. I'd also like to express my gratitude towards the University of Sydney, Discipline of Physiology, the Bosch Institute for providing me this amazing research opportunity.

Lastly, I'd like to acknowledge the other students from the Vision Laboratory, Kevin Leung and Andrea Yong. I have received endless support and had great discussions throughout the countless hours spent in the lab. Through the insightful discussions, I was able to expand my knowledge on and beyond the current research topic, which I'm forever grateful of.

All work apart from that acknowledged was completed by myself, inclusive of all experimentations, statistical and data analysis, and the written documents.

Abstract

The endocannabinoid (eCB) system was found to modulate synaptic transmission in the central nervous system (CNS). The retina carries out complex neural computations that involve several physiological mechanisms, including short and long-term plasticity phenomena. The mechanisms responsible for modifying the strength of retinal synaptic transmission, however, are not fully understood. Previous studies in the Vision Lab showed that bath application of a drug that elevates the concentration of endocannabinoids reduced the peak amplitude of visual-evoked postsynaptic potentials (vePSP) in retinal ganglion cells (RGCs) but paradoxically increased their spiking output. In addition, the rise in endocannabinoid concentration shifted the voltage dependence of the sodium current to the left. The reduction in vePSP amplitude is consistent with the known presynaptic effects of eCBs on synaptic transmission whilst it was postulated that the increase in spiking output could be mediated by TRPV1 receptors, which are nonselective ligand gated cation channel sensitive to eCBs and a broad range of other stimuli. This study investigated the potential role of TRPV1 channels in the modulation of RGCs excitability by recording their electrical activity in wild-type and TRPV1 knock-out mice using whole cell patch clamping techniques. We found that the endocannabinoid anandamide acts on TRPV1 channels to increase cell excitability. Increasing the levels of anandamide in the absence of TRPV1 channels, however, led to the activation of RGCs at more hyperpolarised potentials, suggesting that other targets of anandamide are involved in RGC modulation. Moreover, the TRPV1 agonist and antagonist capsaicin and capsazepine are likely to have non-specific effects as application of capsazepine was able to reduce cell excitability in the TRPV knockout mice (TRPV1-/-).

Table of Contents

Figures and Tables

List of Figures

List of Tables

Abbreviations

eCB	Endocannabinoid system
CNS	Central Nervous System
vePSP	visual-evoked postsynaptic potentials
LGN	Lateral Geniculate Nucleus
TRPV1-/-	Transient Receptor 1 Potential Vanilloid Knock Out
RGC(s)	Retinal ganglion cells
THC	of Δ^9-tetrahydrocannabinol
AEA	Anandamide
2-AG	2-arachydonoyl glycerol
DSI	Depolarisation-induced Suppression of Inhibition
DSE	Depolarisation-induced Suppression of Excitation
CB1R	Cannabinoid Receptor type 1
CB2R	Cannabinoid Receptor type 2
NAPE	N-arachidonoyl Phosphatidylethanolamine
DAG	Diacylglycerol
FAAH	Fatty acid amide hydrolase
MGL	Monoacylglycerol Lipase
COX-2	Cyclooxygenase-2
TRP	Transient Receptor Potential
NKCC	Na^+-K^+-$2Cl^-$-co-transporter
NT	Neurotransmitter
iR	Ionotropic receptor
mR	Metabotropic receptor
Ca^{2+}	Calcium ions
Na^+	Sodium ions
K^+	Potassium ions
TRPV	Transient Receptor Potential Vanilloid
IV	Current-to-voltage
PBS	Phosphate buffer saline
CAP	Capsaicin
IO	Input-output
V-half	50% of the maximum Na^+ current
LE-PSP	light evoked post synaptic potential
ΔVm	Difference in membrane potential
CPZ	Capsazepine
TEA	tetraethylammonium
I_h	hyperpolarisation-activated cation channels
Cl^-	Chloride

1. Introduction

1.1 The Retina

1.1.1 Introduction

The retina consists of a complex neuronal network that converts light energy into electrical signals containing specific features of the visual world. The retina developmentally originates from the same embryonic tissue, ectoderm, as the rest of the brain, and it is therefore classified as a part of the central nervous system (CNS). Anatomically, it is the innermost layer of the eyeball, lining its posterior curvature. It can be divided into the inner neural layer and outer pigmented layer. The inner neural layer contains multiple cell layers and types, responsible for signal conversion and processing. The output of this sensory information leaves the retina from the optic disk, carried through the optic nerve formed by the ganglion cell axons. In terms of vision, these visual signals then travel through the optic nerve, and some axons will cross over at the optic chiasm to the opposite side of the brain, continuing as optic tract and reaching the lateral geniculate nucleus (LGN) of the thalamus. The retino-recipient neurons from the LGN then project to the primary visual cortex and the other cortical areas. This is the visual pathway that is involved with conscious visual perception. Other retino-recipient brain nuclei are involved with several other non-conscious visual functions such as pupillary reflex, control of circadian rhythms and other functions.

1.1.2 Retinal cell types and its neural network/organisation

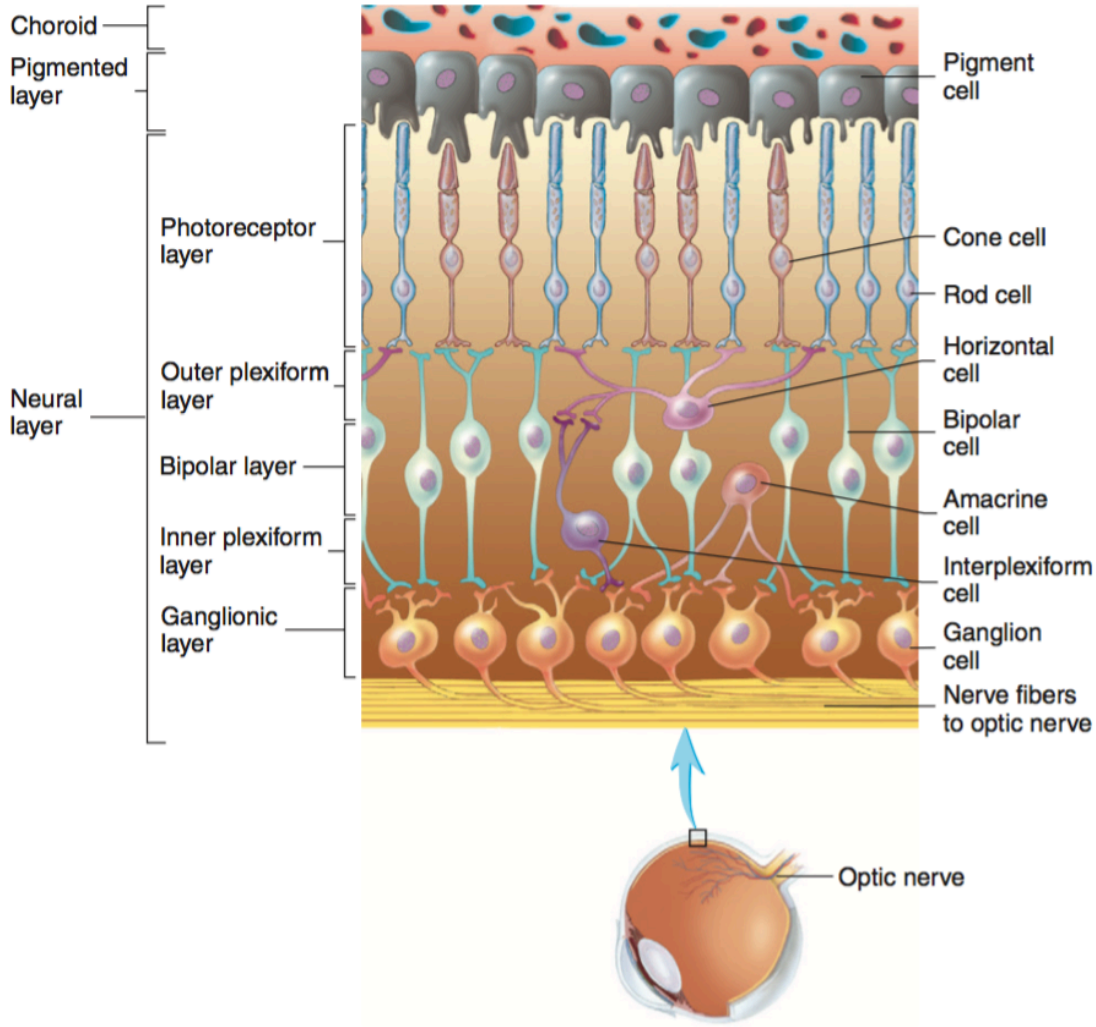

Figure 1.1.Retinal cell organisation and its neural layers. *The choroid, pigmented and neural layer of the retina are illustrated. The neural layer-formed by three neuronal layers, consists of photoreceptors (rods and cones), bipolar cells, and ganglion cells; and two plexiform layers, where neurons synapse with each other (adapted from Silverthorn 2013).*

The retina is a highly organised tissue consisting of three neuronal and two synaptic layers. The five main types of neurons are: photoreceptors (rods and cones), bipolar cells, horizontal cells, amacrine cells, and ganglion cells. The cell bodies (somas) of different cell types are grouped together forming neural layers such that the cell bodies of rods and cones form the outer nuclear layer. On the other hand, the somas of horizontal, amacrine and bipolar cells make up the inner

nuclear layer, and ganglion cells form the ganglion layer. In addition, there are two synaptic layers, also called plexiform layers, where neurons make synaptic contacts with each other. Specific wavelengths of light entering the eye can activate photoreceptors where light energy is then converted into electrical energy; this constitutes the first step of vision. Photoreceptors first transmit visual signals to bipolar and horizontal cells in the outer plexiform layer. Bipolar and amacrine cells then make contacts with each other and with the dendrites of ganglion cells in the inner plexiform layer. Ganglion cells then send action potentials to different visual areas in the brain for further processing.

Photoreceptors are responsible for the process of phototransduction, in which light is converted into an electrical signal. Light first enters the eye via the cornea, passes through the aqueous humor, the lens, vitreous humor, then travels through several relatively transparent neuronal layers of the retina before reaching the outer segments of photoreceptors (Silverthorn, 2013). Rods are responsible for scotopic vision, thus, function best at low light conditions, such as night vision, whereas cones are responsible for photopic vision, such as daytime vision and are responsible for colour and high-acuity vision. Furthermore, in the primate retina, rods and cones have a 20:1 ratio (Mustafi et al., 2009). Rods are mostly located in the peripheral parts of the retina and cones are located at the fovea and the central region of the retina. Thus, rods and cones enable human to see a wide range of light intensities such as very dim at night or very bright on a summer day.

Old world primates, and humans, have three different types of cones. The cones enable them to detect wavelengths from 400nm to 700nm of the visible spectrum. However, cones of other animals tend to have different wavelength sensitivities to primates. For example, cones of rodents are sensitive to light from 360nm to 510nm, with two cone types containing opsins with distinct peak sensitivities, making these animals functionally dichromats (Haverkamp et al., 2005). Thus, rodents used in vision experiments require the right wavelengths to stimulate the corresponding photoreceptors optimally.

Within the retina, there are two main pathways for visual processing: vertical and horizontal. The horizontal pathway involves less change in comparison with the vertical pathway. The two pathways will be further discussed in later paragraphs (*1.1.3*). As signals travel down from photoreceptors to ganglion cells via the two visual processing pathways, convergence happens. Convergence describes when signals from two or more cells synapse onto one cell. In the retina, multiple rod and cone photoreceptors synapse to a single bipolar cell. Similarly, multiple rods also synapse to a single bipolar cell. There are two main classes of bipolar cells: ON and OFF bipolar cells, the former being activated (depolarised) in response to increases in light intensity and the later activated in response to decreases in light intensity. ON bipolar cells are depolarised by decreases in glutamate release from photoreceptors in response to light stimulation, while OFF bipolar cells are hyperpolarised by light (Silverthorn, 2013). Their different responses to changes in glutamate concentration are due to different types of glutamate receptors they express in their dendritic tips. ON bipolar cells express metabotropic glutamate *mGLUR6* receptors in their dendrites, whereas OFF bipolar cells express ionotropic glutamate receptors (Masland, 2012). Retinal ganglion cells (RGCs) receive synaptic inputs from bipolar and amacrine cells. The cell bodies of RGCs constitute the innermost part of the retina. Their axons exit the eye and send action potentials to the other areas of the brain for further processing. In other words, ganglion cells are the final output neurons of the eye. Thus, the study of the physiological properties of RGCs provides a window into how retina process visual information. Rodents, especially mice have been widely used to study the properties of ganglion cells. So far, in the mouse, more than thirty-two different types of RGCs have been identified (Baden et al., 2016). Different criteria have been used to classify RGCs according to their morphological, physiological and, or molecular characteristics. Distinct morphological differences have been described based on the cell soma size, dendritic tree size, density and branching patterns. Historically, homologous cell types in different types of animals have been given different names. Boycott and Wassle (1974) proposed one of the earliest morphological classifications relating to the physiological functions

of RGCs. Four morphological distinctive cell types were discovered in cat retina: alpha, beta, gamma and delta RGCs. They were related to the physiological subclasses: sustained (X), transient (Y) and W cells respectively (Boycott and Wassle, 1974).

Alpha cells have large soma size, with branched, widespread dendritic trees. They have been found in all types of mammals that have been studied so far, comprising 3% of the entire RGC population in cats (Wassle, 2004). In primates, parasol RGCs (M-cells) are suspected to be homologous to the alpha cells (Wassle, 2004). Current research has shown three types of alpha RGCs in mice: ON sustained, OFF sustained, and OFF transient RGCs (Sanes and Masland, 2015) with an additional fourth type, On-transient RGC recently discovered (Krieger et al., 2017). Another well characterized RGC type is the beta cells. They have a smaller dendritic field, and are more densely organized, comprising about half of the total RGC population in cats (Wassle, 2004). They are thought to be highly involved with the visual acuity system due to the aforementioned morphological characteristics. Midget ganglion cells (P-cells) are thought to be the homologous version in primates (Sanes and Masland, 2015, Wassle, 2004).
The physiological classifications will be further discussed in 1.1.4.

1.1.3Vertical and horizontal visual pathways in the retina

As previously mentioned, two different processing pathways have been identified in the retina, the vertical and the horizontal pathways. In the vertical visual pathway, RGCs receive inputs from photoreceptors via bipolar cells. Except for the fovea, neuronal circuits in the retina display a high degree of convergence. The fovea is free of blood vessels, and the neurons post-synaptic to photoreceptors are laterally displaced, so that photoreceptors receive light directly without being scattered or obscured by other structures, and have a one to one relationship with their bipolar cells. At the periphery of the retina, 15-45 photoreceptors converge their signals to a single bipolar cell, which in turn then passes the signal onto RGCs.

On the other hand, in the horizontal signal processing pathway, horizontal and amacrine cells, modify signal transmission along the vertical pathway. Horizontal cells receive synaptic inputs from photoreceptors and synapse back onto photoreceptors and with bipolar cells. They are inhibitory neurons that release GABA and cause lateral inhibition, an adaptation mechanism that enables vision under an extensive wide range of light intensities. Amacrine cells synapse onto bipolar and ganglion cells, as well as onto other amacrine cells (Masland, 2012).

Despite these visual pathways, ganglion cells are the recipient of all signals in the retina, they then transmit action potentials to the rest of the brain for further processing. Understanding the electrophysiological properties of the ganglion cells allows us to understand the early visual processing that occurs in the retina.

1.1.4 Centre-surround organisation of receptive fields in the retina

The receptive field of any sensory neuron refers to the specific region of the sensory space in which a stimulus will produce a response in that neuron. In the case of RGCs, light stimulation within its receptive field activates their downstream neurons, which pass the signal down to the ganglion cell where they elicit a response. In the visual system, Hartline (1938) extended the definition of the receptive field to the change of light in a particular area of the visual space that can drive electrical responses and elicit neuronal firing in a RGC. The visual field of RGCs can be divided into two areas, the centre and the surround (Kuffler, 1953). This organisation of the receptive field allows the use of contrast to understand how visual information is processed, as a result of the two visual pathways, as well as horizontal and amacrine cells' inhibitory characteristics (Silverthorn, 2013). There are two antagonistic areas in the receptive field of RGC, termed the ON and OFF regions as shown in **Figure 1.3**. Increase in light luminosity in the centre or the ON region causes ON cells to fire action potentials. On the contrary, OFF cells fire action potentials when the luminosity in the centre or ON region is decreased (dark spot). When light

shines on the surrounding region of an ON cell, then the response of the cell is inhibited and stops firing.

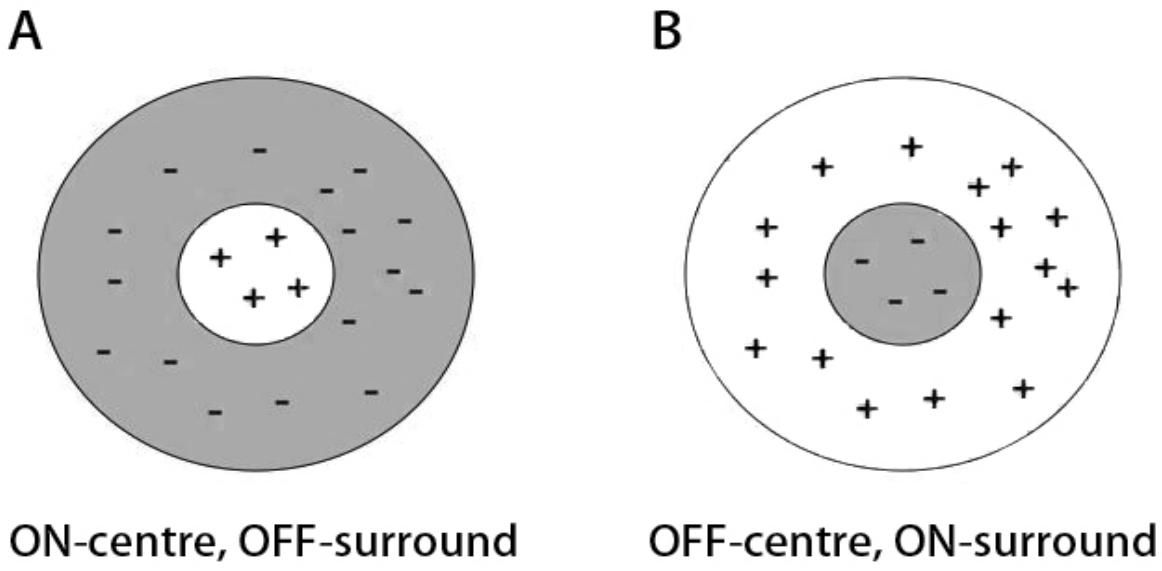

Figure 1.2. Representation of ON-centre, and OFF-centre receptive fields of retinal ganglion cells. *A. ON-centre, OFF-surround receptive field organisation. B. OFF-centre, ON-surround receptive field organisation. ("+" for on, "-" for off)*

Physiologically, there are three main types of RGCs: ON centre/OFF surround, OFF centre/ON surround, and ON-OFF ganglion cells. This refers to their receptive fields' sensitivity to light as each ganglion cell receives visual information from a specific part of the visual field. **Figure 1.2** illustrates the three different response patterns of RGCs. Ganglion cells with ON centre/OFF surround receptive field configuration are excited when light stimulates the centre of their receptive field, and are inhibited by light shone onto the surround. ON-type ganglion cells branch in the innermost part of the inner plexiform layer of the retina (close to the RGC cell bodies) and synapse with the axon terminals of ON-type bipolar cells. The opposite light response occurs in OFF centre/ON surround fields, where action potentials occur when the light is removed or stimulated by a dark spot. The OFF-type ganglion cells branch in the outermost part of the inner plexiform layer of the retina (close to the inner nuclear layer) and synapse with the OFF-bipolar cells. Whereas, ON-OFF ganglion cells fire action potentials at the beginning and the end of light

stimulation, and their dendritic trees branch in both zones of the inner plexiform layer, making a "bistratified" morphology (Nelson, 2007). This organisation uses the difference in contrast between the centre and the surrounding part of the receptive field to depict visual information. More advanced research methods in recent years have also shown other types of RGCs such as brisk transient (Y) cells, direction-selective ganglion cells, colour-coded ganglion cells of the primate retina and melanopsin containing ganglion cells (Wassle, 2004).

A recent review points out the definitive types of RGCs in the mouse are: four types of ON-OFF directionally selective cells, three types of ON directionally selective cells, four types of alpha RGCs, five types of intrinsically photosensitive melanopsin-containing RGCs, Local Edge Detectors, and three types of J-RGCs (Sanes and Masland, 2015). Moreover, there remains many identified but yet to be completely characterised RGCs as choosing the right markers remains challenging for RGC classification.

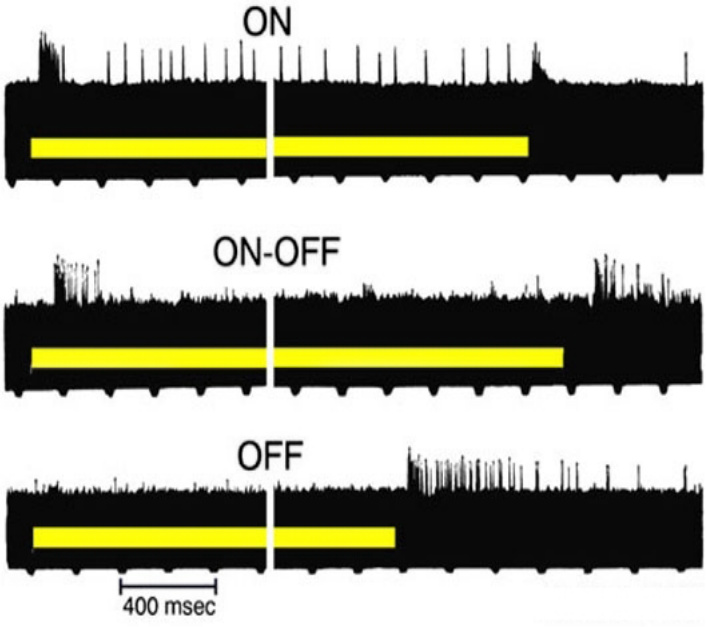

Figure 1.3. ON-type, OFF-type, and ON-OFF type retinal ganglion cell responses to light stimulation (yellow bars). *Picture adapted fromHartline (1938).*

1.2 Endocannabinoid System in the Retina

1.2.1 General Characteristics of the Endocannabinoids

The endocannabinoid system (eCB) of the CNS is a more recently described neurotransmitter system that alters neuronal excitability (Schwitzer et al., 2016) and thus, regulates a whole range of physiological activities, from pain sensation (Cravatt et al., 2001), motor learning (Kishimoto and Kano, 2006), to neuroplasticity and appetite (Di Marzo et al., 2001). Their vast effects on physiological processes are due to the fact that the eCB receptors are located throughout the central and peripheral nervous systems. The eCB system has already been described in the cerebellum (Good, 2007, Kishimoto and Kano, 2006, Di Marzo et al., 2001), hippocampus (Hashimotodani et al., 2007, Lee et al., 2015), basal ganglia (van der Stelt and Di Marzo, 2003), and other regions of the CNS. eCBs are lipid mediators involved in different biological processes. In the body, the most bioactive eCBs are anandamide (arachidonylethanolamide; AEA) and 2-arachidonoylglycerol (2-AG). Δ^9-tetrahydrocannabinol (THC) is the most active cannabinoid of the cannabis plant and mimics the action of eCBs.

1.2.2 Neuroplasticity of the Endocannabinoid System

As previously mentioned, eCBs play a modulatory role in many parts of the CNS, one such role is neuroplasticity. Synthesis and release of eCBs occur on demand as the result of increased activity in post-synaptic neurons. eCBs are released from postsynaptic neurones and act retrogradely, leading to inhibition of presynaptic neuron, and a short-term reduction in postsynaptic activity (Middleton and Protti, 2011). Retrograde transmission of eCBs system allows this short-term depression effect. Once eCBs are released, they activate presynaptic cannabinoid receptor 1, and leads to the hyperpolarisation of the presynaptic terminal, which decreases GABA or glutamate release The two most commonly described short-term plasticity phenomena are known as

depolarisation-induced suppression of inhibition (DSI) and depolarisation-induced suppression of excitation (DSE) (Diana and Marty, 2004). DSI is triggered by postsynaptic depolarisation resulting in eCBs release, which induces a transient inhibition of inhibitory neurotransmitters (GABA or glycine) from pre-synaptic neurons. DSE functions in a similar fashion, whereby release of excitatory neurotransmitters (glutamate) is suppressed. Recent studies by Middleton and Protti in 2011 have demonstrated the modulation of synaptic transmission and synaptic plasticity in ganglion cells by exo- and endo-cannabinoids.

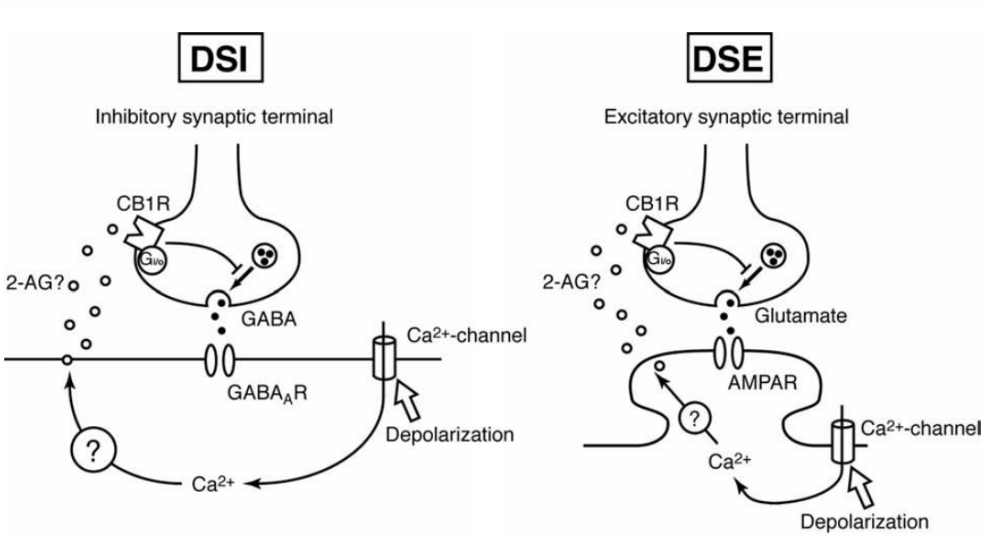

Figure 1.4. Current models for depolarisation-induced suppression of inhibition (DSI) and depolarisation-induced suppression of excitation (DSE).

1.2.3 Endocannabinoids in the Retina: Receptors, Ligand, and Enzymes

There are two primary types of G protein-coupled eCB receptors: cannabinoid receptor type 1 (CB1R) and type 2 (CB2R). CB1R receptors have been shown to be present in the retina across different animal species such as tiger salamander, goldfish, rat, mouse, chick and monkey (Schwitzer et al., 2016). They are found in the main types of retinal cells: photoreceptors, horizontal cells, amacrine cells, and ganglion cells (Straiker et al., 1999). The presynaptic location of CB1R on glutamatergic and GABAergic interneurons has been widely demonstrated. Their modulatory effect on synaptic transmission consists of a reduction in the release of glutamate and GABA from presynaptic terminals (Elphick and Egertova, 2001). A recent study by Penzo and

Pena (2009) demonstrated the postsynaptic location of CB1R in adult chick brain as well. CB2Rs were found on photoreceptors, horizontal cells, amacrine cells, bipolar cells and ganglion cells (Cecyre et al., 2013). Both types of receptors are also present in human retina (Schwitzer et al., 2016).

There are two major types of endogenous ligands that stimulate the CB receptors: N-arachidonoylethanolamide (anandamide, AEA) and 2-arachidonoylglycerol (2-AG). Anandamide is synthesised from N-arachidonoyl phosphatidylethanolamine (NAPE). Diacylglycerol (DAG) is hydrolysed by two DAG-lipase to produce 2-AG.

The three enzymes responsible for the degradation of eCBs are fatty acid amide hydrolase (FAAH), monoacylglycerol lipase (MGL) and cyclooxygenase-2 (COX-2). In mouse retina, FAAH is detected in all major cells types except cones (Schwitzer et al., 2016). MGL has been identified in mouse ganglion cells, while COX-2 was shown only in rods and bipolar cells in mouse retina, and ganglion cells in rat retina.

Apart from anandamide's well-known effect on the eCB system, it was also found to exert versatile effects by directly modulating other ion channels as it also binds to the Transient Receptor Potential (TRP) family channels. Anandamide is capable of directly inhibiting ion currents mediated by L-type Ca^{2+} channels, and TASK-1 K^+ channels (Di Marzo et al., 2002). Moreover, recent research (Vardi et al., 2000, Miraucourt et al., 2016) demonstrated that anandamide modulates cell excitability by binding to CB1R mediated Na^+-K^+-$2Cl^-$-co-transporter (NKCC1) channels. By reducing Cl^- level in RGCs, glycinergic currents are increased, which then facilitate voltage gated Na^+ channels to recover from their inactivation state (Vardi et al., 2000, Miraucourt et al., 2016). Membrane potential is then hyperpolarised, which leads to enhanced intrinsic excitability of RGCs. Furthermore, anandamide also acts as a endovanilloid, binding to the TRP family channels, which will be discussed later under the TRP channel chapter (**Chapter 1.3**).

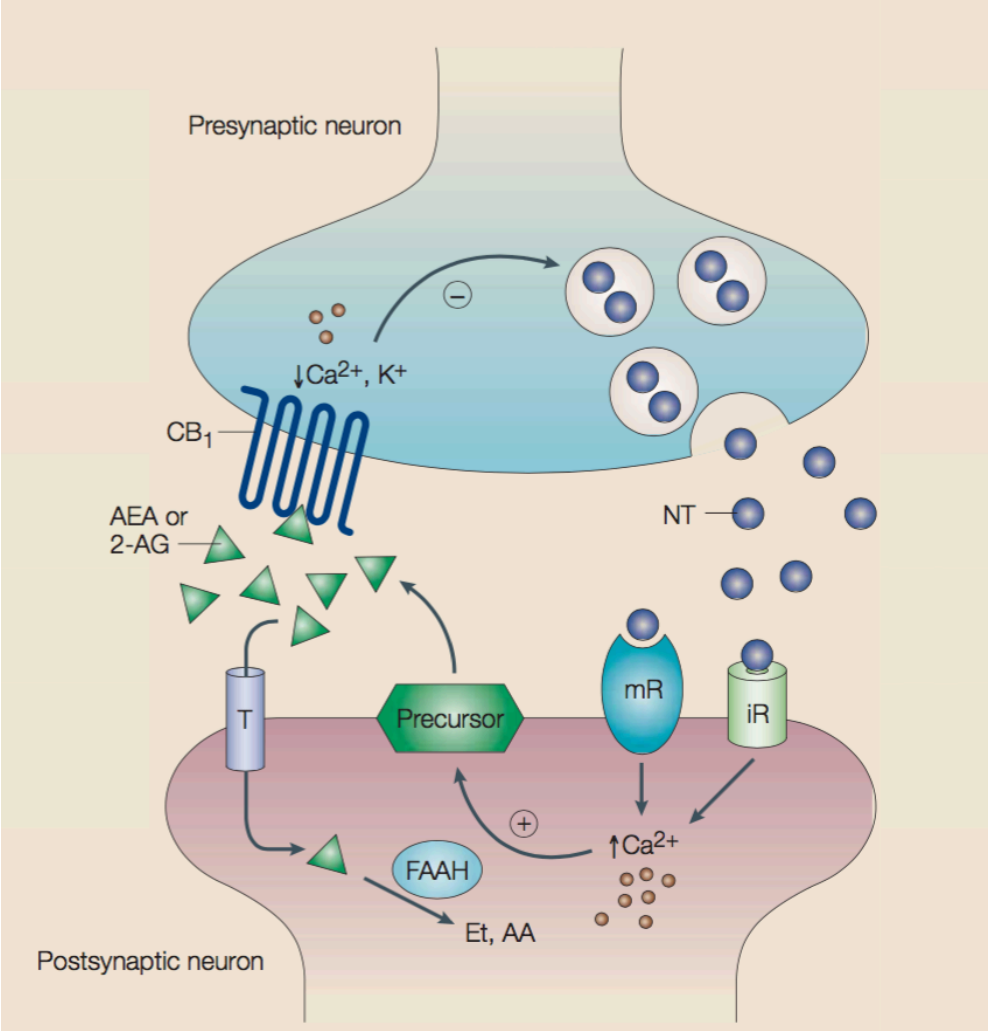

Figure 1.5.Modulatory effects of endocannabinoids by retrograde transmission at synaptic terminals. *Upon the release of neurotransmitters (NTs), binding of NTs to ionotropic (iR) and metabotropic (mR) receptors leads to an increase in Ca^{2+} intracellular concentration. AEA (anadamide) or 2-AG (2-arachidonoyl glycerol) is released from a postsynaptic neuron, and binds to presynaptic CB1 receptors, which inhibit Ca^{2+} channels and activate K^{+} channels. This in turn decreases NT release. Membrane-transport system (T) takes up the leftover endocannabinoids and degrades them via enzymes: fatty acid amide hydrolase (FAAH), monoacylglycerol lipase (MGL) and cyclooxygenase-2 (COX-2).Picture adapted from Guzman (2003).*

A study by Middleton and Protti (2011) demonstrated the application of a CB1R agonist WIN55212-2 was able to suppress both glutamatergic and GABAergic currents in ganglion cells. Moreover, the same group showed WIN55212-2 could reduce retinal responses to light stimulation, which could be reversed by the CB1R antagonist, AM251 (Middleton and Protti, 2018)

Interestingly, recent studies from the Vision laboratory (Protti et al., 2015, Yates, 2014, Leung, 2016, Yong, 2016) has shown a paradoxical effect when anandamide levels are elevated. This was achieved by directly administrating exogenous anandamide and blocking the degrading enzyme FAAH using URB597 to retinal wholemounts in the mouse. The physiological or exogenous increased level of anandamide was thought to decrease the number of action potentials in RGCs. However, by using the patch-clamping technique, the amplitude of light-evoked postsynaptic potential was decreased but led to an increase in the number of spikes (Yates, 2014, Protti et al., 2015, Leung, 2016, Yong, 2016). As the amplitude of the post-synaptic potential represents input into RGC and action potential represents the cell's spike output, this unexpected result illustrated URB597 or anandamide increases cell excitability (Protti et al., 2015) as shown in **Figure 1.6**.

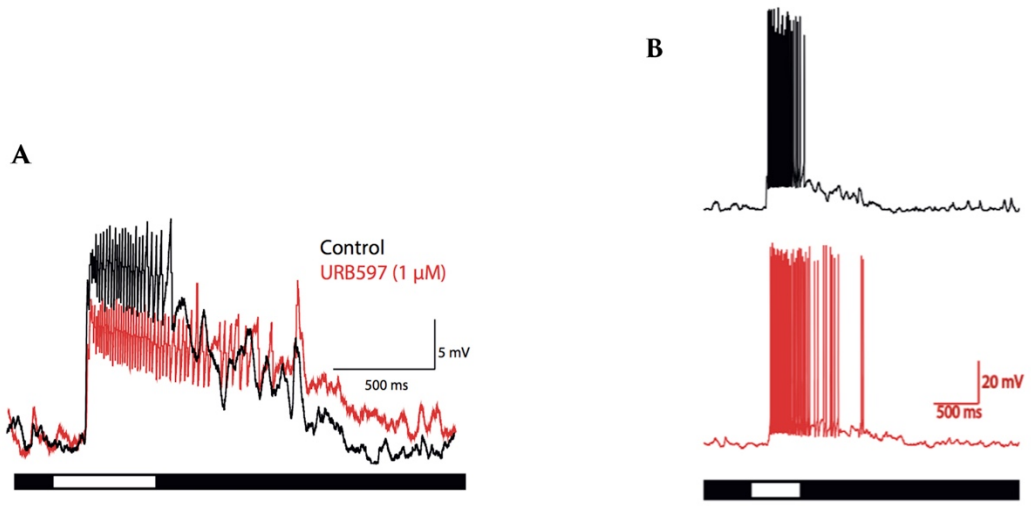

Figure 1.6. Application of URB597 creates a paradoxical effect on retinal ganglion cells. *(A)Light-evoked postsynaptic potential was reduced after application of URB597 (red trace). (B) Light-evoked response of an ON retinal ganglion cell increased in spike count after application of URB597.*

1.3 TRP Channels in the Retina

1.3.1 General properties of TRP channels

Transient Receptor Potential (TRP) channels are relatively non-selective channels permeable to cations, including sodium and calcium, with six transmembrane segments, and play important roles in sensory physiology. A variety of external stimuli including light, touch, sound, temperature and chemical can excite TRP channels. TRP channels were initially discovered due to *trp* mutation in the fruit fly *Drosophila*, which altered the fly's electroretinogram resulting in missing a sustained phase (Cosens and Manning, 1969). In mammals, TRP channels have a high degree of sequence homology, especially in the putative functional regions (Song and Yuan, 2010). However, they have diverse activation mechanisms, vary in permeability to cations, and can be categorised into two groups and a total of seven subfamilies based on their sequence and topological differences (Venkatachalam and Montell, 2007). Five channels belong to Group 1 including TRPC, TRPV, TRPM, TRPA, and TRPN, and two other channels belong to Group 2 including TRPP and TRPML.

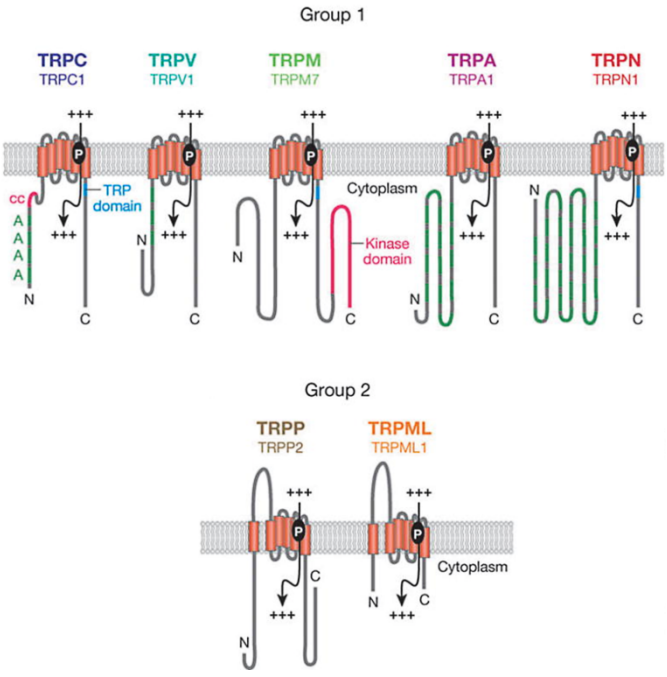

Figure 1.7. The TRP superfamily consists of five Group 1 subfamilies and two Group 2 subfamilies. They are calcium-permeable cation channels with six transmembrane segments. *Picture adapted from (Venkatachalam and Montell, 2007).*

1.3.2 General characteristics of TRPV1 channels

The Transient Receptor Potential Vanilloid (TRPV) subfamily is divided into two groups: TRPV 1-4 and TRPV5, 6. TRPV1 is a non-selective ligand-gated cation channel, which can be activated by a wide range of physical and chemical stimuli (Chavez et al., 2010, Venkatachalam and Montell, 2007). It was first identified by Julius and colleagues in the search for channels activated by vanilloid compound capsaicin, which is the hot ingredient from hot chilli peppers (Ryskamp et al., 2014). It can also be activated by eCBs, and other exogenous lipids (Leonelli et al., 2009). Although it has primarily been located on nociceptive neurons in the peripheral nervous system, these receptors have also been found throughout the CNS (Chavez et al., 2010, Leonelli et al., 2009). Of interest is that Nucci and colleagues (2007) demonstrated the presence of TRPV1 channels in rat retina through functional experiments. The group discovered anandamide binding ability is reduced to CB1 and TRPV1 in ischemic-reperfused retinas, which could induce cell loss in RGC layer on ischemic insult. Later, Sappington and colleagues (2009) showed trpv1 mRNA was expressed in RGC, with robust TRPV1 proteins localised in the cell bodies and axons. Recent research by Jo and colleagues (2017) discovered that TRPV1 expression is confined to a subset of ganglion cells, which peaks in the mid-peripheral mouse retina. In addition, their results showed a colocalization of CB1R and TRPV1 in RGCs.

1.3.3 Possible explanation of the paradoxical effect observed the RGCs

One possible explanation for the aforementioned paradoxical effect of URB597 is through the activation of TRPV1 channels. As anandamide is a partial agonist for CB1 receptor, but a full agonist for TRPV1 receptor, inhibition of FAAH would lead to an increase of eCBs and activate not only CB1 receptors but also TRPV1 channels, which have high Ca^{2+}permeability. Increased cytoplasmic calcium concentration would activate calcineurin, which is a Ca^{2+} dependent phosphatase implicated in dephosphorylation of Na^{+}channels. This would lead to an increase in Na^{+}channels activity and therefore increased action potential firing of ganglion cells.

Previous studies from the Vision lab had provided the foundation to the current hypothesis. **Figure 1.8** illustrates the input-output function of RGCs in response to current injection under the effect of URB597 and capsazepine. The input-output function was constructed from current injection protocols and describes cell excitability. The number of spikes produced in a RGC was plotted as a function of the magnitude of the change in membrane potential for each current step and then fitted with a sigmoidal curve. Thus, a shift in the input-output function indicates the change in cell excitability.

As previously mentioned, URB597 is a FAAH inhibitor, which elevates the levels of eCBs, and capsazepine is a TRPV1 antagonist. The number of spikes was plotted against amplitude of depolarising step for individual cells, and the average input-output function was drawn. A leftward shift with URB597 application indicates an increase in cell excitability, which was reversed by the application of capsazepine (**Figure 1.8**).

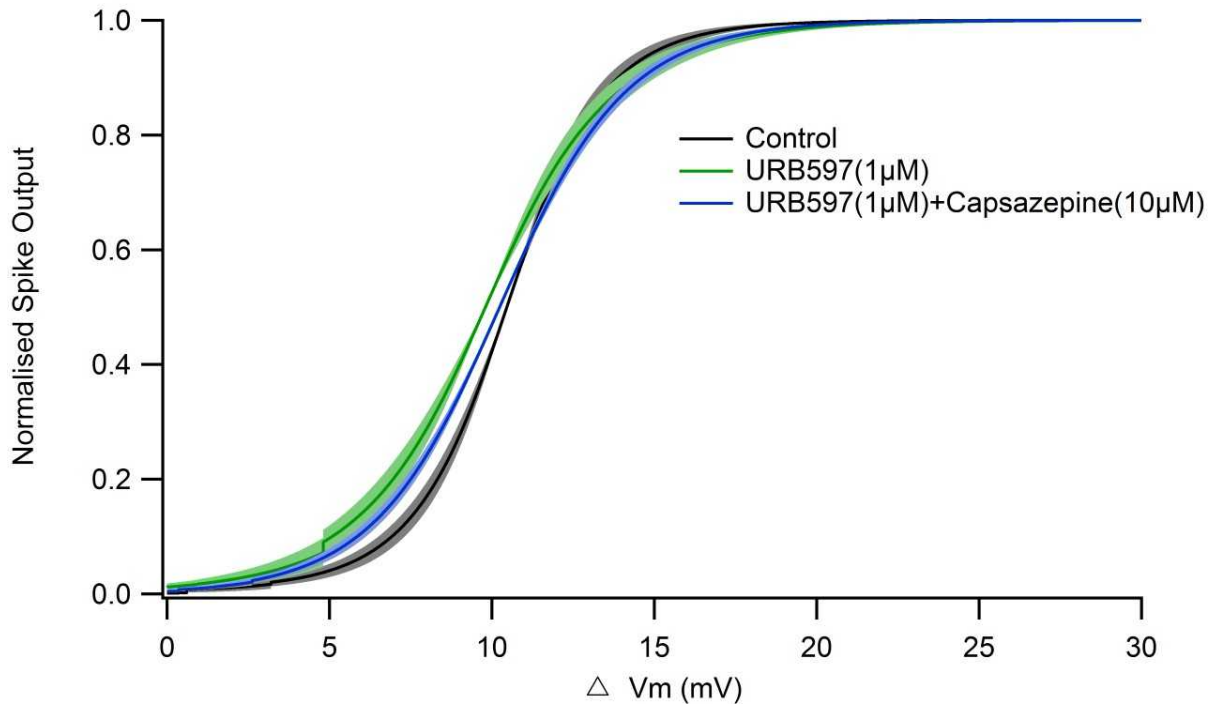

Figure 1.8.Input-output relationships of ganglion cells in response to current injection under control, URB597, and URB+Capsazepine condition. Spike responses were normalised to control condition. *Upon URB597 application, the observed left shift of the curve (green) was reversed by a right shift after application of capsazepine (blue). Solid line represents the average of pooled sigmoidal fits, shaded area indicates SEM.*

Another method to assess membrane excitability is through the analysis of the current-to-voltage (IV) relationship recorded under voltage-clamp configuration. This is crucial as the voltage-gated Na^+ currents are responsible for generating action potentials. As shown in **Figure 1.9**, the IV curve significantly reduced with URB597 application, which indicated raised level of Na^+ entry and spike output.

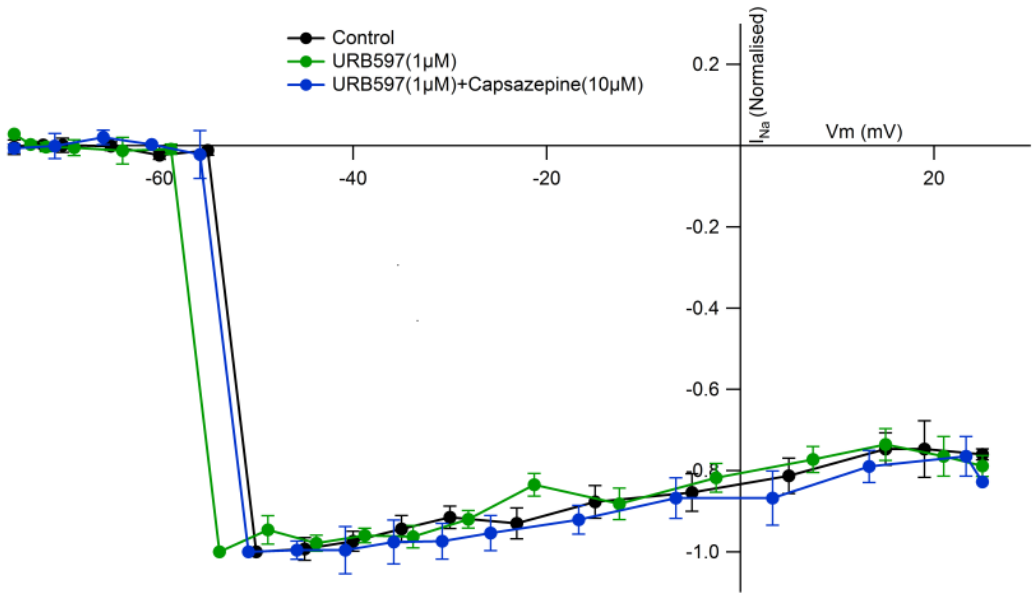

Figure 1.9.Current-voltage (IV) relationships illustrate a left shift in Na^+ entry from control after application ofURB597, then a right shift from URB to URB+Capsazepine. *The average IV plot (±SEM), normalised to peak Na^+ current is shown. Amplitude of Na^+ entry was plotted against membrane potential of RGCs as IV curves. A leftward shift was observed with URB597 (green trace) condition followed by a rightward shift upon capsazepine (blue trace) application.*

1.4 Hypothesis and Aims

The overall aim of this project was to investigate the roles that TRPV1 channels play in the modulation of membrane excitability in RGCs, in particular, their possible involvements in the eCB system. The specific aims are:

1. To study the effects of TRPV1 channel agonist capsaicin on RGC excitability. Since TRPV1 channels are nonselective ligand gated cation channels, we predict bath application of capsaicin on retinal whole mounts will cause an influx of cations into ganglion cells, leading to an increase in their excitability.
2. To determine the effects of anandamide on TRPV1 channels and its modulation of RGC excitability using URB597 and capsazepine. As anandamide is an agonist of TRPV1 receptors, an increase in ganglion cell excitability is expected. URB597, a FAAH inhibitor, elevates the levels of eCBs and leads to an increase in cell excitability, thus, its effects are expected to be reversed by the co-application of capsazepine (TRPV1 antagonist). Thus, little or no change in ganglion cell excitability is expected.
3. To further validate Aim 2 by using *TRPV1-/-* knockout mice. In these knockout animals where TRPV1 channels have been removed, results could be compared to those obtained from control animals. Differences between these groups could reveal other functions of TRPV1 channels.

The above aims will be achieved by pharmacological modulation on the eCB system in wild-type (control) and TRPV1 knock-out mice. Patch clamp technique was employed to obtain electrophysiological recordings from the cell bodies of RGCs. Cell excitability will be examined by generating input-output functions from current clamp recordings, and Na^+ and K^+ currents will be recorded under voltage clamp configuration to produce current-to-voltage (IV) relationships. A mouse model was chosen for the current study based on the following reasons: 1) Results collected could be compared to the data obtained from previous experiments conducted by the

same lab. 2) Mouse is a common animal model thus allows comparison to published results. 3) Genetically modified *TRPV1-/-* mice are accessible.

Based on background knowledge, it was hypothesised that: TRPV1 channel activation by eCBs leads to an increase in RGC excitability. Application of a TRPV1 agonist (capsaicin) and an antagonist (capsazepine) were used for wild type animals. To test whether or not the URB-induced postsynaptic effects are mediated by TRPV1 channels, URB597 in combination with TRPV1 antagonist capsazepine was used for TRPV knockout animals. If anandamide-induced increase in cell excitability was due to binding of TRPV1 channels, we hypothesise the following:

1. Application of capsaicin will increase cell excitability. Na^+ and K^+ current will increase in amplitude, X-half of the input-output function will decrease, and spike output will increase.
2. Application of capsazepine will modify cell excitability, changing Na^+ and K^+ currents and the input-output function.
3. Using knockout animals, where TRPV1 channels are absent, application of URB597 elevates the level of anandamide but no effects on RGC excitability would be seen if anandamide acts via TRPV1 channels.
4. In the absence of TRPV1 channels, co-application of URB597 and capsazepine on knockout animals is not expected to produce any change in cell excitability.

2. Materials and Method

2.1 Ethics Approval

Procedures and experimentation on all animals used were approved by the Animal Ethics Committee of the University of Sydney. Guidelines issued for animal experiments by the Australian Code of Practice for the Care and Use of Animals for Scientific Purposes, and National Health and Medical Research Council of Australia, were followed.

2.2 Solutions Used in Experiments

An extracellular solution was made up of 8.8g of AMES medium (US Biological) and 1.9g of sodium bicarbonate in 1L of Milli-Q water. It was used to bath the retina for dissection and electrophysiological recordings. AMES medium is made of many inorganic salts, amino acids, vitamins, and other compounds to keep the retina alive after dissection as well as maintaining its electrical activity. The extracellular solution was continuously bubbled with 5% carbon dioxide and 95% oxygen to buffer the solution at pH of 7.4 while keeping the retinal tissue oxygenated.

Intracellular solution used for electrophysiological recordings consisted of: K^+-Gluconate (140mM), HEPES (10mM), EGTA (10mM), $MgCl_2$ (4.6mM), ATP-Na^+ (4mM), and GTP-Na^+ (0.5mM) (Huang et al., 2013). The osmolarity was kept around 278mOsm, about 10mOsm lower than the extracellular solution in order to help giga-seal formation between the tip of the micropipette and the cell membrane. 1% (in volume) of fluorescent dye Lucifer yellow was also added to the intracellular solution prior to patching for the purpose of morphological identification of cells and antibody staining.

2.3 Tissue Preparation

Two mouse strains were used for the experiments, C57bl/6J (N = 30) were used as wild-type (control) animals and TRPV1-/- (B6.129X1-*Trpv1*^{tm1Jul}/J, N = 48) were used for the knockout experiments. The TRPV1-/- mouse line was obtained from Prof. Bernard Balleine. These mice are homozygous for the targeted mutation; their phenotype is normal but they display no pain response and show reduced aversive responses to high temperature and acidity. These mice live longer than wildtype mice, maintain a youthful metabolic profile, and have improved special memory (Caterina et al., 2000).

Animals were dark adapted for at least 2-hours before anaesthesia with isoflurane (Henry Schein) followed by euthanasia by cervical dislocation in the dark under infra-red illumination or under dim red light. Infra-red viewers (FJW Optical Systems, Find-R-Scope Infrared) attached to a microscope (Olympus SZX7) allowed visualisation of the eye structures and the retina while dissecting in the dark. Eyes were removed using curved scissors and transferred to a beaker containing AMES solution and then to a Petri dish with AMES solution continuously carboxygenated. Dissection of the eye was done under a microscope (Olympus SZX7), after removal of the cornea and iris, lens was taken away for retinal detachment from the sclera. Before detachment of the retina, the eyecup was cut into halves to harvest hemi-retinae. This cut flattens the retina, so that it can be put under a grid where it remains relatively flat. Afterwards, vitreous humour was carefully removed from the retina without damage. One hemi-retina was mounted inside a recording chamber with the ganglion cell layer up, and held down by a grid made of platinum wire and dental floss threads.

The chamber was then placed under an upright microscope (Olympus BX50WI), and continuously perfused with carboxygenated extracellular solution. A CCD camera (JENOPTIK D-07739) was connected to the microscope and computer monitor to allow visualisation of the tissue under infrared light (see **Figure 2.1**).

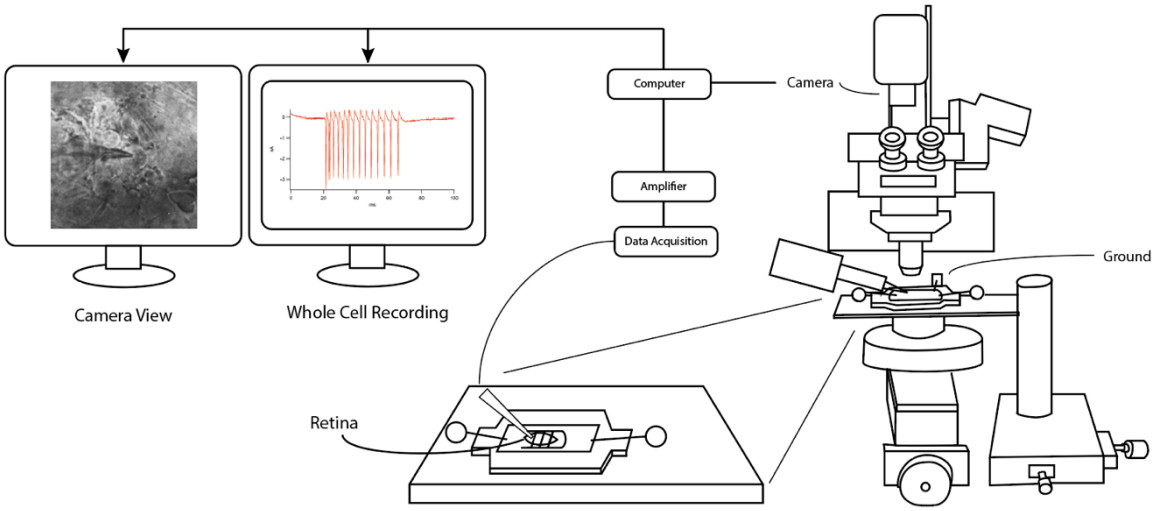

Figure 2.1. Experimental setup for patch clamping mouse retinal tissue and data acquisition. *Visualisation of the cell body is gained by infrared light imaging captured by a digital camera, and relayed to the computer. Cell membrane potential is kept stable (~ -60mV) using a feedback loop between the computer and the cell and injecting different amount of currents (voltage clamp mode). The same feedback loop is also used to inject constant current. Cell responses such as amplitude of the changes in membrane potential and spikes were acquired, amplified and recorded. Recordings of the cell is displayed in red on the right screen.*

2.4 Electrophysiological Recordings made from Ganglion Cells

In order to carry out electrophysiological recordings, physical access to the cell body is required. This was achieved by firstly tearing a small hole in the inner limiting membrane to expose the soma of ganglion cells using a pulled glass pipette driven by a micro-manipulator (Sutter MP-225). Next, a newly pulled glass pipette of resistance 6-10MΩ was filled with intracellular solution containing the fluorescent dye Lucifer yellow. Positive pressure was applied before entering the bath with the pipette, which was used to approach and target RGCs using a micromanipulator. The pipette was then lowered onto the soma surface until a dimple was visible. The positive pressure was subsequently released, and negative pressure was gently applied to achieve a giga-seal. After obtaining a giga-seal, a short pulse of negative pressure was applied until the cell membrane opens. Membrane potential was maintained at -60mV before performing several recording protocols using an EPC8 patch clamp amplifier (HEKA Electronik). PatchMaster software was used, protocols were then repeated under different pharmacological conditions, as described below.

2.5 Protocols Used to Make Recordings from Ganglion Cells

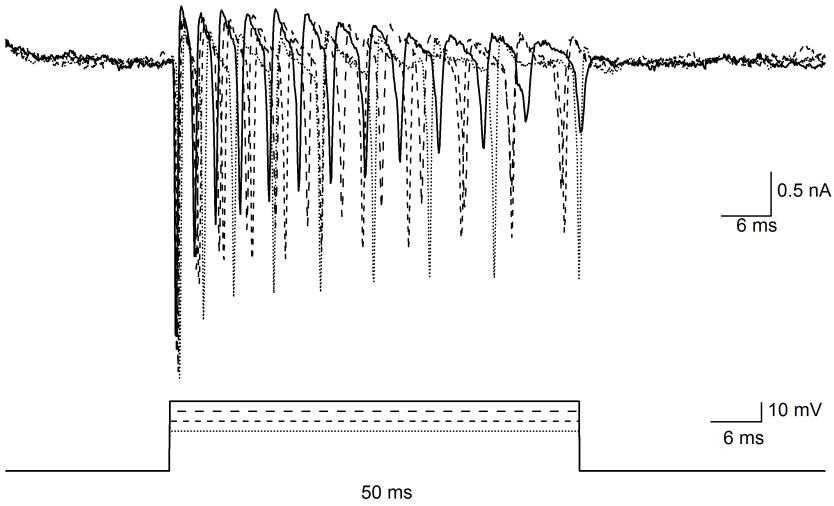

Figure 2.2. Representative voltage clamp membrane currents with depolarisation recorded from the cell body of a ganglion cell. *(A)The inward Na^+(downward) and outward (upward) K^+ currents representation from a typical ganglion cell are shown. (B) Stimulation of a ganglion cell was achieved using currents ranged from -75mV to +35mV with 5mV steps for 100mselicited inward Na^+(downward) and outward (upward) K^+ current corresponds to A.*

2.5.1 Voltage clamp protocols used to stimulate ganglion cells

To explore the effects of pharmacological modulators of the endocannabinoid system and agonist and antagonist of TRPV1 channels on RGCs excitability, RGCs were held from -75mV to +35mV, at intervals of +10mV for 100ms. A total of 12 steps were applied to the cell. Note that there were changes made to the protocol to achieve better resolution around the peak inward Na^+ current. The cell membrane holding potential changed from 12 steps to 24 steps as shown in **Figure 2.3**. After modification of the membrane holding potentials, RGCs were held at intervals of +5mV for the first 12 steps and intervals of +10mV for the following six steps for 100ms as shown in **Figure2.3B**. The peak amplitude of inward Na^+ currents from each step was extracted later to build current-to-voltage (IV) curves.

While whole-cell patch clamp technique is widely used for synaptic electrophysiological studies, direct dendritic recordings have exposed the space-clamp error of the voltage clamp (Williams

and Mitchell, 2008). This error is due to neurons are not perfectly spherical, and somatic patch clamp could only have accurate control of the membrane potential of the somatic and perisomatic area. The apical dendritic voltage escape could sequentially distort the somatic measurement (Williams and Mitchell, 2008). This will be further discussed in Discussion (**4.3**).

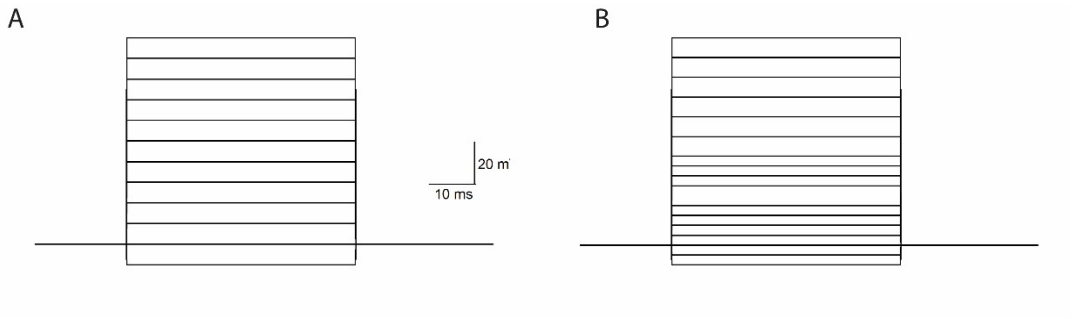

Figure 2.3 Holding potentials of ganglion cells under voltage clamp configuration. *(A). There was a total of 12 steps of holding potentials ranged from -75mV to +35mV at intervals of 10mV for 100ms. (B). First 12 steps of holding potentials ranged from -75mv to +5mV with 5mV intervals and six steps of holding potentials from +5mV to +35mV at interval of 10mV for 100ms*

2.5.2 Current-injection protocol into the cell bodies of ganglion cells

Apart from current injections or during experimental protocols, the resting membrane potential of the cell was always kept at -60mV. Any current required to inject into the cell corresponds to the leak current.

In order to investigate the excitability properties of ganglion cells in current-clamp configuration, 24 current steps at increment of +5pA amplitude was applied. Currents ranged from +15pA to 125pA were injected for 100ms into the cell bodies of RGCs to elicit action potential firing as shown in **Figure 2.4**.

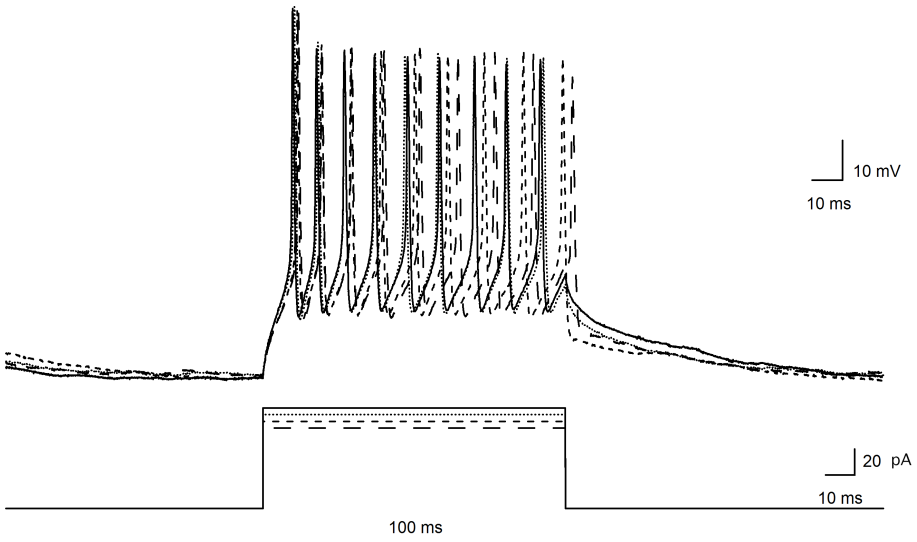

Figure 2.4 Sample recording traces of current injection recorded from a typical ganglion cell.
Sample action potentials in response to four steps of current injections (60, 65, 70, 75 pA).

2.5.3 Light-stimulation protocols used to stimulate ganglion cells

Two protocols were used to measure light evoked responses in current clamp mode.

The first protocol consisted of five light stimuli of similar light intensity. This was achieved by applying full field stimulation with a blue (455nm) LED (THOR LABS DC 4104) at an intensity of 1.12^{10} photons/μm^2*s through the microscope optics (2.24 x 107 photons/um2/s with ND6, ND10 and polariser filters). Following this, another stimulation protocol was applied in which 10 constant intensity light pulses of varying duration (range: 2.25ms - 192.5ms) were applied.

2.6 Data Analysis of Ganglion Cell Responses

Custom-written routines in IGOR Pro 6.0 (Wavemetrics) were used to analyse electrophysiological recordings obtained from Patchmaster (HEKA Electronik). Input-output functions of ganglion cells were built from spike output and amplitude of depolarisation/light-evoked postsynaptic potential were recorded under current clamp mode. The relationships alone

with their key parameters were further normalised and pooled to compare between different pharmacological conditions.

2.6.1 Current-voltage relationships and inward Na^+ currents of ganglion cells

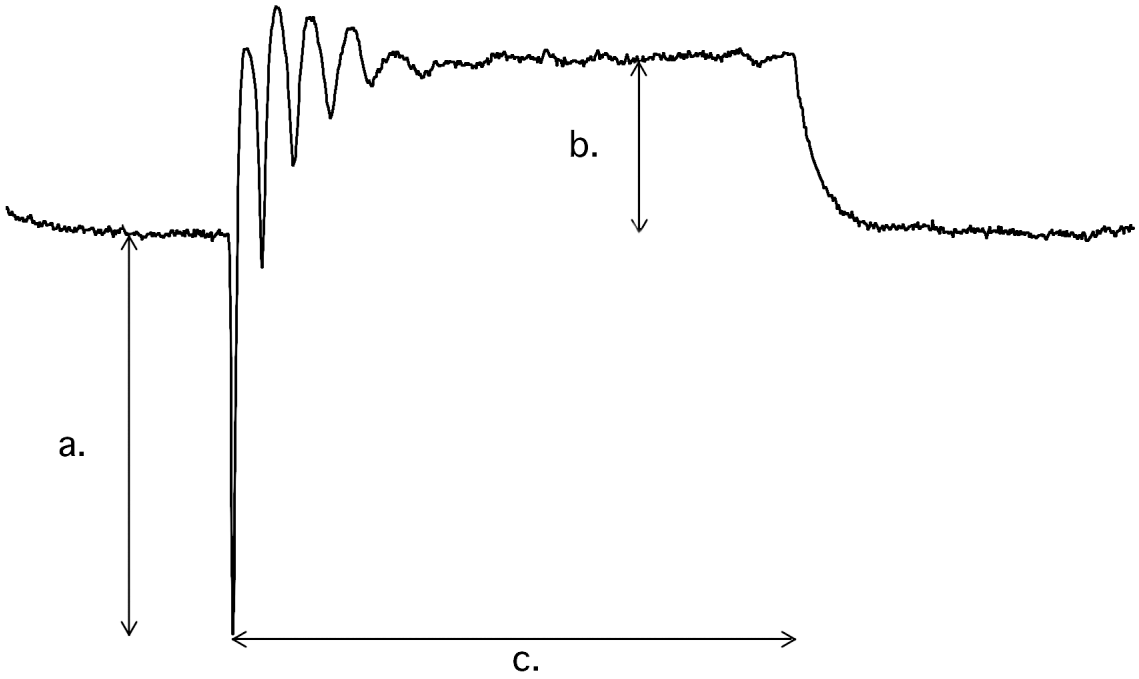

Figure 2.5 Analysis of a voltage clamp trace recorded from a ganglion cell illustrating parameters collected for further data analysis*. a: the amplitude of inward Na^+ current;b: the amplitude of outward K^+ current; c: the number of inward Na^+ spikes.*

Voltage gated Na^+ and K^+ channels open at different membrane holding potentials, moving in the opposite directions. Positive K^+ currents (b) leaving the cell can be seen in **Figure2.5** as an upward deflection of the membrane potential, and positive Na^+ currents (a) going into the cell will be indicated as the downward deflection. Also, Na^+ and K^+ channels have different kinetic properties and opening at different rates, with Na^+ opens much faster than K^+ channels (Hodgkin and Huxley, 1952). Amplitudes of both inward Na^+ and outward K^+ were measured for the control and two pharmacological perfusion conditions (**Figure 2.5**). Then each amplitude was plotted against the corresponding holding voltage for the construction of current-to-voltage (IV) plots and

subsequent quantification of V-half. V-half represents the value at half-height which is 50% of the maximum Na^+ current (see **Figure2.6**).

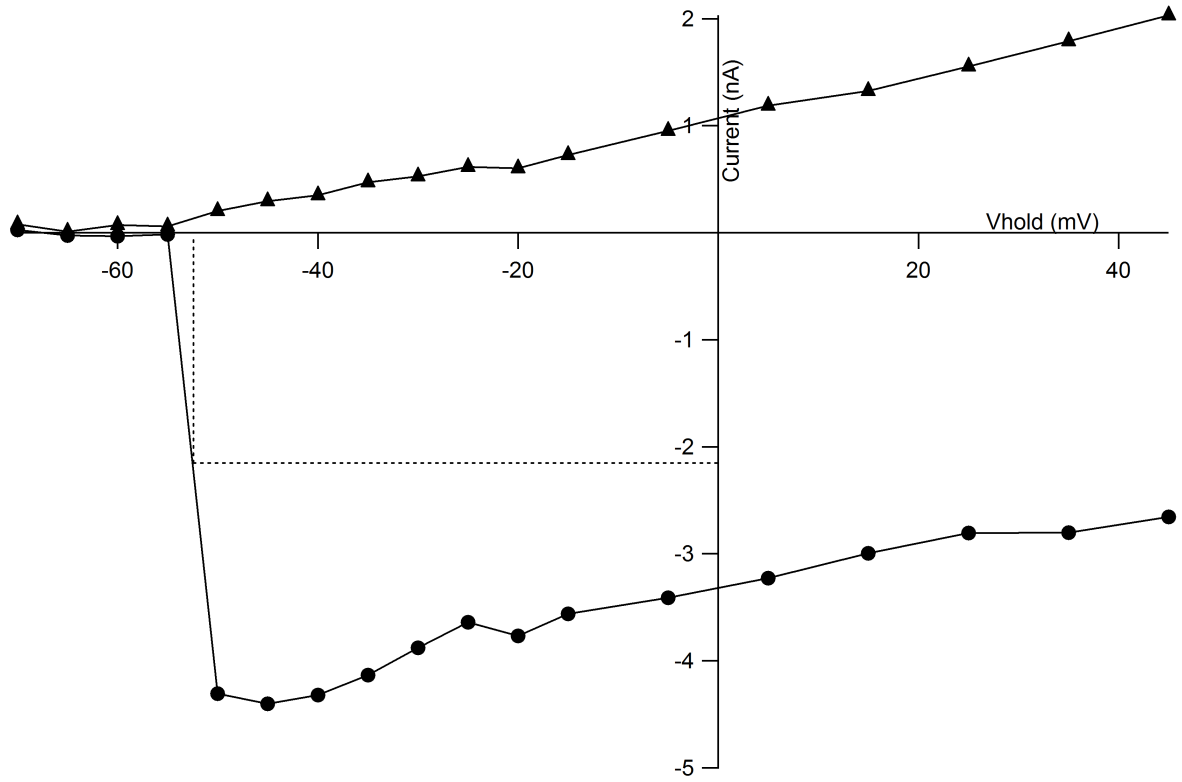

Figure 2.6 Sample trace of an IV curve of inward Na^+ and outward K^+ current amplitude (y-axis) in response to membrane depolarisation (x-axis). *The dash line indicates V-half which is 50% of the maximum Na^+ current.*

The amplitude of maximum inward Na^+ current, 50% of the maximum Na^+ current (V-half), the total number of inward Na^+ events, and the peak outward K^+ current were extracted from the IV curves. A two-tailed Wilcoxon matched-pairs signed rank test was performed between the control and the first drug condition, as well as between the first drug and the second drug conditions.

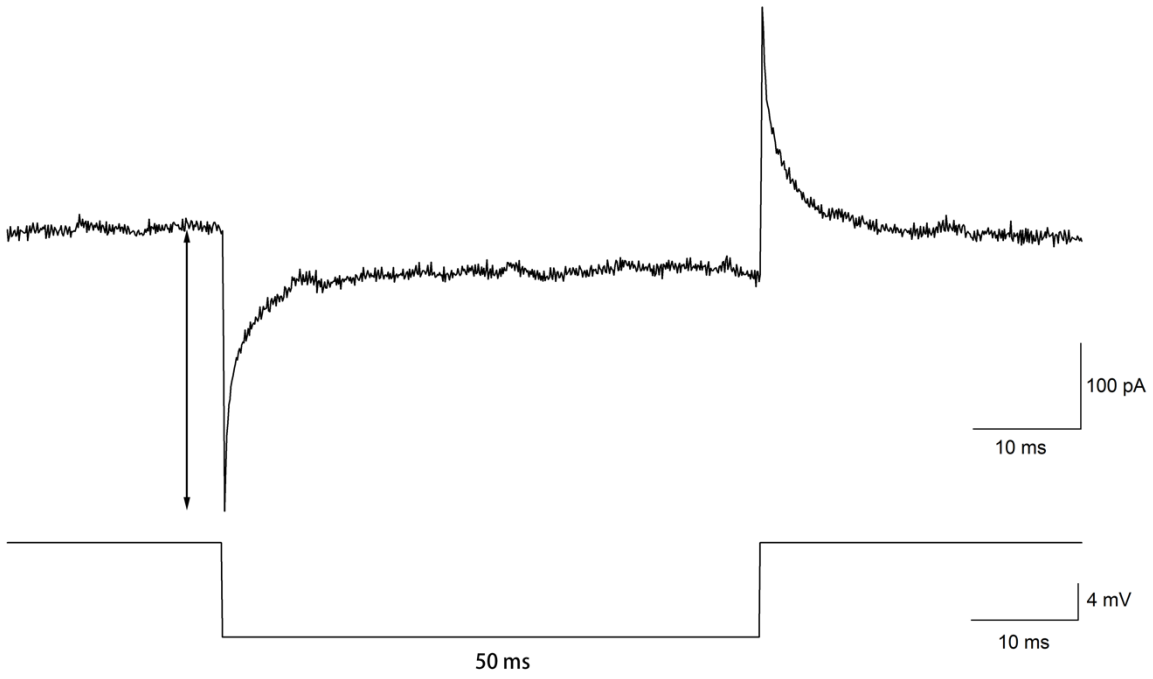

Figure 2.7 Amplitude of the inward current was measured to indicate the degree of cell access. *Cell access for the control and the two pharmacological conditions were measured for the purpose of examining stability of recordings, and thus ruling out that changes in excitability were due to differences in electrical access to the recorded cell.*

2.6.2 Pulse

A short change of -10mV in the holding membrane potential allows direct observation of change in cell access measured under voltage clamp, as shown in **Figure 2.7**. This measurement is crucial for comparison of cell access before and after each pharmacological condition. A dramatic change in cell access could lead to poor quality of electrophysiological recordings, resulting in large alteration in RGC excitability. Such cells were eliminated as not to confuse their results with the actual effects of drug perfusion.

2.6.3 Current injections into the cell bodies of ganglion cells

In order to generate the input-output functions of RGCs, measurements of the amplitude of membrane depolarisation and the number of action potentials (spikes) were obtained. A threshold of -30mV was set to detect spikes. Amplitude of the depolarisation was measured by removing spikes using linear interpolation of the membrane potential 4ms before and around 10ms after

each spike (Di Marco et al., 2009). The difference between resting membrane potential and peak depolarisation is measured as ΔVm. For the construction of the input-output plots, the number of spikes is plotted against ΔVm and was fitted with a sigmoidal function:

$$base + \frac{max}{1 + \exp\big((xhalf - x)rate\big)}$$

base: the minimum point of output, where the sigmoidal curve crosses the y-axis.

max: the maximum point of output, where the sigmoidal curve plateaus.

x-half: the membrane potential (x-axis) when 50% of maximum output occurred.

rate: the slope of the sigmoidal curve.

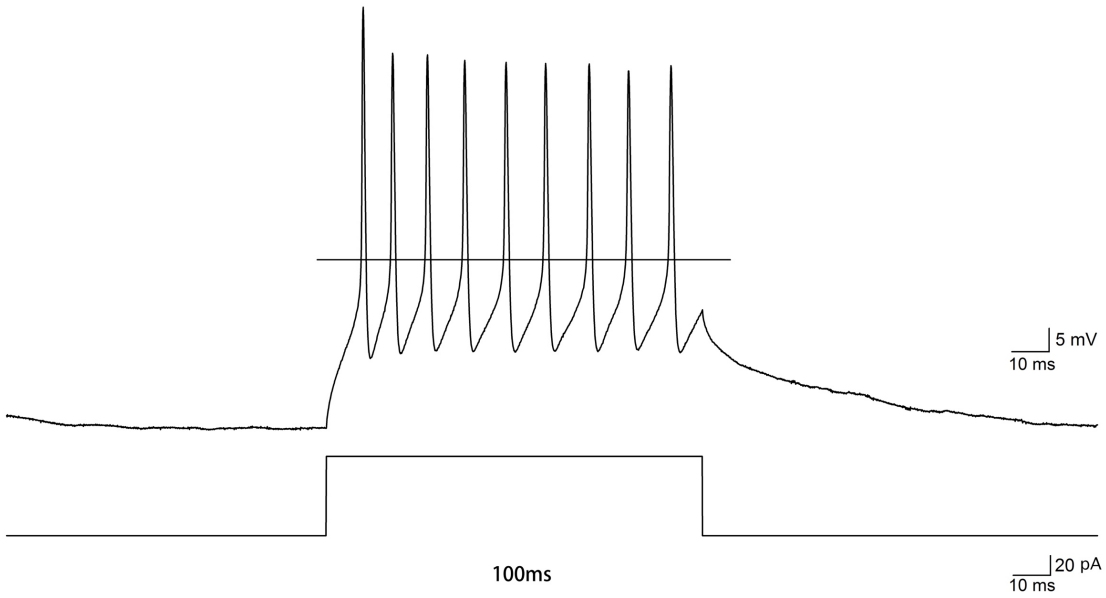

Figure 2.8 Analysis of a current injection trace recorded from a typical ganglion cell. *Amplitude of the membrane potential and the total number of spikes measured at threshold of -30mV were used for further data analysis.*

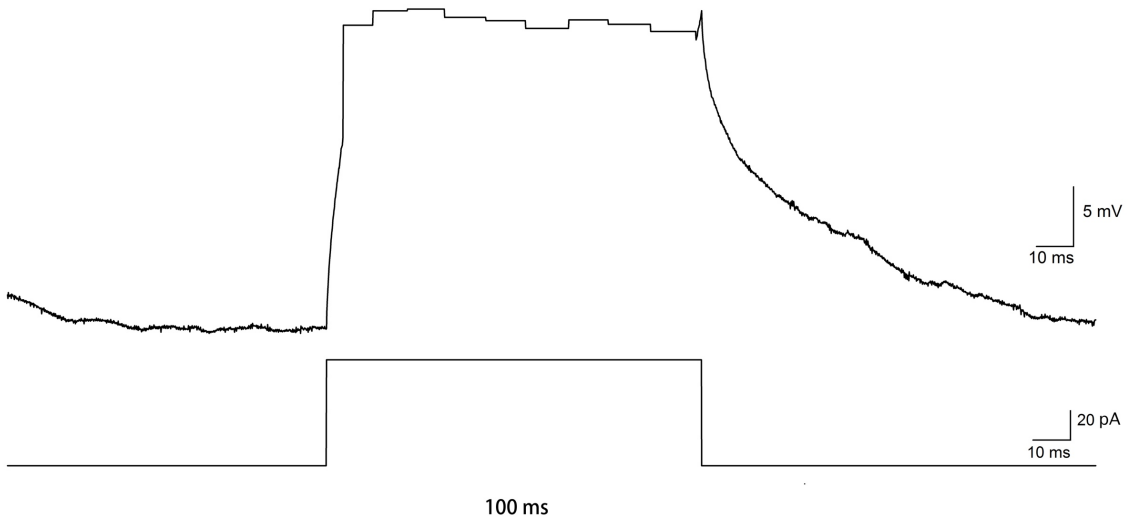

Figure 2.9 Sample trace of current injection of a typical ganglion cell after smoothing. *Action potentials were removed, the smoothed curve was used to measure the change between resting membrane potential and depolarised potential (ΔVm).*

The total number of spikes were measured directly between time interval indicated by the bottom trace in **Figure 2.8**. Amplitude of the depolarisation was measured after smoothing out spikes at the set threshold of +30mV (**Figure 2.9**). As neuronal input-output relationship is described by sigmoidal curve function, a curve fit generated for individual RGC (Rudolph and Destexhe, 2006, Lafon et al., 2017, Hocking, 2016). Also, this approach enables the comparison across multiple cells as explained in the following paragraph.

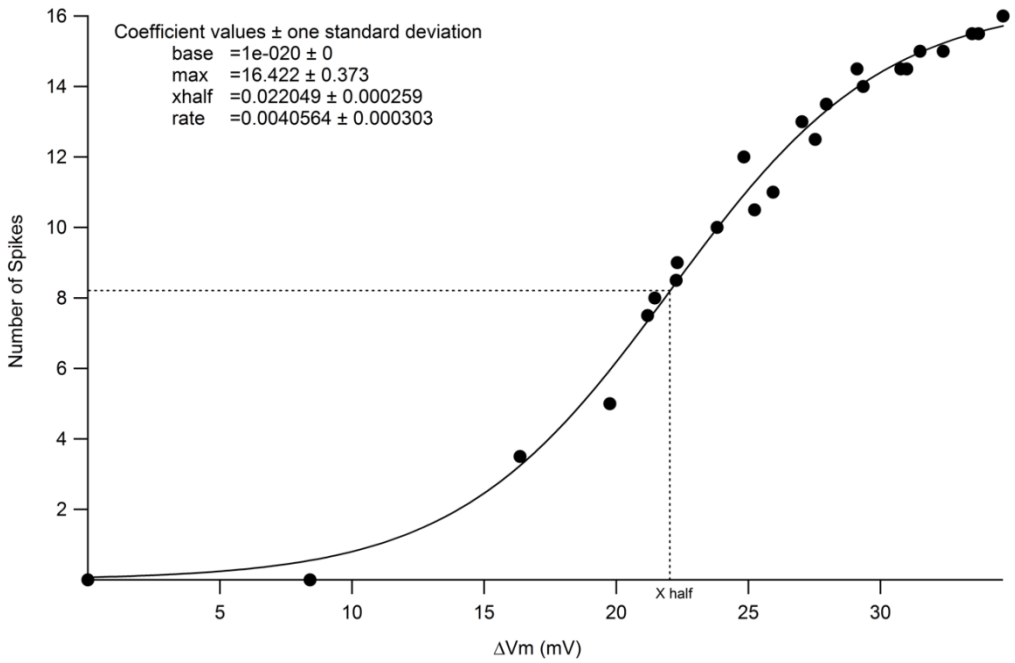

Figure 2.10 Spike-amplitude relationship curve. *Number of spikes output was plotted against amplitude of depolarisation. A sigmoidal curve was fitted through data points with curve parameters indicated on the top left-hand corner of the figure. Sigmoidal curve fitted parameters were collected for further statistical comparisons between control and various conditions.*

Parameters of individual sigmoidal fits were then collected from the input-output curves, which were first normalised against control condition, pooled and then averaged. Procedures are as follows: first, fits were regenerated by using the sigmoidal function parameters: base, max, x-half and rate as shown in **Figure 2.10**. Next, they were normalised to the maximum amplitude, aligned to X-half and averaged to generate the mean input-output function for control and different drug conditions. The mean function of the drug condition was first normalised against one for its maximum value to compare the change in X-half. Then, the drug condition sigmoidal fit was further normalised against the control condition in regard to each maximum spike output value to directly illustrate the change in maximum output. A two-tailed Wilcoxon matched-pairs signed rank test was performed to compare X-half (half-height) of the control and drug conditions.

2.6.4 Light responses collected from ganglion cells

Quantification of light-evoked responses was made in a similar way to that of the aforementioned current injection analysis. Amplitude of membrane potential and total number of action potentials in response to light stimulation were measured (see **Figure2.11**).

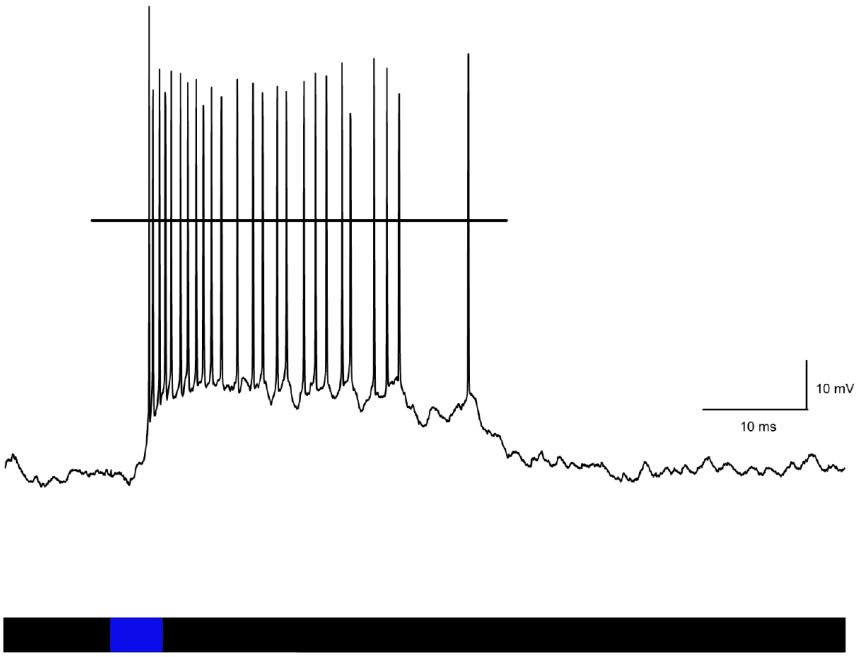

Figure 2.11 Sample trace of light response recorded from a typical ganglion cell. *Action potential firing in response to blue LED light stimulation (5ms) was quantified to obtain the total number of spikes and amplitude of the light evoked post synaptic potential (LE-PSP).*

For wide field constant luminosity and constant duration light stimulation (5ms duration) protocol (**Figure2.11**), direct statistical analysis was performed for the average of amplitude of light evoked post synaptic potential (LE-PSP) and total number of spikes.

For wide field constant luminosity with increase stimulus duration protocol (**Figure 2.12**), input-output sigmoidal functions were generated**.** Figure 2.13 demonstrates five sample RGC responses with its' corresponding light stimulation of various duration. Further, Figure 2.14 demonstrates a sample response of a single RGC to the increasing light duration. In a similar way to the statistical analysis for current injection protocols, sigmoidal parameters were used to reconstruct curves, which were then normalised and pooled. Statistical analysis was performed to compare X-half in order to compare RGC excitability.

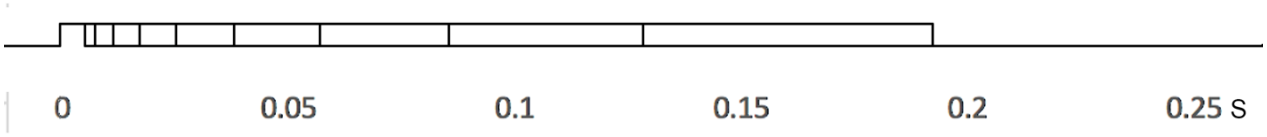

Figure 2.12 Duration of ten light stimulations of the same intensity. *Stimulation time is listed as following: 0.00525s, 0.00775s, 0.0115s, 0.01725s, 0.0255, 0.03825s, 0.05725s, 0.08575s, 0.1285s, 0.1925s.*

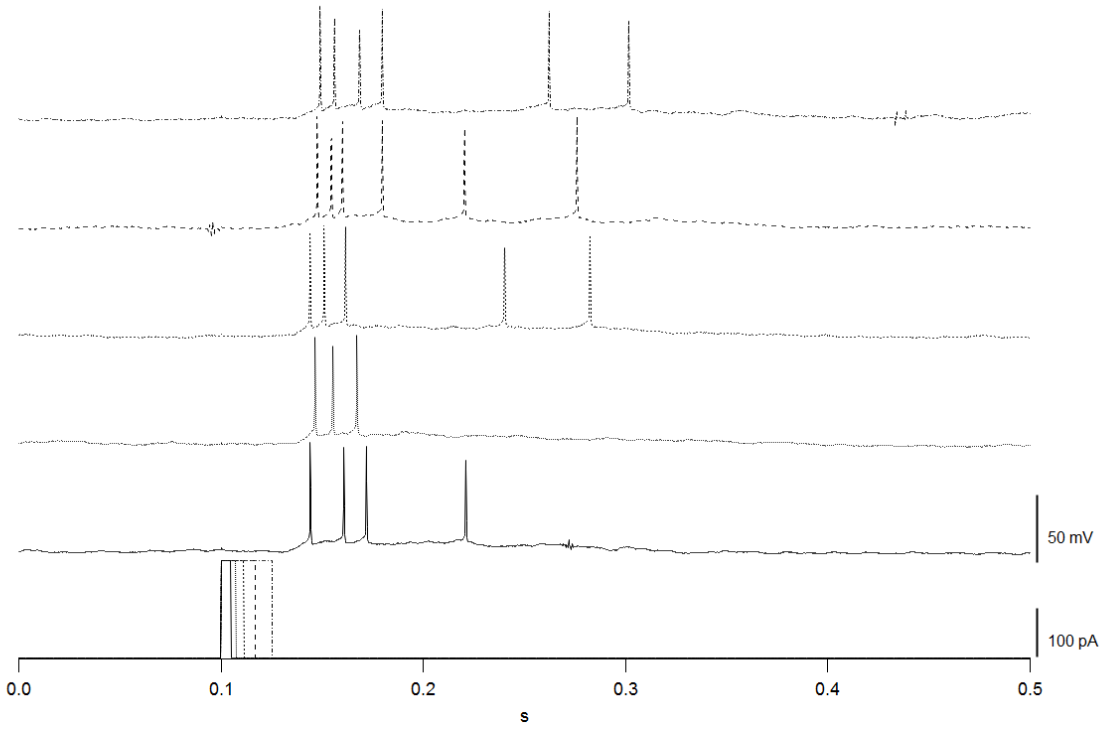

Figure 2.13 **Five s*ample traces of RGC response to same intensity different duration light stimulation.***

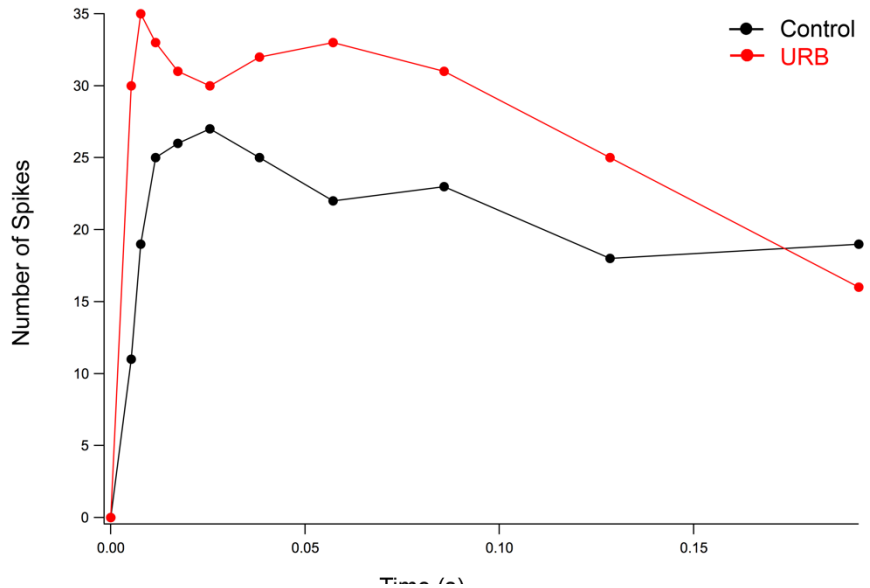

Figure 2.14 Sample relationship of the RGC response (number of action potential spikes) to increased light stimulation of the same intensity. *Spikes counts were generated using the same method described in* ***2.6.3****.*

1.6.5 Statistical analysis

Different statistical tests were used to analyse statistical significance between control and drug conditions. For paired data comparison, two-tailed Wilcoxon tests were used to analyse the change in X-half for input-output function, V-half, peak Na^+, peak K^+ currents and total number of Na^+ events were extracted from the I-V relationship. This statistical test was used due to the variability between each ganglion cell response and the non-normal distribution of data. As for presentation, Box-and-whisker plots were used, presenting median, first and third quartiles, along with the minimum and maximum data points. The Kolmogorov-Smirnov tests were used for comparison between sigmoidal fits (normalised to one) for input-output functions built from current clamp recordings. This test can detect overall differences including shift, slope, and shape of the input-output functions between control and drug conditions, rather than single point comparison of X-half values.

2.7 Morphological analysis to determine ganglion cell types

As previously mentioned, 1% fluorescent dye Lucifer Yellow was included in the intracellular solution. The dye fills up the cell, which allowed us to obtain information about the morphology

of the patched cell. Upon finishing electrophysiological recordings, the micropipette was carefully retracted from the cell minimising damage to the cell body. The retinal tissue was then fixed with 4% paraformaldehyde for 30 minutes, followed by three phosphate buffer saline (PBS) washes at ten minutes' intervals. Afterwards, the tissue goes through antibody staining as follows:

i. Five days of incubation of retinal tissue with anti-Lucifer yellow antibody (rabbit IgG, 1:10000, Invitrogen).
ii. On the fifth day, wash the tissue in PBS for at least eight hours.
iii. Sixteen hours' incubation of Alexa594 conjugated to goat anti-rabbit IgG (1:500, Invitrogen) followed.
iv. Mounting of the tissue with FluorSave medium (Merck Millipore) for confocal imaging.

After obtaining microscopic images using a Leica SPII confocal microscope, images were stitched using Image J. Classification parameters developed by (Sun et al., 2002) including soma size, dendritic field size of the ganglion cells to obtain quantitative data. These parameters were measured in ImageJ, and the current study classified RGCs into four subcategories: A, B, C, and D. A-type has a dendritic diameter of around 300µm and a radiant dendritic branching pattern. B-type has a dendritic diameter around 173µm and a dense dendritic branching pattern. C-type has an average dendritic field diameter of 241µm and less dense dendritic tree. D-type have thin curvy dendrites and an average of 150µm dendritic diameter. Cells that did not fit the above criteria were grouped as unclassified.

3. Results

3.2 The effects of capsaicin on retinal ganglion cell properties in wild type mice

To investigate the potential involvement of TRPV1 channels on RGC excitability, electrophysiological recordings were obtained in response to current injection and voltage clamp protocols before (control) and after perfusion with the TRPV1 channel agonist capsaicin (CAP). Input-output functions that describe cell excitability were constructed from current injection protocols by quantifying the number of spikes elicited in a RGC as a function of the magnitude of the change in membrane potential for each current step. To assess the voltage dependence of Na^+ currents, current-to-voltage (IV) relationship was analysed in response to the different cell holding potentials.

Physiological responses were recorded from different types of RGCs. From a total of 79 RGCs that were electrophysiological recorded, 25 cells were morphologically identified after visualisation and scanning under a confocal microscope. Ganglion cells were classified into four subgroups: A, B, C or D according to criteria published by Sun and co-workers (2002). Due to the relatively limited number of cells of each subgroup successfully patched and morphologically identified, we were not able to analyse the correlation between morphological classification and electrophysiological properties. Furthermore, we are only confident about three main morphological type classifications: A, B, and C as we rarely patched D cells although cells were chosen randomly. **Figure 3.1** shows representatives of the three main RGC subtypes. **Figure 3.1A** is an A-type RGC with a soma diameter of 16.7 µm. It has four primary dendrites displaying relatively even pattern covering a large dendritic field. **Figure 3.1B** illustrates a B type RGC with a soma diameter of 15.2 µm, with a small dendritic tree localised distinctively unilaterally**. Figure 3.1C** represents a C-type RGC, with 12.6 µm soma diameter and a medium sized dendritic field. This particular cell has a comet-like aspect which is characteristic of the C6 subtype of C cells.

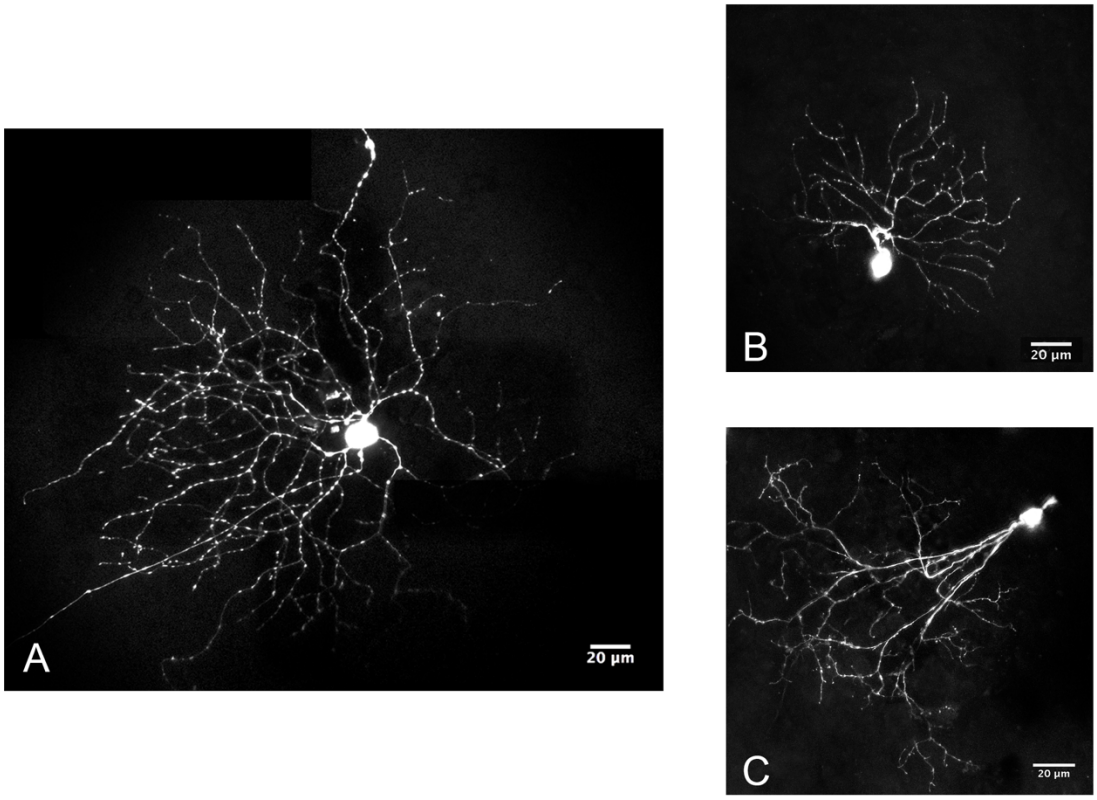

Figure 3.1. Photomicrographs showing example cells of each of the three main ganglion cell morphological types. *(A) An A-type RGC with a large dendritic field. (B) A B-type RGC with thin, curvy dendrites and a small dendritic field. (C) A C-type RGC with dendrites extending in one direction and of a large dendritic field.*

3.2.1 Input-output relationship in response to current injection

In order to examine the impact of capsaicin on the excitability of ganglion cells, the current injection protocol was used. The mean input-output function was constructed using RGC spike output and EPSP. The figures below display representative recordings and stimuli and demonstrate the construction process of the input-output curves.

Figure 3.2 shows representative recordings of the response of a RGC to injection of a current step before and after bath application of the TRPV1 channel agonist capsaicin (10 µM). A concentration of 10 µM was chosen because preliminary studies performed by Yong (2016), Leung (2016) showed it was effective in modifying the excitability properties of RGCs. The strength of the responses to current injection was increased upon bath application of capsaicin. In

the control condition, the total number of spikes was 10 compared to 16 spikes during drug condition - an increase of 60%.

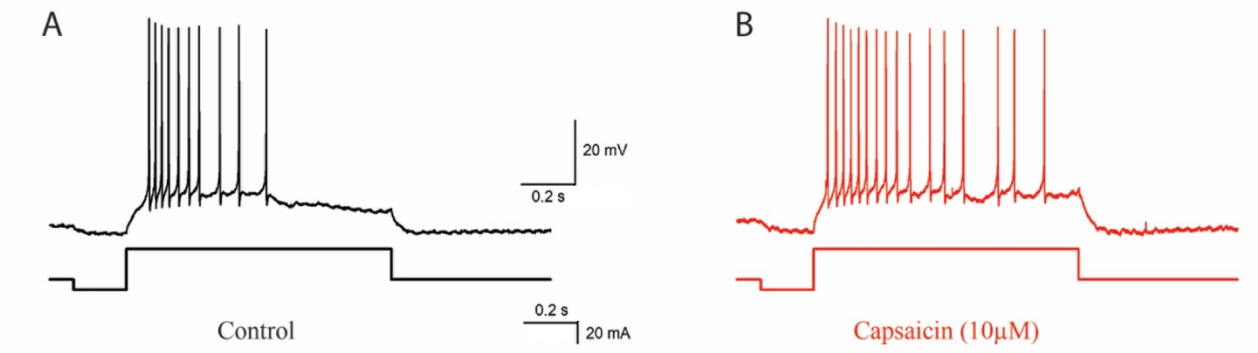

Figure 3.2 Representative spike output in response to the same level of membrane depolarisation under control and capsaicin conditions from a single RGC. *It is clear that application of 10 µM capsaicin (red trace on the right) increased the number of spikes.*

Current injection protocols were applied to RGC in control and capsaicin conditions to generate input-output functions. RGCs were first recorded under control conditions with 12 steps of currents injected into the RGC while holding membrane potential at -60mV. The total number of spikes was counted in both control and capsaicin conditions as illustrated in **Figure 3.2**. The total number of spikes (y-axis) was then plotted against the change in membrane potential (ΔVm on x-axis), and fitted with sigmoidal curves. Thus, these curves represent the cell's input-output function as shown in **Figure 3.3**.

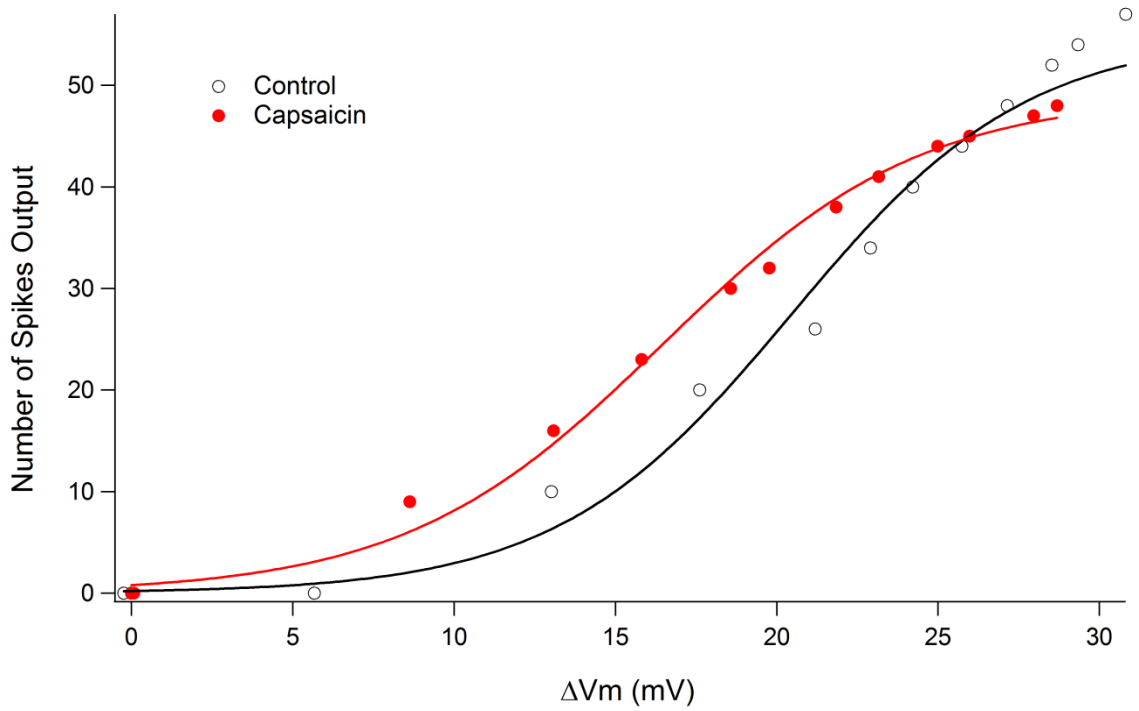

Figure 3.3 Representative input-output relationships in response to current injection from a single RGC under control and capsaicin conditions. *The total number of spikes is shown on the y-axis, it is plotted against the change in membrane potential (ΔVm) on x-axis and are shown as dots. Solid lines represent fitted sigmoidal curves under control condition (black) and under capsaicin condition (red). A leftward shift of the sigmoidal curve in capsaicin condition reflects an increase in spike output at similar level of ΔVm.*

Subsequently, by using parameters obtained from each sigmoidal fits, two normalised input-output functions were generated using custom-written routines in IGOR Pro 6.0 (Wavemetrics) for all cells recorded in both control and capsaicin conditions. Control input-output functions were pooled, aligned to their X-half and averaged as shown in **Figure 3.4A**. Note that similar procedures were carried out with input-output functions generated for capsaicin treatment. In **Figure 3.4A**, input-output function of capsaicin condition was normalised against the maximum output in control condition, to compare the maximum spike output in the presence of capsaicin against control conditions.

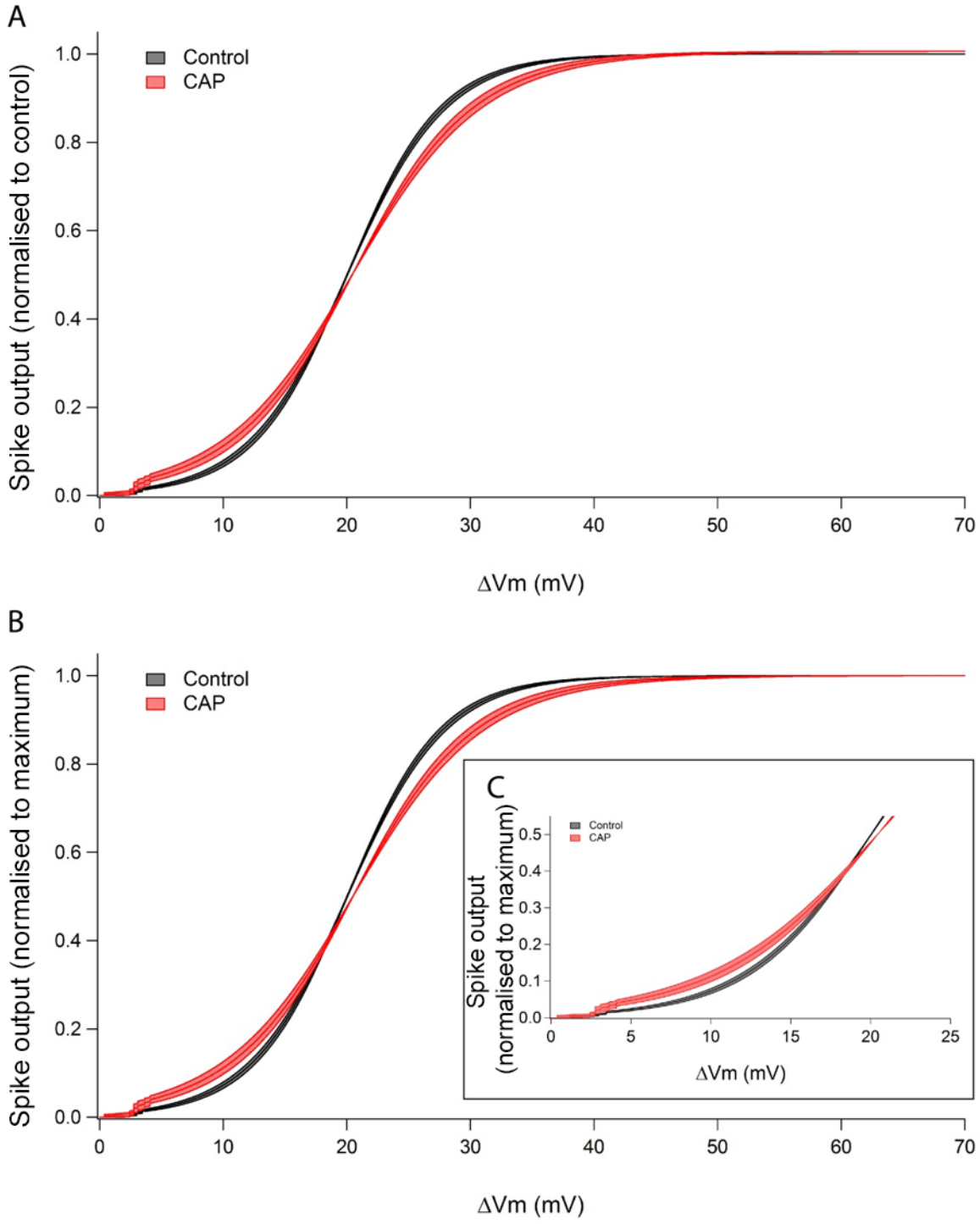

Figure 3.4. Current injection responses in control and capsaicin conditions (n = 7). *(A) Input-output relationship in response to current injection in control and capsaicin condition, normalised to control. Spike output on the y-axis is plotted against ΔVm, which represents the difference between resting membrane potential and depolarisation potential. A slight right shift from control to capsaicin condition in the mean fitted curve is shown. (B) Input-output relationship in response to current injection in control and capsaicin condition, normalised to 1. Kolmogorov-Smirnov test showed a statistically significant overall difference in the input-output relationship between the two groups ($p < 0.0001$). (C) A magnified section of input-output function from (B) for 0 to 25mV of ΔVm. An increase in output for the same ΔVm can be clearly demonstrated in this magnified insert.*

After the addition of capsaicin (10μM) to the bath, the mean input-output relationship of seven RGC exhibited no apparent change in maximum spike output. However, as shown above in **Figure 3.4A**, at lower input levels (below 15 mV) RGCs recorded in the presence of capsaicin had a higher level of spike output. This can be clearly seen when both mean input-output curves were normalised to 1 in **Figure 3.4B** and **Figure 3.4C**. In particular, when the early rising phase of the curve is magnified in **Figure 3.4C**, a stronger spike output for the same amount of change in membrane potential can be observed upon application of capsaicin.

Figure 3.4B shows that there is no change in X-half values. Under control condition, derived X-half value was at 17.5 ± 0.29 mV and in the presence of capsaicin it was 18.0 ± 0.49 mV, these values were found to be not statistically significant (Wilcoxon test, n=7, $p > 0.1$; see **Figure 3.5)**. Figure 3.5 illustrates X-half for the control and capsaicin conditions using box-and-whisker plot. The advantage of using box plot is median, first and third quartiles, the minimum and the maximum data points are all represented on each plot providing more information. In conclusion, Capsaicin produced an increase in output for the same ΔVm from 0 to 25mV, but no change in X-half could be seen.

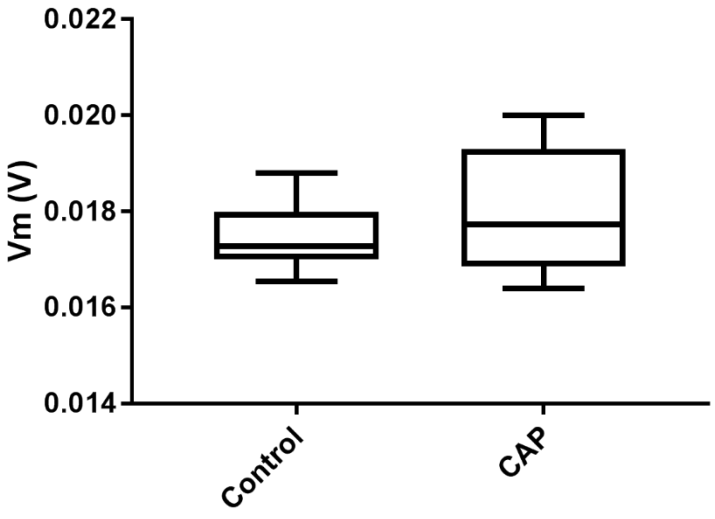

Figure 3.5. Capsaicin produced no change in the mean X-half (n=7, p > 0.05) for a population of seven ganglion cells. *No statistical significant change is see (Wilcoxon test: p > 0.1).*

3.2.2 Effects of capsaicin on the current-to-voltage relationships in RGCs

Current-voltage (IV) relationships for Na^+ and K^+ currents were recorded in control condition and after bath application of capsaicin (**Figure 3.6)**. In the representative **Figure 3.6**, after bath application of capsaicin, Na^+ current had fewer inward currents spikes, and their maximum amplitude was smaller. IV curves allowed us to assess the potential involvement of TRPV1 channels in modulating the excitability properties of ganglion cells. RGCs were held at 12 different voltages from -75mV to +35mV with +10mV per incremental step. Peak inward Na^+ and K^+ currents in response to each holding membrane potential were quantified and plotted against holding potential of each step as shown in **Figure 3.7**.

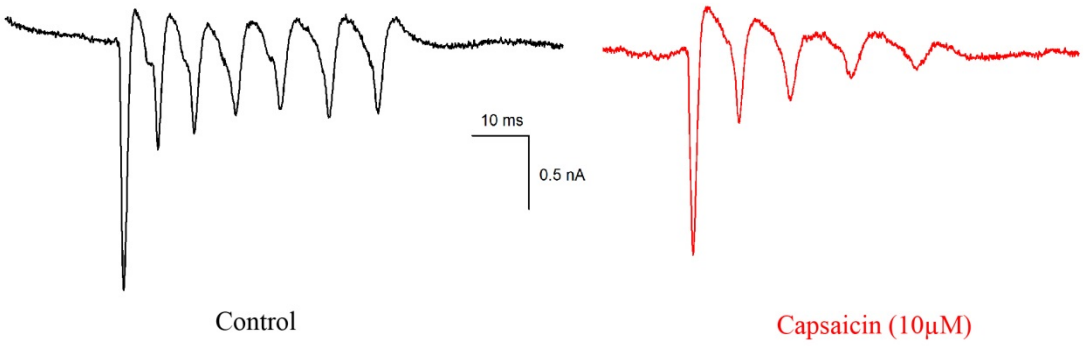

Figure 3.6 Representative single voltage clamp recording trace of Na^+ and K^+ currents for a single RGC under control and capsaicin conditions. *For this cell, there was a small reduction in peak Na^+ current and reduced inward Na^+ events. No obvious change in K^+ currents could be seen.*

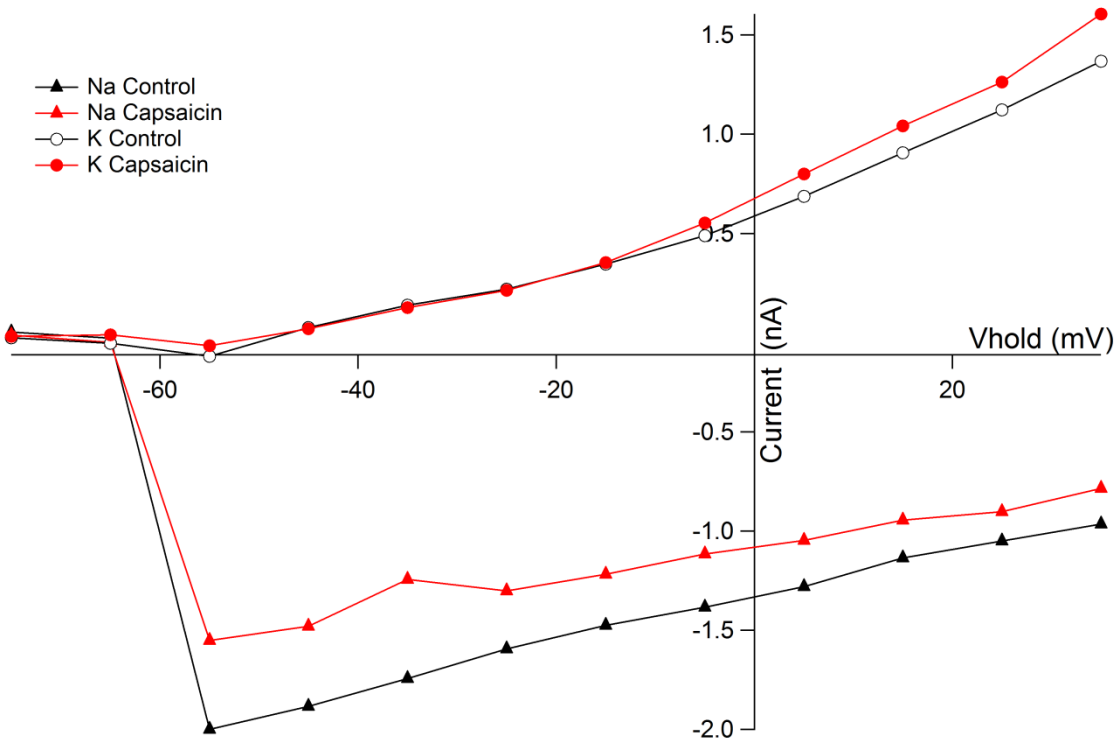

Figure 3.7 Representative current-to-voltage (IV) relationship obtained from a ganglion cell in control (black) and capsaicin (red) conditions. *Na^+ (triangle) and K^+ (circle) currents were plotted against various holding membrane potentials to build an IV relationship. For this ganglion cell, there was a reduction in peak inward Na^+ current, as well as a small increase of the peak outward K^+ current.*

To generate a normalised IV relationship, Na^+ and K^+ currents of each cell were divided by their peak Na^+ and K^+ currents respectively. Then, an average of the individually normalised currents was taken across the 12 recorded RGCs to produce the final normalised IV relationship as shown in **Figure 3.8**. Four properties of IV relationship in ganglion cells were examined. They were: 1) the total number of inward currents carried by Na^+ (Na^+ events), 2) the peak amplitude of Na^+ current, 3) the membrane potential at which 50% of the peak Na^+ current was reached (V-half), and 4) the peak amplitude of the outward K^+ current.

Under control condition, Na^+ currents were activated at a holding potential around -55mV, and reached a maximum mean value of -2.07 ± 0.28 nA (n=11) at -50mV (**Figure 3.8**). After bath application of capsaicin (10µM) for 5 minutes, the magnitude of the Na^+ current observed at -55mV increased, producing a steeper slope which shifted the V-half to the left, as shown in **Figure 3.9A**. The Na^+ current reached a peak current of -1.71 ± 0.174 nA (n=11) also at -50mV

but it was significantly reduced ($p < 0.05$) in size compared to the control condition as seen in **Figure 3.9B**. No significant difference was found in the total number of Na^+ events as illustrated in **Figure 3.9C** and in peak K^+ current in **Figure 3.9D**.

The finding of Na^+ potential indicates capsaicin allows RGCs to be activated at more hyperpolarised potentials, though producing a smaller amplitude. And capsaicin produced no change in K^+ channel.

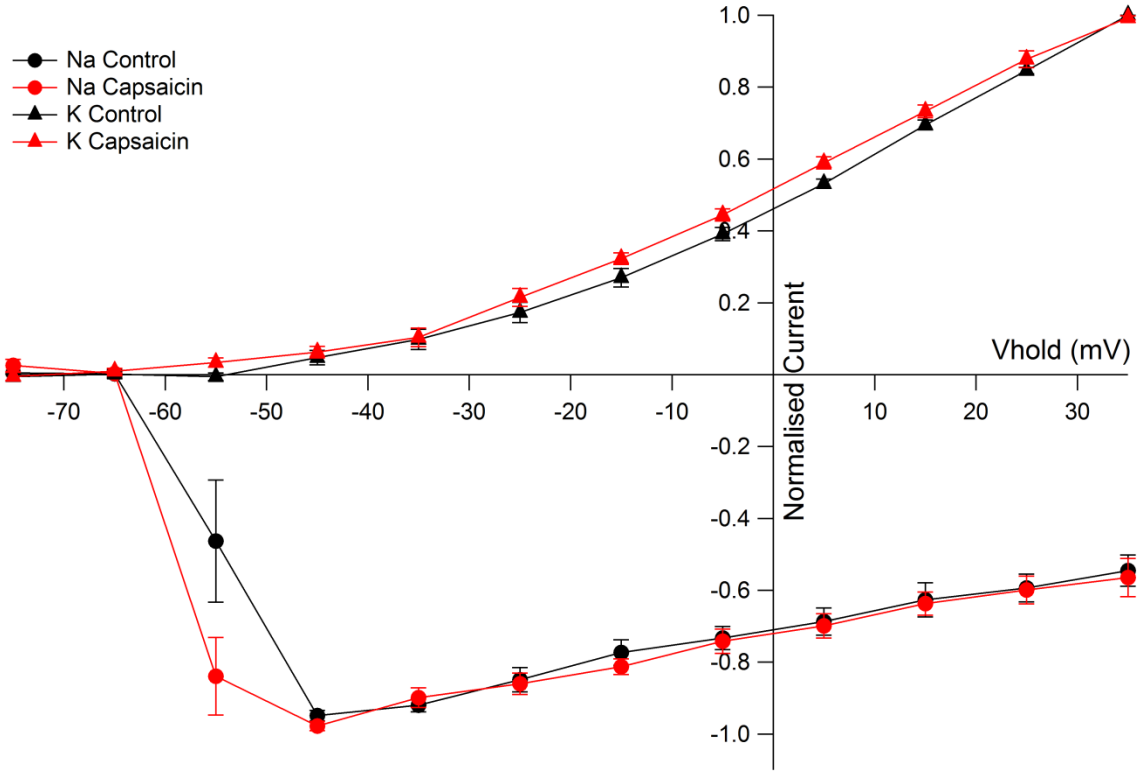

Figure 3.8 IV responses of RGCs in control (black) and capsaicin (red) conditions (n = 12). *IV relationship shows a larger Na^+ (dot) current at a lower holding membrane potential under capsaicin condition. Amplitude of Na^+ and K^+ (triangle) current entry was plotted against membrane potential of RGCs to produce IV curves. Average IV curves (± SEM) normalised to peak Na^+ and K^+ are shown.*

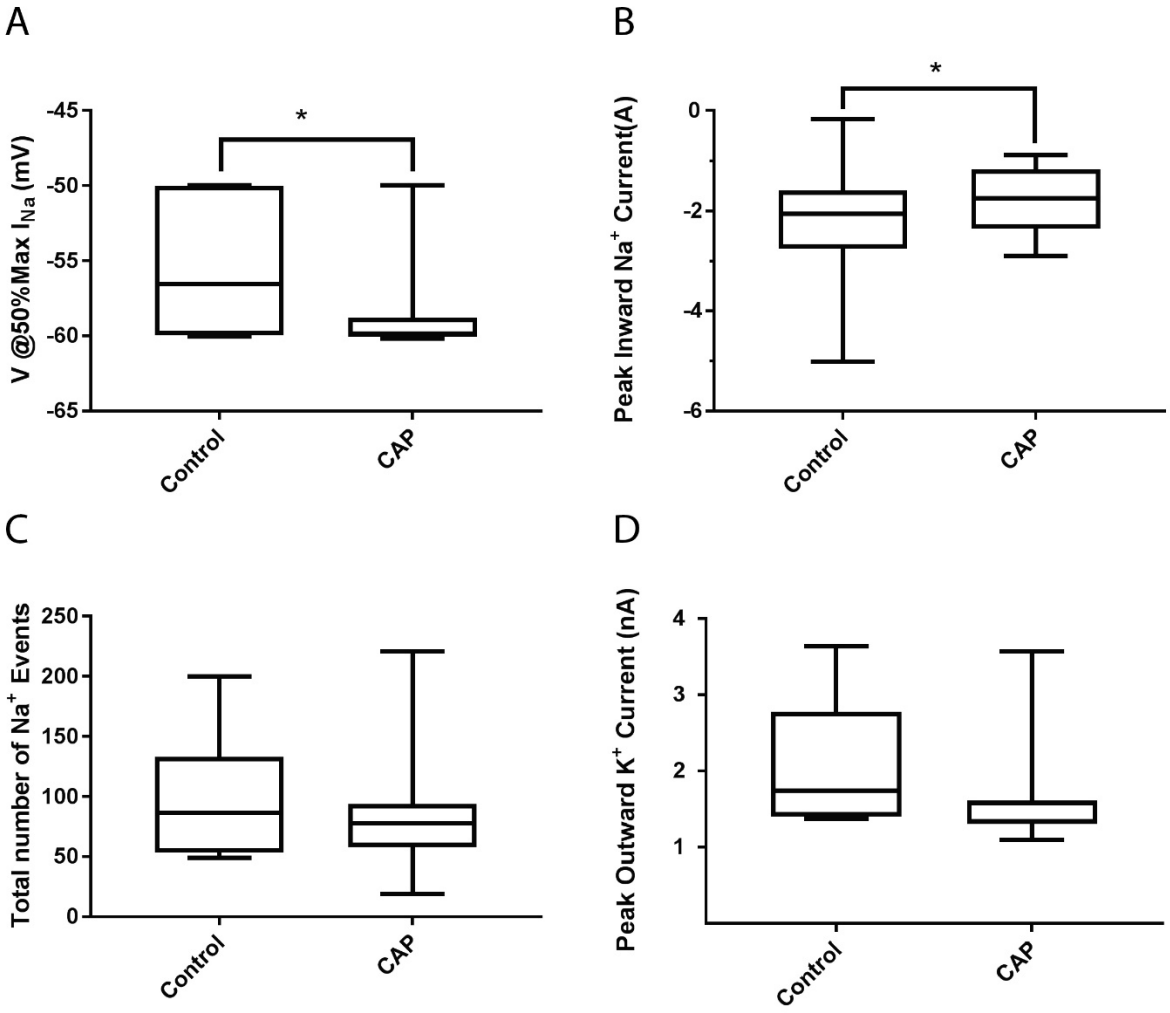

Figure 3.9 Application of the TRPV1 channel agonist capsaicin changes excitability of ganglion cells. *(A) A significant reduction in V-half was observed with application of capsaicin ($p < 0.05$). (B) A significant decrease in peak Na+ amplitude was observed under capsaicin condition ($p < 0.05$). (C) Little change in the total number of Na+ events were observed with capsaicin ($p > 0.05$). (D) No significant change can be seen in peak K+ current between control and drug conditions ($p > 0.05$).*

3.3 The effects of capsazepine on retinal ganglion cell excitability properties in wild type mice

To further investigate the involvement of TRPV1 channels, the antagonist capsazepine was used to compare RGC excitability properties with the control condition. A concentration of 10 μM was chosen based on values used in the literature. Therefore, one would predict after application of capsazepine, the responses of the cell would be similar to those obtained from the control condition. Previous experiments from the Vision lab (Middleton and Protti, 2012; Yates, 2014) showed that eCB are constitutively released in the retina. Based on eCB binding to TRPV1

channels and producing an increase in excitability in RGC, TRPV1 antagonist capsazepine was hypothesised to reduce RGC excitability.

Similar to the experimental design used to study the effects of capsaicin, input-output functions and current-to-voltage relationship were extracted and analysed. However, some modifications were made to the stimulation protocols. For current injection protocols, the duration of the current steps was shortened from 0.5s to 0.1s, and smaller intervals of 5pA rather than 10pA between steps were used to obtain a better estimate of V-half value. A total of 24 current steps were injected to examine spike output of RGCs. This modification enabled recordings to be made in order to detect smaller changes in membrane potential and to avoid plateau of spike output and over stimulation of the cell. The current-to-voltage protocol was also modified to deliver smaller holding potential intervals to produce a better resolution at peak Na^+ current.

1.3.1 Input-output relationship of ganglion cells

To examine the effect of capsazepine on RGC excitability, current injection protocol was used to record RGC's spike output and EPSP for both control and capsazepine conditions.

The input-output function of ganglion cells after application of capsazepine, produced with the modified protocol, had a significantly smaller number of spikes due to shorter duration of stimulation in comparison with the capsaicin results from previous section. In general, no change was found in the parameters characteristic of the input-output relationship. Wilcoxon test shows no difference in maximum spike output ($p > 0.05$, $n = 14$) despite **Figure 3.10A** visually shows a small reduction in the maximum spike output. As for the X-half, **Figure 3.10B** shows no change, which is confirmed by Wilcoxon test in **Figure 3.11** ($p > 0.05$, $n = 14$).

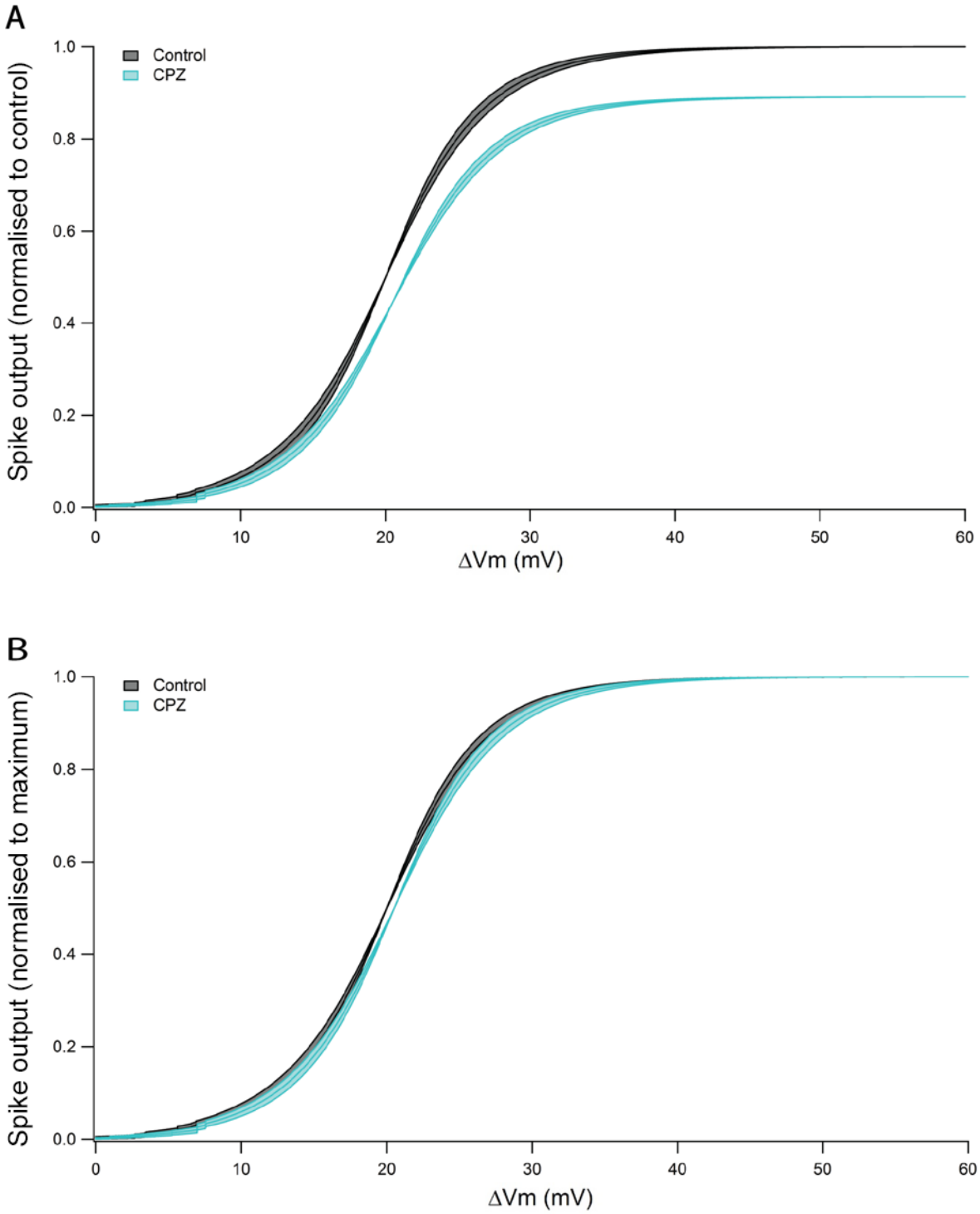

Figure 3.10. Current injection responses of ganglion cells in control (black) and capsazepine (blue) conditions (n = 14). *(**A**) Input-output relationship of ganglion cells in response to current injection in control and capsazepine conditions. Curves were normalised to control condition. Spike output on the y-axis is plotted against ΔVm, which represents the difference between resting membrane potential and depolarisation potential. Capsazepine application produced an obvious right shift in the mean fitted curve from control. (**B**) Input-output relationship of ganglion cells in response to current injection in control and capsazepine conditions. Both curves were normalised to 1 and no obvious change was observed. Kolmogorov-Smirnov test showed a statistically significant overall difference in the input-output relationship between the two curves ($p < 0.0001$).*

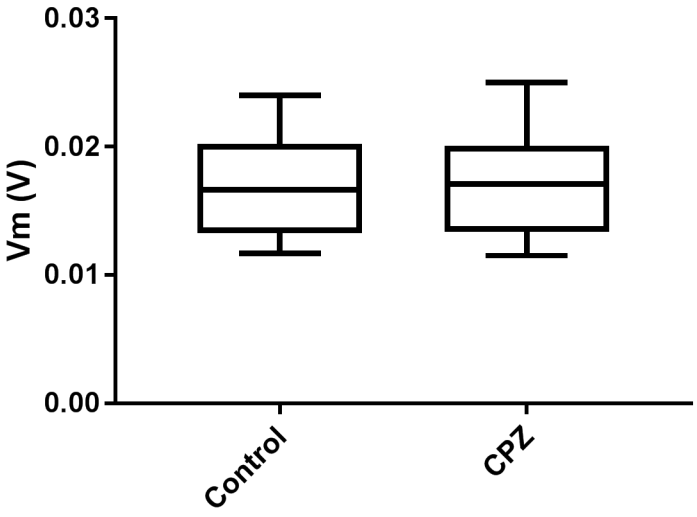

Figure 3.11 Capsazepine produced a non-significant (p > 0.05) increase in X-half of ganglion cells. *Control condition had a X-half value of 16.7 ± 1.0μV, and is very similar to the capsazepine condition which had a X-half value of 17.2 ± 1.1μV.*

3.3.2 Current-to-voltage relationship of ganglion cells

Whole cell voltage clamp was then used to examine the effect of capsazepine on Na^+ and K^+ ion channels, which reflects the excitability of the RGCs. As previously mentioned, the IV protocol used to test the effects of capsazepine on ganglion cell excitability was modified to 18 steps of holding membrane potential. Each step was increased by +5mV starting from -75mV to -5mV, and +10mV per increment step starting from -5mV to +35mV. The purpose of this protocol modification was to produce a better resolution for the IV relationship, especially around the activation and peak of the inward Na^+ current.

Figure 3.12 shows the normalised mean current-to-voltage response for control and capsazepine conditions. Addition of capsazepine caused a significant change in peak Na^+ at -45mV from -2.3±0.1nA in control condition to -1.8±0.6nA (n=12) (**Figure 3.13B)**. However, this change did not lead to a significant change in V-half as shown in **Figures 3.12** and **3.13A.** Also, there was no change in peak K^+ current (**Figure 3.13D**). Though, **Figure 3.13C** shows that the total number of inward Na^+ currents was significantly reduced by capsazepine.

To sum up, the reduction in the total number of Na^+ events and peak Na^+ current suggests a decrease of cell excitability was produced by capsazepine.

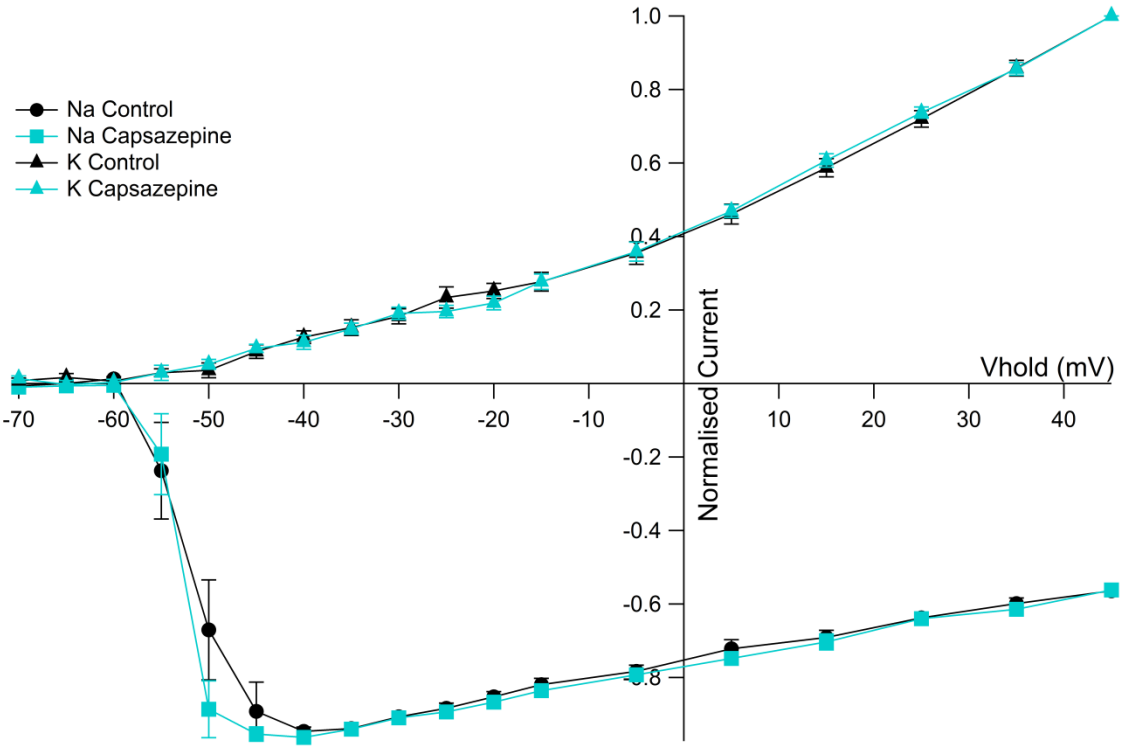

Figure 3.12 IV response of RGC in control and capsazepine conditions (n = 14). *IV relationship shows a larger Na^+ current at a lower holding membrane potential under the influence of capsazepine. Amplitude of Na^+ current entry was plotted against membrane potential of RGCs to produce IV curves. Average IV curves (± SEM) were normalised to the peak Na^+.*

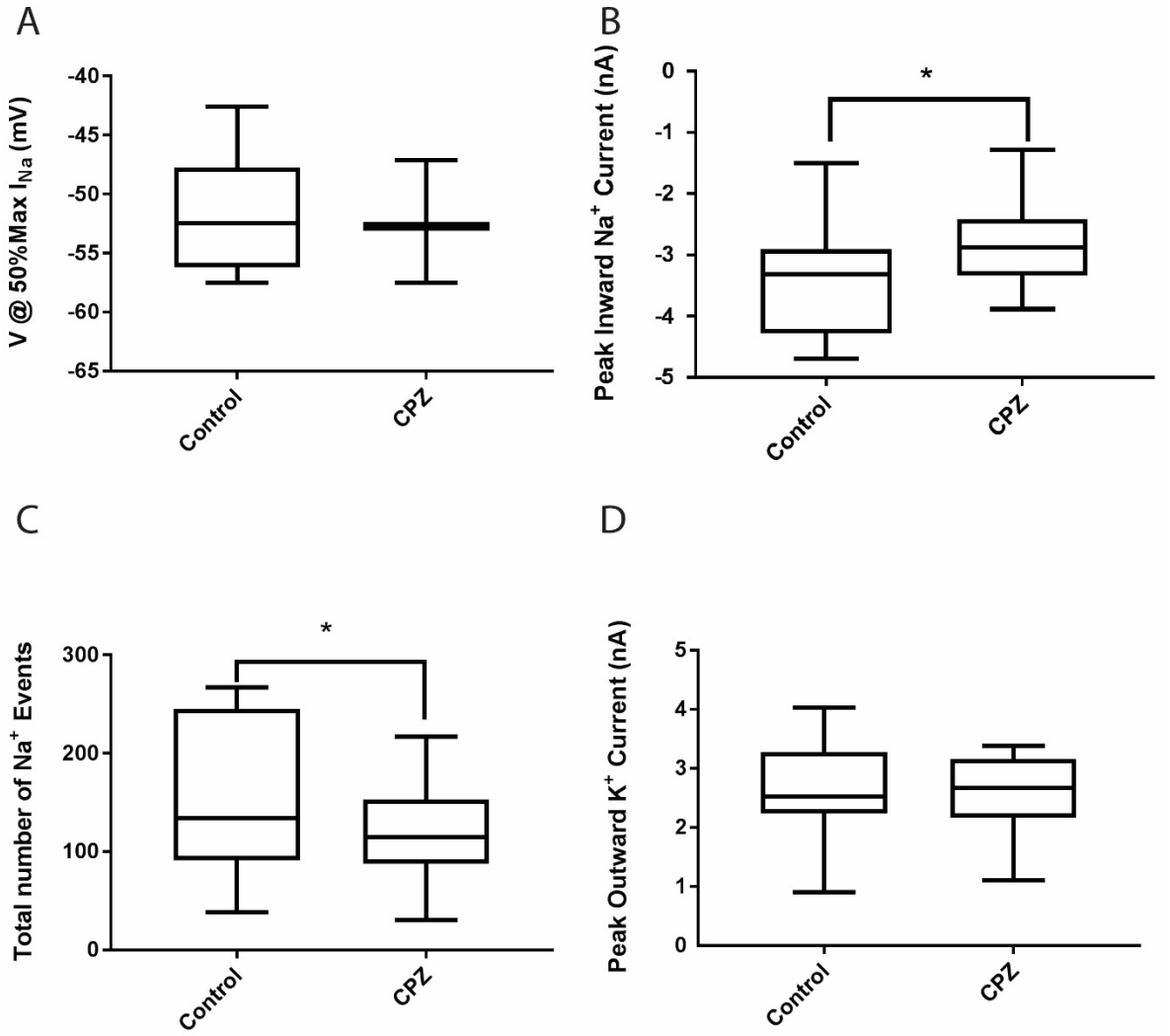

Figure 3.13 Application of the TRPV1 channel antagonist capsazepine changes RGC excitability. Population data are shown. *(A) A significant ($p < 0.05$) reduction in the total number of Na^+ events were observed with capsazepine. (B) The peak Na^+ amplitude was significantly ($p < 0.05$) less negative in capsazepine condition. (C) Capsazepine caused no significant ($p > 0.05$) change in V-half. (D) A non-significant ($p > 0.05$) reduction in K^+ current is produced by bath application of capsazepine.*

3.4 The effects of URB597 and URB597+Capsazepine on ganglion cell excitability properties in TRPV1-/- mice

In order to further test whether or not the observed effects of capsaicin and capsazepine were due to a specific effect on TRPV1 channels, recordings were obtained from RGCs of TRPV1-/- mice. A total of 48 RGCs from TRPV1-/- animals were successfully patched, of which 20 cells underwent pharmacological treatment with the FAAH inhibitor URB597, which increases the endocannabinoid concentration by blocking the degrading enzyme of anandamide. Although all cells were attempted with capsazepine application, only 13 were successfully recorded, had good cell access and remained healthy after co-application of URB597 and capsazepine. Due to the above stringent criteria, as a result, data presented in this section of the thesis is limited. Current injection and current-to-voltage protocols were similar to those employed in **Section 3.3**.

In addition to the current-injection and voltage-clamp protocols, light stimulation was also carried out with a full field flash with a blue LED to investigate the effects of drugs on the physiological responses of RGCs. A total of ten RGCs displayed responses to light stimulation. In these experiments, two different light stimulation protocols were used to record light-evoked responses in current clamp mode. In one of these protocols, its luminosity was kept constant whilst stimulus duration was varied (10 different durations). In the other light-stimulation protocol, five repeats of a stimulus of constant luminosity and time duration were delivered to determine an average value. Thus, comparisons could be made between control and treatment conditions. Spike count and the amplitude of light-evoked postsynaptic potentials were quantified to produce input-output functions.

3.4.1 Input-output relationship in response to current injection

Figure 3.14 illustrates the input-output curve of ganglion cells in the control condition produced by current injection protocol, for URB597 (1μM) and co-application of URB597 (1μM) with capsazepine (10μM) conditions. Comparison between the three groups was made separately

because the total number of cells obtained in URB597 and capsazepine conditions was different due to the difficulties of keeping the cell healthy for the full pharmacological protocol to allow co-application with capsazepine. In **Figure 3.14A** and **3.14C**, spike output obtained from drug conditions were normalised to their previous condition to compare maximum spike output. On the other hand, in **Figure 3.14B** and **3.14D**, responses collected during drug conditions were normalised to their maximum spike output in order to compare any changes in X-half values.

In **Figure 3.14A**, the input-output function that after application of URB597 (1μM) shows a reduction in the maximum spike output compared to the control condition. **Figure 3.16A** shows plots comparing the maximum number of spikes between the two conditions, statistical comparison indicates that URB597 produced a significant drop from 13.0 ± 0.8 spikes to 11.7 ± 0.9 spikes is shown (n=18), denoting decreased cell responsiveness. When mean input-output function of URB597 condition was normalised to maximum spike output of control condition in **Figure 3.14B**, the X-half of the mean input-output curve of both control and URB597 conditions were displayed around 20mV. Thus, bath addition of URB597 (1μM) to the retina led to no change in X-half, which was confirmed to be statistically insignificant by the Wilcoxon test (n=18) shown in **Figure 3.15B**.

After administering capsazepine (10μM) to the bathing medium, a total of five minutes of waiting time was allowed before recording resumed. Under co-application of URB and capsazepine, a further reduction of 40% of normalised spike output can be observed in **Figure 3.14C.** By examining the maximum spike output of both conditions, a significant change from 12.2 (± 1.1) to 9.0 (± 0.8) spikes were observed (**Figure 3.16B, n=11)**. **Figure 3.14D** demonstrates no change in the average input-output curve. Wilcoxon test in **Figure 3.15B** confirms the observation in **Figure 3.14D**, showing no change in the X-half value between URB597 and co-application of URB597 and capsazepine conditions. Previous results from the Vision lab in wild-type mice had

shown that the left shift induced by URB597 could be reversed by co-application of URB597 and capsazepine, indicating the involvement of TRPV1 channels. This effect was absent in the current study with TRPV1-/- mice, suggesting that in the absence of TRPV1 channels, capsazepine was not effective in reversing the effects of URB597. Moreover, Kolmogorov-Smirnov test indicates the difference in the general shape of the input-output functions. Kolmogorov-Smirnov test was performed comparing the curves in **Figure 3.14 B** and **D**, when the input-output functions were normalised to the maximum. Although no significant change was found in X-half, Kolmogorov-Smirnov test showed differences between the control, URB597 and co-application of URB597 and capsazepine conditions.

In conclusion, in the TRPV1-/- mice, capsaicin produced a decrease in RGC responsiveness. Co-application of URB and capsazepine could not reverse this effect, and further reduce the output of RGC. Moreover, there is no change in x-half for both capsaicin and co-application of URB and capsazepine.

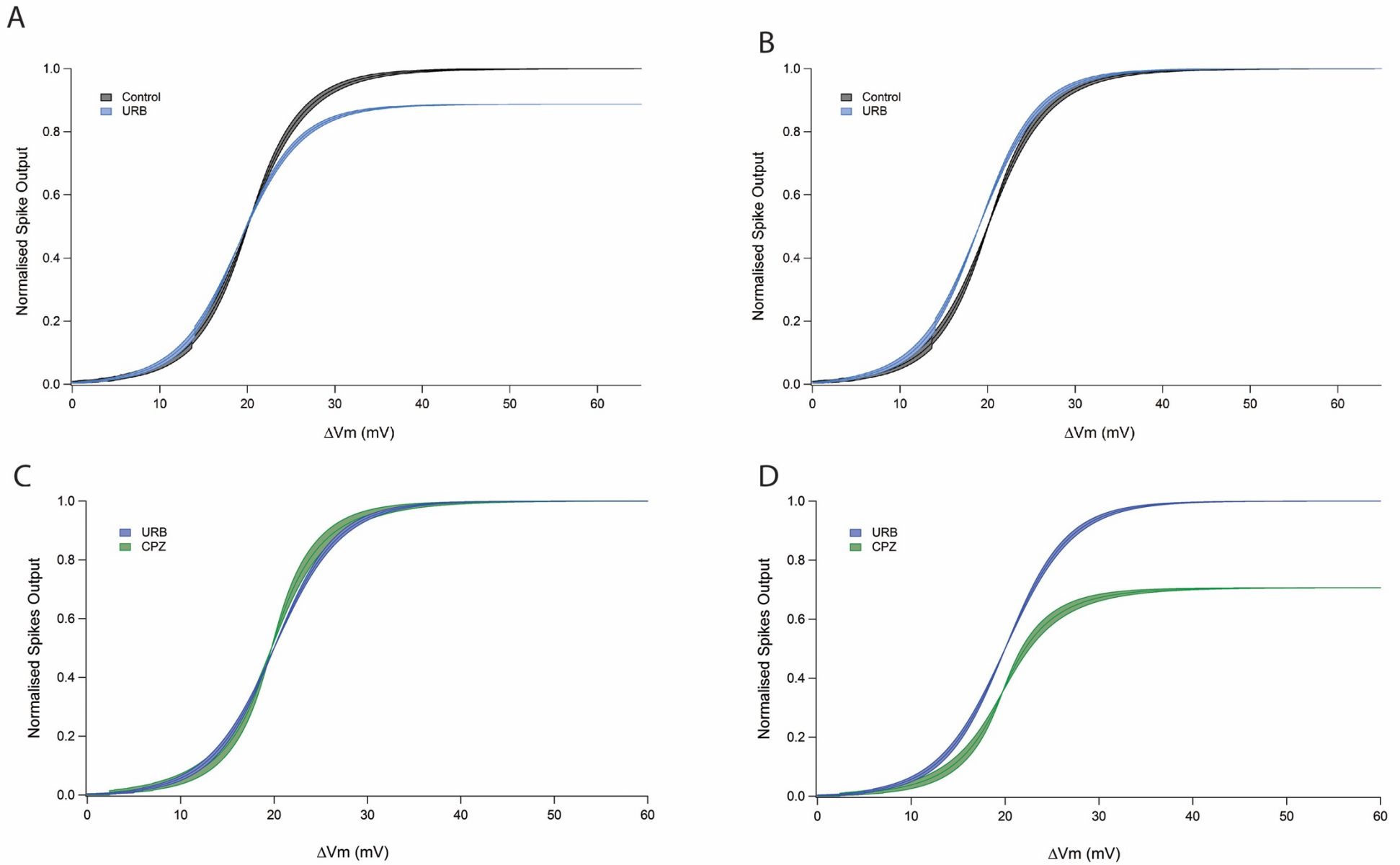

Figure 3.14 *Current injection responses of ganglion cells in control, URB597 and URB597+Capsazepine (URB+CPZ) conditions (n = 10, n = 5 respectively). (A) Input-output relationship in response to current injection in control, and URB condition was normalised to its control values. Spike output on the y-axis is plotted against ΔVm, which represents the difference between resting membrane potential and depolarisation potential. A reduction in RGC output can be observed upon application of URB597. (B) Input-output relationship in response to current injection in control and URB conditions, normalised to maximum spike output. A left shift of URB in input-output function is demonstrated. Kolmogorov-Smirnov test showed a statistically significant overall difference in the input-output relationship between the two curves ($p < 0.0001$). (C) Input-output relationship in response to current injection in URB and URB+CPZ conditions, normalised to control condition. A large decrease in RGC output can be observed by co-application of URB and CPZ. (D) Input-output relationship in response to current Injection in URB and URB+CPZ conditions, normalised to maximum spike output. Although there was no obvious shift can be seen, however, Kolmogorov-Smirnov test showed a statistically significant overall difference in the input-output relationship between the two conditions ($p < 0.0001$).*

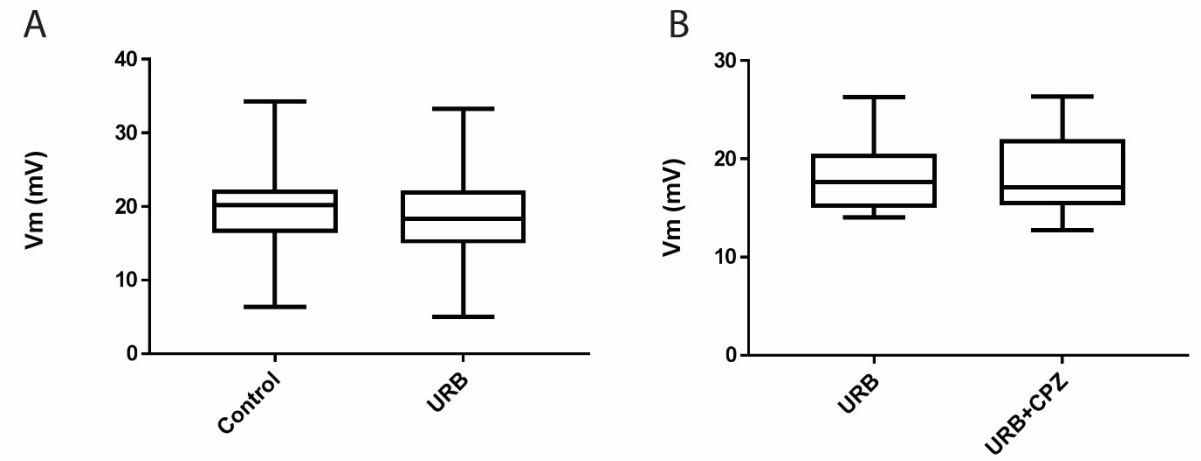

***Figure 3.15*. X-half comparison between control, URB597 and capsazepine conditions.** *Both URB and capsazepine produced little change in X-half values ($p > 0.05$).*

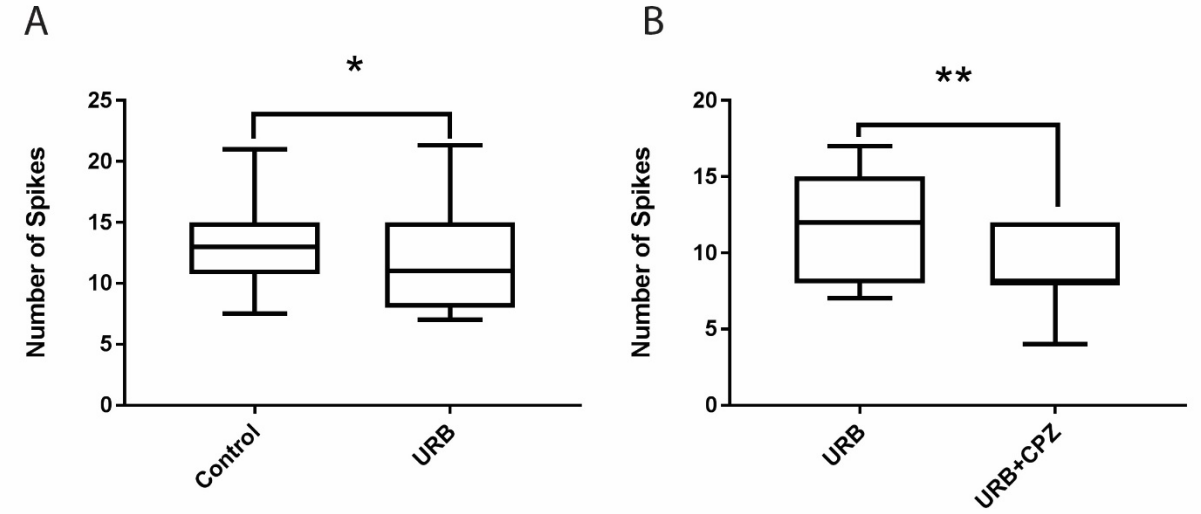

Figure 3.16 Maximum spike output in control, URB597 and co-application of URB597 and capsazepine conditions (n=18, n=11 respectively). *A significant drop in the average number of spikes from 13.0 (± 0.8) to 11.7 (±0.9) from control to URB condition could be observed ($p < 0.05$). When comparing between URB and URB+CPZ, the mean change decreased from 12.2 (± 1.1) to 9 (± 0.8) spikes ($p < 0.001$).*

3.4.2 Input-output relationship of ganglion cells in response to light stimulation

In order to test the effects of URB597 and Capsazepine on the synapses where RGCs receive their inputs and where the eCB system is mostly localised to, light responses were recorded under current clamp mode. A full-field flash of constant light intensity with increments in time duration from 5.25 ms to 192.5ms was used to stimulate the RGCs. Input-output functions were constructed in the similar fashion of those in current injection protocols, with normalised spike output (y-axis) against light-evoked postsynaptic potential (x-axis). When this stimulation protocol was applied, as opposed to the current injection protocols, the first one or two sweeps of light stimulation did not elicit any spike output in some RGCs. This lack of responsiveness in the first few sweeps was reflected in the input-output function as the curve started increasing in y-value (normalised spike output) at around 10mV LE-PSP, rather than from the origin (0mV). After addition of URB597 (1μM), the mean input-output function drawn from RGCs responses to URB597 displayed no change in X-half as shown in **Figures 3.17B** and **3.18A**. Also, no change was found in the maximum spike output when tested by Wilcoxon test shown in **Figure 3.19A**. After 5 minutes of co-application of URB597 and capsazepine, the curve appeared to have shifted to the left (**Figure 3.17D)**. Despite the visually apparent shift, X-half values did not show any statistical difference between the tested conditions (**Figure 3.18B)**. **Figure 3.19B** shows plots of the maximum spike output across different drug conditions. As shown in this figure, co-application of URB597 and capsazepine led to a significant reduction in spike output, which decreased from 22.1 (± 4.5) to 16.3 (± 4.1) spikes ($p < 0.001$, Wilcoxon test).

To sum up, application of URB produced no change in the light response of TRPV1-/- mice, while co-application of URB and capsazepine reduced the number of spikes of RGC in response to light.

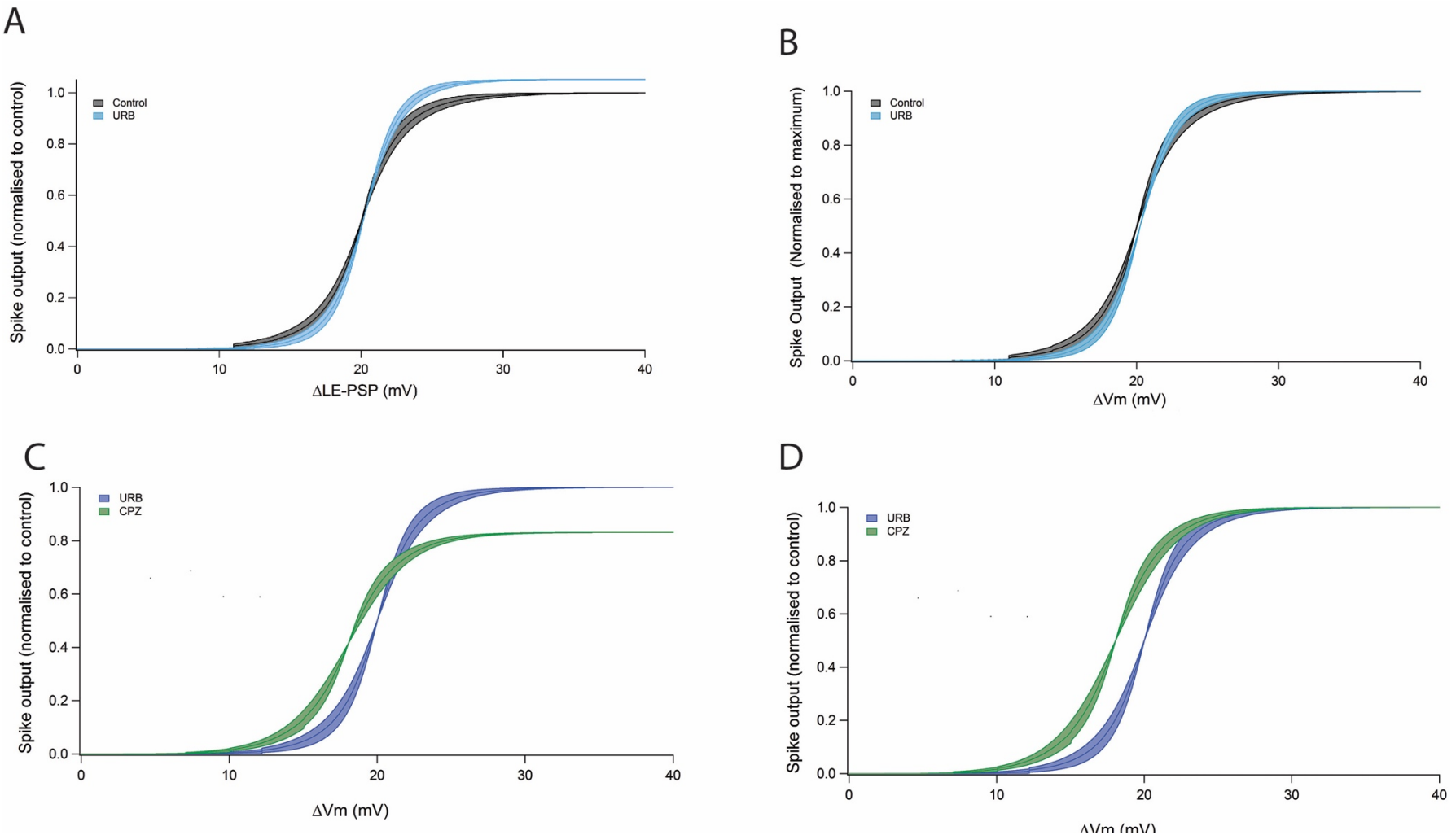

Figure 3.17 Light responses of ganglion cells in control and URB and URB+Capsazepine (URB+CPZ) conditions (n=10, n=5). (A) Input-output relationship in response to constant intensity, increasing time duration light stimulation in control, and URB conditions, normalised to control conditions. *Spike output on the y-axis is plotted against light evoked postsynaptic potential (ΔLE-PSP), which represents the difference between resting membrane potential and depolarisation potential. No obvious change in the average curve for control to URB. (B) Input-output relationship in response to light stimulus in control and URB conditions, normalised to maximum spike output. No obvious change can be observed. Kolmogorov-Smirnov test showed a statistically significant overall difference in the input-output relationship between the two curves (p<0.0001). (C) Input-output relationship in response to constant intensity, increasing time duration light stimulation in URB, and URB+CPZ conditions, normalised to control conditions. A reduction in spike output can be seen by URB+CPZ. (D) Input-output relationship in response to light stimulus in URB and URB+CPZ conditions, normalised to maximum spike output. A shift to the left can be observed. Kolmogorov-Smirnov test showed a statistically significant overall difference in the input-output relationship between the two curves (p<0.0001).*

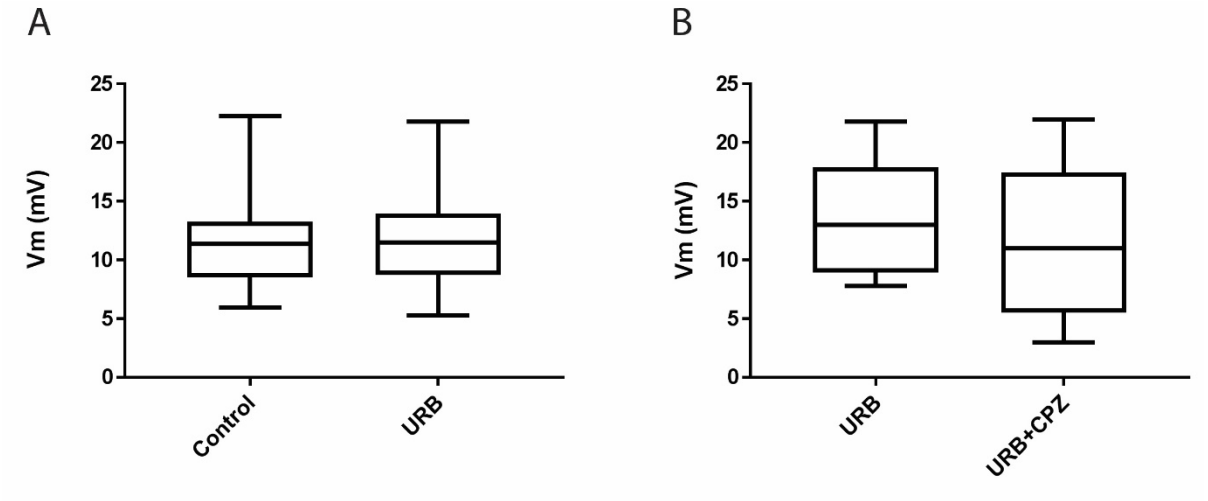

Figure 3.18 Light response X-half values of ganglion cells, comparisons made between control, URB597 and capsazepine conditions*. Both URB and capsazepine produced no change in X-half values (p > 0.05, Wilcoxon test).*

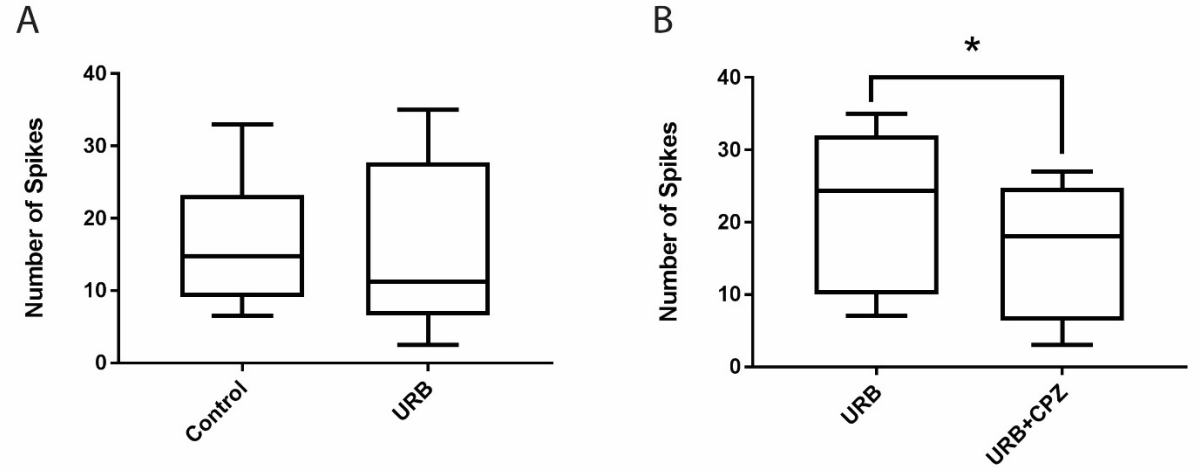

Figure 3.19 Maximum spike output of ganglion cells in control, URB597 and co-application of URB597 and capsazepine conditions (n=10, n=5) are shown*. There was no significant change in the number of spikes in control or URB condition (p < 0.05). When comparing between URB and URB+CPZ, the mean change decreased from 22.1 (± 4.5) to 16.3 (± 4.1) spikes and it was statistically significant (p < 0.001, Wilcoxon test).*

3.4.3 Responses of ganglion cells to stimuli of constant light intensity and constant duration

To further investigate the effects of URB597 and capsazepine on retinal circuitry, another light stimulation protocol was used, with the same light intensity and duration. Spike output and amplitude of light-evoked postsynaptic potentials of RGCs were quantified and compared between control and drug conditions. Comparisons were made between control and URB597, and between URB597 and co-application of URB597 and capsazepine using stimuli with constant duration and light intensity. In control condition, light-evoked spike output had an average value of 11.4 (± 2.1) spikes and LE-PSP had an amplitude of 13 mV. Addition of URB597 (1μM) caused no change in spike output ($n = 10$, $p > 0.1$) in the mean spike count (**Figure 3.20C**). In both of these conditions, the average amplitude of LE-PSPs was 12 mV (**Figure 3.20A)**. After co-application of URB597 (1μM) and capsazepine (10μM), spike output and LE-PSP exhibited no change as shown in **Figure 3.20 C** and **3.20D**.

In brief, no change was produced by both URB597 and co-application of URB597 and capsazepine on the light response of RGCs in TRPV1-/- mice.

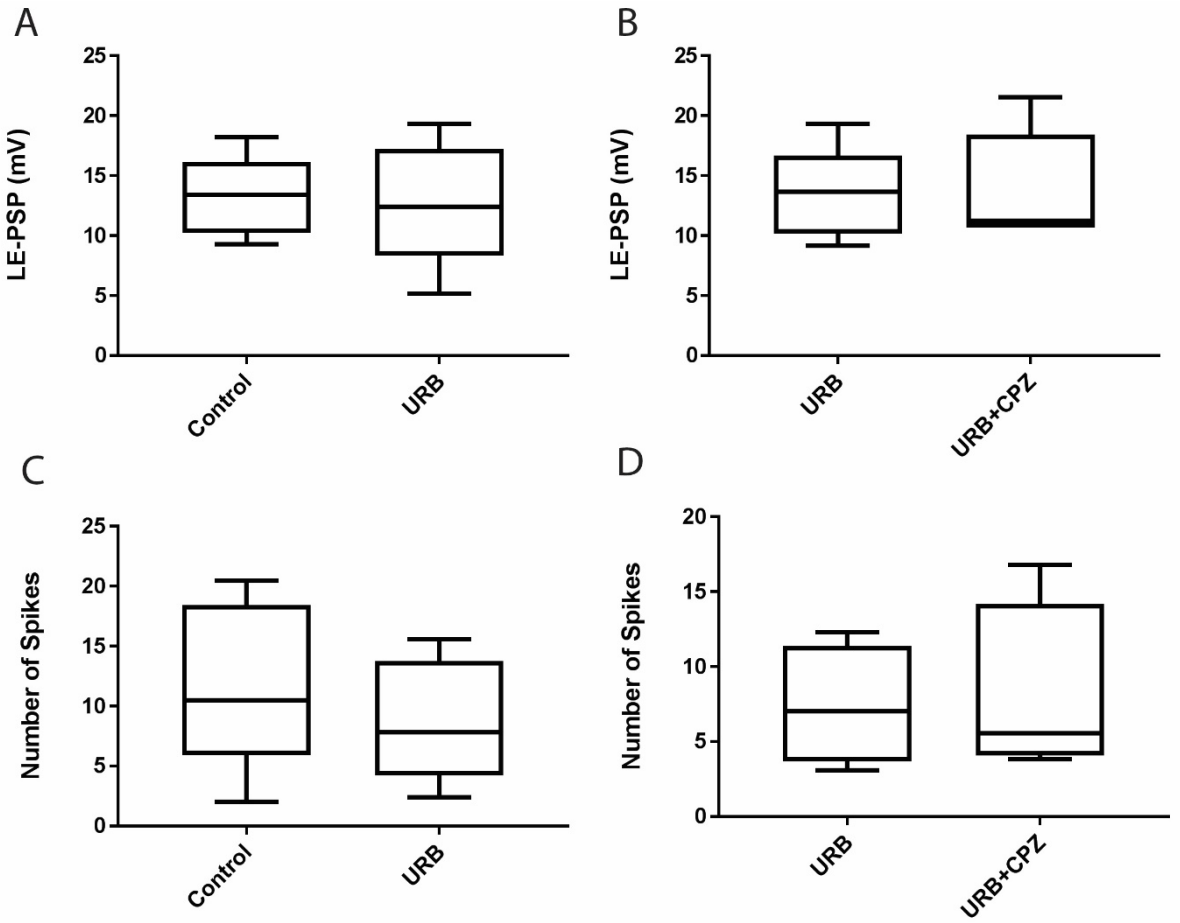

Figure 3.20 Ganglion cell responses to constant intensity and duration light stimulation in control, URB597 and URB+capsazepine conditions. *(A) Light-evoked postsynaptic potential in response to constant light stimulation are shown for the control, and URB597 conditions. No statistical significant change was found between these conditions ($p > 0.1$, $n = 10$). (B) Light-evoked postsynaptic potential in response to constant light stimulation between URB and URB+capsazepine conditions. No change is observed between them ($n = 5$, $p > 0.1$) (C) Number of spike output in response to constant light stimulation between control and URB conditions. No change was found between these groups ($p > 0.1$, $n = 10$). (D) Number of spike output in response to constant light stimulation between URB and URB+CPZ conditions. Little change was found ($p > 0.5$, $n = 4$).*

3.4.4 IV relationship of ganglion cells in voltage clamp

To explore the effects of FAAH inhibitor URB597 (1μM) and TRPV1 channel antagonist capsazepine (10μM) on membrane excitability properties of ganglion cells in the absence of TRPV1 channels, current-to-voltage relationships were investigated.

After addition of URB597 (1μM) to the retina**,** RGCs were activated at a more hyperpolarised potential as shown in **Figure 3.21A**. This shows that the activation of Na^+ currents occurs at a lower membrane potential and suggests an increase in cell excitability, which was also reflected in the negative change in V-half (**Figure 3.22A1)**. V-half value was changed from -50.6 ± 0.9mV to -53.4 ± 1.3mV ($p < 0.05$, n=17). In addition, both the total number of Na^+ events and peak Na^+ current were significantly reduced upon URB597 application. After URB597 application, a significant reduction from 146.8 ± 1.8 to 133.3 ± 29.97 spikes was seen ($p < 0.05$, n = 17, **Figure 3.22B1**). Capsazepine caused a further significant reduction from 135.4 ± 12.6 to 114.1 ± 13.81 spikes ($p < 0.05$, n = 12, **Figure 3.22B2**). As shown in **Figure 3.22C1**, peak inward Na^+ current had a reduction from -2.7 ± 0.2nA to -2.1 ± 0.2nA with URB application ($p < 0.005$, n = 17), and no significant change was observed after co-application of URB597 and capsazepine. Finally, K^+ peak current did not change with URB597 application, but it was reduced from 1.9 ± 0.2nA to 1.4 ± 0.2nA under URB+CPZ condition ($p < 0.005$, n = 12) (**Figure 3.22D1** and **3.22D2**).

In conclusion, a reduction in V-half value was observed with URB application, while capsazepine had no effect. The total number of Na^+ events in control, URB, URB+CPZ conditions decreased. Peak inward Na^+ currents had a reduction after URB application, while no change was present under URB+CPZ condition. Peak outward K^+ had no change under URB condition, and a significant reduction could be seen under URB+CPZ condition.

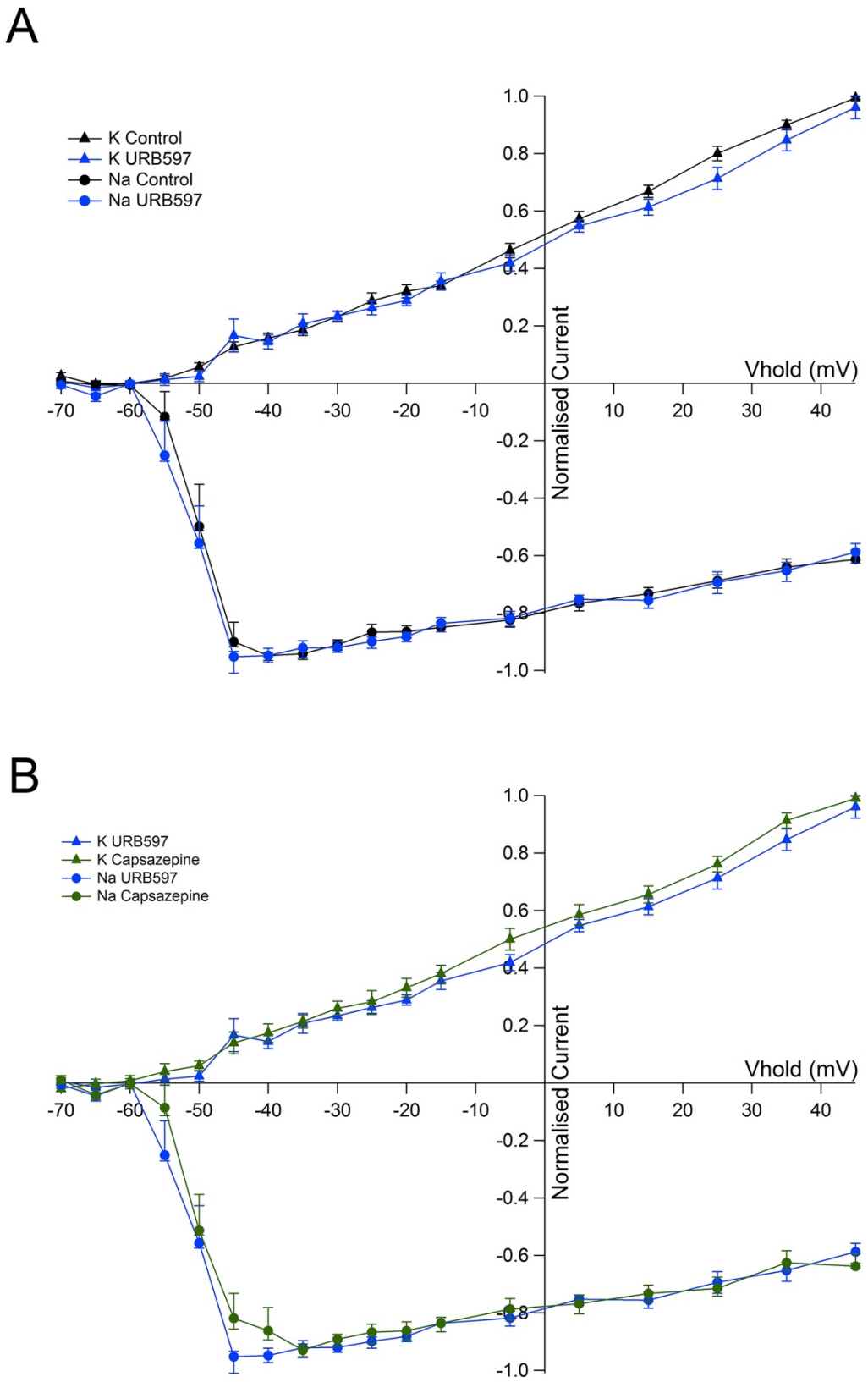

Figure 3.21 IV response of RGC in control, URB597 and URB+capsazepine conditions. (A) Control vs URB IV relationship of ganglion cells showed a larger Na^+ current at a lower holding membrane potential under the influence of capsazepine (n = 18). *Amplitude of Na^+ and K^+ currents were plotted against membrane potential of RGCs to produce IV curves. Average IV curves (± SEM) normalised to peak Na^+ are shown. (B) URB vs URB+CPZ IV relationship illustrated little/no change in capsazepine condition (n = 12).*

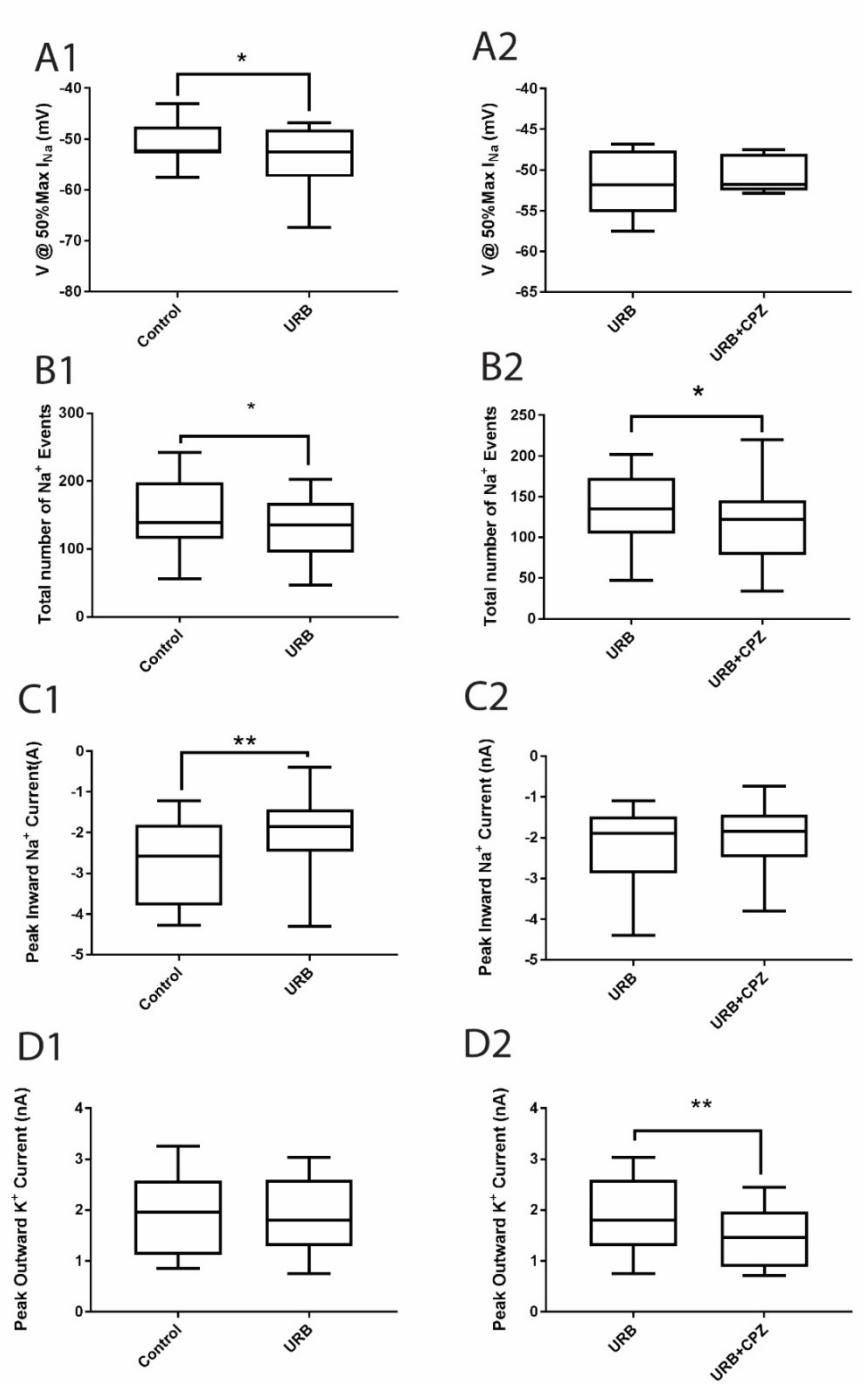

Figure 3.22. Application of FAAH inhibitor URB597 and TRPV1 channel antagonist capsazepine changes RGC excitability. *(A1, A2) A significant reduction in V-half value was observed with URB application, from -50.6 ± 0.9mV to -53.4 ± 1.3mV ($p < 0.05$, $n = 17$). There was no change in V-half after capsazepine was applied. ($p > 0.05$, $n = 12$). (B1, B2) Total number of Na^+ events in control, URB, URB+CPZ conditions. A significant reduction from 146.8 ± 1.8 to 133.3 ± 29.97 spikes after URB application was observed ($p < 0.05$, $n = 17$). Capsazepine caused a further significant reduction from 135.4 ± 12.6 to 114.1 ± 13.81 spikes ($p < 0.05$, $n = 12$). (C1, C2) Peak inward Na^+ currents in control, URB, and URB+CPZ conditions. A reduction was observed from -2.7 ± 0.2 to -2.1 ± 0.2nA after URB application ($p < 0.005$, $n = 17$). No change was present under URB+CPZ condition ($p > 0.05$, $n = 12$). (D1, D2) Peak outward K^+ currents in control, URB, and URB+CPZ conditions. Little/no change was present under URB condition ($p > 0.05$, $n = 17$). A significant reduction from 1.9 ± 0.2 to 1.4 ± 0.2nA could be seen under URB+CPZ condition ($p < 0.005$, $n = 12$).*

The tables below sum up all the changes observed in the Results section. **Table 3.1** provides a summary of the input-output function including the observed shift, mean change in X-half, and its' significance, as well as Kolmogorov-Smirnov test results. Overall, there was no change in the X-half value, despite all Kolmogorov-Smirnov tests showed significant differences in the general shape of the sigmoidal curves. In table 3.2, the parameters drawn from the I-V relationship were compared between control and drug conditions. A leftward shift in the I-V curve indicates increased excitability, which was shown for capsaicin condition in the wild-type animals and the URB597 condition for the TRPV1-/- animals. This leftward shift consequently led to decreased value in V-half for capsaicin and URB597 conditions. A reduction in the magnitude of Na^+ currents could be observed for all the drug conditions. As for Na^+ events, capsazepine (wild-type), URB597 (TRPV1-/-), and co-application of URB697 and capsazepine reduced the number of Na^+ events. However, no change in K^+ current was found in any of the drug conditions.

Table 3.1. Summary of input-output function of retinal ganglion cells to different drug conditions. *Current-clamp was used for generation of table 3.1.*

Drug conditions	Hypothesis of cell excitability	Observed shift	Mean change in X-half(mV) ± SEM	Significance: X-half (Wilcoxon test)	Significance: X-half/V-half (Kolmogorov-Smirnov test)
Capsaicin (wild type)	Increase	-	+0.49±0.59	ns	****
Capsazepine (wild type)	Decrease	-	+0.45±0.39	ns	****
URB597 to URB+Capsazepine (TRPV1-/-)	No change to decrease	- to -	-0.98±0.86 to -0.27±0.11	ns to ns	****
Light Response: URB597 to URB+Capsazepine (TRPV1-/-)	No change to decrease	NA to -	NA to -1.9±1.3	NA to ns	****

***p < 0.05 **p < 0.01 ***p < 0.001; ← Leftward/Additive shift; → Rightward/Subtractive shift**

NA=not applicable, due to small sample size

Table 3.2. Summary of current-to-voltage of the retinal ganglion cells to different drug conditions.

Drug conditions	Observed shift	Mean change in V-half (mV) ± SEM	Significance V-half (Wilcoxon test)	Mean change in max amplitude of Na^+ Current (nA)	Significance: max amplitude of Na^+ Current (Wilcoxon test)	Mean change in total number of Na^+ events	Significance: total number of Na^+ events	Mean change in max amplitude of K^+ Current (nA)	Significance: max amplitude of K^+ Current (Wilcoxon test)
Capsaicin (wild type)	←	-3.5±1.3	*	+0.51±0.21	*	-16.5±8.3	ns	-0.257±0.47	ns
Capsazepine (wild type)	-	-1.2±1.2	ns	+0.56±0.21	*	-31.57±12.4	*	-0.029±0.177	ns
URB597 to URB+Capsazepine (TRPV1-/-)	← to -	-2.8±1.1 to 2.4±1.7	* to ns	+0.61±0.17 to +0.27±0.12	** to *	-13±5.5 to -21±8.0	* to *	-0.41±0.13	ns

***p < 0.05 **p < 0.01 ***p < 0.001; ← Leftward/Additive shift; → Rightward/Subtractive shift**

4. Discussion

This study aimed to characterise the potential role TRPV1 channels play in retinal ganglion cell excitability. Two experimental conditions were examined in RGCs of wild-type animals using: 1) capsaicin, a TRPV1 agonist and 2) capsazepine, a TRPV1 antagonist. Another experimental approach was to study the modulation of the eCB system in TRPV1-/- animals that lacked TRPV1 channels. In this set of experiments, URB597, a blocker of the degrading enzyme of the eCB anandamide was used to elevate anandamide concentration. This was followed by co-application of URB597 and capsazepine to further investigate whether TRPV1 channels are the target protein involved in modulating RGC excitability by eCB. The results of the current study suggest TRPV1 channels are tonically activated, although they do not seem to be the only target of anandamide that contributes to the modulation of RGC excitability. Other membrane proteins, such as NKCCl or TRPM channels, might potentially contribute to the changes seen in RGC excitability by anandamide and will be considered later in this Discussion section.

4.1 TRPV1 channel modulates retinal ganglion cell excitability

4.1.1 Activation of TRPV1 channel increases RGC excitability at a low cell input

Our results indicated no change in X-half for I-O function in RGCs of wild-type mice with capsaicin application, but a change in the overall shape of the input-output relationship. A Kolmogorov-Smirnov test was used to compare the shape of the two sigmoidal fits

(normalised to 1), and this test indicated statistical significance between control and capsaicin conditions. Although there was a lack of change in X-half value, RGCs displayed an increased spike output in the early phase of the curve in response to small changes in ΔVm. These changes indicate that a weaker depolarisation led to a bigger spiking output which means there is an increase in cell excitability of ganglion cells. This partially agrees with our hypothesis postulating that capsaicin increases cell excitability. Previous findings from our lab on the effects of URB597 (Protti D.A., 2015, Yates, 2014, Yong, 2016) showed an increase in cell excitability. The hypothesis of our current study stated that application of URB597 would raise the level of anandamide. Anandamide is an endovallinod, and it acts on TRPV1 channels by allowing influx of Ca^{2+} ions into the cell which in turn would increase cell excitability (Caterina et al., 1997). Thus, the increase in cell output in the initial phase of the input-output function by directly activating TRPV1 channels using capsaicin is aligned with previous studies and supports the working hypothesis. However, this effect was not observed for the whole of the input-output function, namely larger depolarisations did not elicit more action potentials. One possible explanation for the above observation is that current injection was held for 0.5 seconds. This prolonged stimulation would have caused plateau depolarising responses in some RGC with large current injections. In other words, responses saturated after a certain level of stimulation. Thus, a protocol modification was carried out for the later experiments, by shortening the stimulation time to 0.1 seconds. This change in protocol resulted in less spike output, a much smaller change in plateaued depolarisation response, and larger depolarisation. Another possible explanation could be a

result of the compartment-specific effect of capsaicin. In other CNS regions such as the dentate gyrus, anatomical evidence suggests that CB1 and TRPV1 are co-localised (Cristino et al., 2006). Chávez et al. (2014) demonstrated that by activating TRPV1 with capsaicin or anandamide, somatic but not dendritic inhibitory transmission was reduced in rat and mouse dentate gyrus. The same group also found that the depressing effect on somatic inhibition was absent in TRPV1-/- mice, suggesting a modulatory role of TRPV1 channels on GABAergic synaptic transmission. These results indicate that in the dentate gyrus, the supressive effect of TRPV1 channels works in a compartment-specific manner. In relation to our results, only somatic whole-cell patch clamp recordings were obtained, where no change in the magnitude of depolarisation induced by current injection could be observed. However, as the only somatic response was recorded, we could not be certain of what effects might have taken place in other compartments, such as the dendrites. Thus, although the effects of capsaicin might be compartment-specific, dendritic and somatic responses could potentially show different results.

4.1.2 Effects of capsaicin on sodium and potassium currents of ganglion cells

Under voltage clamp mode, RGCs were held at different membrane potentials to measure inward Na^+ and outward K^+ currents. Current-to-voltage (IV) relationships were built from sodium and potassium currents and then plotted against corresponding membrane potentials.

The recorded membrane potential at which 50% of Na^+ current (V-half) occurred was measured as an estimation of voltage-gated sodium channels activation. Although this measurement does not provide the most accurate parameter to quantify the voltage-dependent properties of voltage-gated Na^+ channels (such as activation and inactivation constants), it allows analysis of the relationship between membrane potential and Na^+ channel activation whilst being able to carry out current-clamp recordings from the same cell. Experiments blocking K^+ currents with caesium and tetraethylammonium would be required to obtain more accurate recordings of the voltage-dependent properties of Na^+ channels, but this would preclude measurements of the input-output relationships as action potentials would not repolarise in these conditions, and therefore spiking behaviour would be markedly affected. The conditions of the voltage-clamp recordings in this study are therefore a compromise that at least allowed measurement of an estimate of the voltage-dependence of Na^+ channels whilst being able to investigate RGC excitability in current-clamp conditions. Application of capsaicin produced a leftward shift in V-half measured from IV curves, indicating that RGCs required weaker depolarising steps to elicit Na^+ entry, thus indicating that cell excitability was increased. This leftward shift in V-half provides support of the observed shift to the left in X-half of the I-O relationship. The peak amplitude of the Na^+ current, however, was reduced. This finding is not in alignment with our hypothesis. One possible explanation is that it could be due to the reduction in cell access resistance. In order to analyse the effects of capsaicin, a total of five minutes' drug perfusion time was allowed to fully deliver the drugs through the retinal tissue. Patch clamp recordings are very sensitive and once the cell

membrane is patched, any changes in the external environment or the perfusion system can disrupt the quality of recordings, thus affecting cell responses. Although we have eliminated cells that had more than 30% reduction in access resistance and a change of >200pA in leak current, several cells still had around 10% reduction in access resistance which could potentially result in the observed decrease in Na^+ current amplitude. Patch clamp is a challenging technique with relatively low success rates, and after exclusion of many cells, the total sample number in this study was not as high as in the initial experimental design.

In regard to K^+ channels, little change was observed after capsaicin application. This finding is also in contradiction with our initial hypothesis which predicted that capsaicin would increase ganglion cell excitability. Previous experiments found that URB597 application caused a significant increase in late-stage potassium current in large RGCs but not small RGCs (Protti D.A., 2015, Yates, 2014, Yong, 2016). A possible explanation for the lack of effect in this study is because of unintentional sampling bias. Although cells were randomly patched, it is possible that many of the cells we recorded from did not express TRPV1 channels as a recent study (Jo et al., 2017) showed that only around 17% of RGCs express TRPV1 channels. Given that in this study, a total of 76 RGCs were successfully patched but only 25 of them could be classified into cell types, we cannot provide an estimate of whether or not they expressed TRPV1 channels. Several challenges such as tissue degradation can occur during treatments of retinal tissue for immunocytochemical staining. Tissue was initially fixed for 30 minutes then incubated in antibody solutions for at least a week. Because of tissue degradation and/or tearing of the tissue due to its fragile nature, only one-

third of the recorded RGCs were successfully imaged under a confocal microscope. Using their morphological features, they were classified into cell types according to criteria used by Sun and colleagues (2002). Because of a low sample number, it was not possible to link RGC cell types to their physiological responses for statistical comparisons. Hence, the lack of change in K^+ current might be due to the RGCs recorded were mostly small cells although they were randomly selected for recordings.

The previously observed K^+ current modulation by anandamide could be due to its binding to CB1R mediated Na^+-K^+-$2Cl^-$-co-transporter (NKCC) 1 channels. Miraucourt and colleagues (2016) demonstrated an increase in RGC excitability after blocking NKCC1 using NKCC1 inhibitor bumetanide in *Xenopus* tadpoles. The NKCC1 co-transporter has also been localised in rodent ganglion cells (Vardi et al., 2000), which suggests its possible involvement in modulating cell excitability in mouse RGCs.

4.1.3 TRPV1 channels in Ganglion cells are tonically active

The TRPV1 antagonist capsazepine was used to investigate the effects of TRPV1 channel inactivation on RGCs responses and excitability properties. Similar to experimental procedures with capsaicin, RGCs were recorded in current- and voltage-clamp mode, and input-output relationships and current-to-voltage relationships were normalised and pooled to estimate RGC excitability. The hypothesis predicted that by blocking TRPV1 channels using capsazepine, RGC excitability would be reduced.

Results from experiments in current clamp conditions showed decreased cell excitability as observed in the input-output curves. When I-O relationship of capsazepine condition was normalised to the control, a decrease in spike output was observed as the KS test showed the difference in curves. This decrease in cell excitability caused by capsazepine supports the hypothesis that anandamide acts through TRPV1 channels. Anandamide is a potent agonist of TRPV1 channels, and capsazepine being the TRPV1 channel antagonist, competes with anandamide for binding. Blocking of TRPV1 channels by capsazepine leads to a reduction in Ca^{2+} influx (van der Stelt et al., 2005) and activation of second messenger pathways that modulate RGC excitability. To our surprise and contrary to our hypothesis, no change in X-half could be observed. Capsazepine is an antagonist, rather than an inverse agonist of TRV1 channel, and consequently its inhibitory effect is affected by the amount of anandamide present. Previously, Leung (2016) demonstrated that URB597 application to retina whole mounts increased cell excitability presumably by increasing the levels of anandamide as this effect could be reversed by co-application with capsazepine. Furthermore, the IV relationship also showed reduced RGC excitability. Although V-half did not have a significant change, the reduction in cell excitability was reflected as a significant reduction in the total number of Na^{+} events. Besides, the peak Na^{+} current was significantly reduced in size. Similar to the effects found with capsaicin, there was no change in potassium currents.

In summary, attenuation in spike output, decreased peak Na^{+} current, and total number of Na^{+} events confirmed the hypothesis of a reduction in cell excitability under capsazepine

conditions. However, contrary to our prediction on the hypothesis, no change in X-half, V-half and peak K^+ currents were observed.

4.2 The endocannabinoid anandamide modulates cell excitability in the absence of TRPV1 channels

4.2.1 Anandamide increases cell excitability in the absence of TRPV1 channel

TRPV1-/- mice were used to investigate the effects of anandamide modulating the retinal levels of eCBs in the absence of TPV1 channels. The effects of raising anandamide levels with URB597 on RGC excitability were first examined. Co-application of URB597 and capsazepine was subsequently used to investigate whether a reversal effect would still be present in the absence of TRPV1 channels.

Input-output relationship with application of URB597 and co-application of capsazepine

As observed in current injection experiments (Results 3.4.1), application of URB597 produced a decrease in cell excitability in the absence of TRPV1 channels. No change in X-half was observed, and a significant reduction in cell output was observed as the spike output was reduced. This reduced excitability is in agreement with our hypothesis. The original hypothesis was based on the idea that anandamide activates TRPV1 channels which in turn cause increased excitability as TRPV1 channels are found on the cell membrane and cytoplasmic reticulum (Turner et al., 2003). Furthermore, it was proposed that activation of the membrane TRPV1 channels would increase Ca^{2+} influx, and activation of TRPV1

channels in the cytosolic compartment would cause an increase in intracellular Ca^{2+} leading to an increase in cell excitability. In addition to being an eCB, anandamide is known to be an endovanilloid (Starowicz et al., 2007, Zygmunt et al., 1999) which binds to TRPV1 and increases Ca^{2+} currents into the cell. This increase in intracellular Ca^{2+} concentration is known to modulate Na^{+} channel phosphorylation (Auld et al., 1988), leading to a change in cell excitability. Previously, it was demonstrated a paradoxical effect of increased spike output with decreased synaptic input with application of URB597 and anandamide in RGCs of wild-type mice (Protti et al., 2015, Leung, 2016, Yates, 2014). Thus, with TRPV1 channels absent in the knockout mice, Ca^{2+} concentration would not increase and no downstream effects such as increased cell excitability would be expected.

The results obtained after co-application of URB597 and capsazepine showed a decrease in cell excitability. No significant change in X-half was observed, as confirmed by Wilcoxon test. However, a significant reduction in the spike output was observed. This reduction in cell excitability is contrary to our hypothesis. A possible explanation of this reduced RGC output is non-specific binding of TRPV1 agonist and antagonist. Although TRPV1 channel is known as the 'capsaicin receptor', capsaicin was shown to also exhibit a range of TRPV1-independent mechanisms such as activation of voltage-gated inward and outward currents, and binding to the CB1 receptor (Ryskamp et al., 2014). Likewise, capsazepine was also found to produce physiological effects in TRPV1-/- mice. It was found that capsazepine exerts antagonism on voltage-activated Ca^{2+} channels (Docherty et al., 1997), acetylecholine

receptors (Liu and Simon, 1997), hyperpolarisation-activated cation channels (I_h) (Ray et al., 2003), and stimulation of amiloride-sensitive ENaC channels (Yamamura et al., 2004). In relation to our results, in the absence of TRPV1 channel, capsazepine may have blocked voltage-activated calcium channels and led to a reduction in cell excitability.

4.2.2 The Effect of Anadamide and Capsazepine on Light Response of RGCs in the absence of TRPV1 channel

Using the same current-clamp recording protocol, the effect of light stimulation was explored. Stimulation of RGCs using light, the natural stimulus, was employed as a more physiological approach to investigate cell excitability. The current injection protocol used in previous sections involved a series of injections of depolarising currents into the RGC soma to cause a change in membrane potential and consequently elicit firing of action potentials. This is different from physiological stimulation as synaptic inputs take place in the dendrites rather than in the soma. Given that the retina is a complex yet highly organised structure, using light stimulation reproduces the conditions where RGCs receive a collection of synaptic signals and its response reflects the effects of the drug on the entire circuitry.

Input-output relationship for light response with application of URB597 and co-application of capsazepine

Similar to the results observed with current injection protocols, there was no change in X-half upon application of URB597, or with co-application of URB597 and capsazepine, as

observed in the I-O functions. As for spike output, URB597 did not cause any effect upon application in the TRPV1 knockout animals. Thus, confirming our hypothesis that the increase in cell excitability works by anandamide binding to TRPV1 channels. Co-application of URB597 and capsazepine reduced the spike output significantly, in alignment with the results of our current injection protocol. Apart from the previously discussed non-specific binding of capsazepine, in the case of light stimulation, bleaching of the retinal tissue and upstream effects should also be considered. In these experiments, light responses were attenuated in order to prevent photoreceptor bleaching. As the retinal pigment epithelium layer must be detached for infrared illumination coming from the condenser to illuminate the tissue for visualisation of cells, photoreceptor pigment could not be regenerated after photoisomerisation, which inevitably led to some degree of bleaching (Werner, 2014). Although two neutral density filters were used to attenuate the light stimulation, it was still observed in many cases that the cell responses became weaker over time. Thus, only a small sample size could be used for the final statistical comparison, which had an impact on the statistical power. Secondly, the shift in X-half value could be due to non-specific binding of capsazepine (Schmidt, 2009) to voltage-activated Ca^{2+} channels (Docherty et al., 1997), acetylcholine receptors (Liu and Simon, 1997), hyperpolarisation-activated cation channels (I_h) (Ray et al., 2003), and/or stimulation of amiloride-sensitive ENaC channels (Yamamura et al., 2004). Although capsaicin was widely recognised to be specific to TRPV1 channels, Shen and co-workers found that in *TRPV1*$^{-/-}$ mouse, a complete disruption of ON bipolar cell function was present (Shen et al., 2009). Initially, capsaicin-induced responses within rod and

cone ON bipolar cells appeared to be indistinguishable from the effects mediated by light and mGluR6 antagonist, which pointed in the direction of TRPV1 channel. Though, in *TRPV1*$^{-/-}$ mice, light responses of the ON bipolar cells were unaffected. However, the light responses were eliminated in the TRPM knockout animals (Shen et al., 2009).

However, only partial reduction of the amplitude of capsaicin amplitude was seen in TRPM$^{-/-}$ mice, suggesting other possible sensors in ON bipolar cells (Morgans et al., 2009). As bipolar cells are upstream in the retinal circuitry, and the inability of categorising RGC cell type into subtypes such as ON or OFF cells due to the nature of the stimuli used in this study (full field and short duration), or cell morphology, the response produced could have multiple contributors. Thus, non-TRPV1-mediated effects by capsaicin and capsazepine should be taken into careful consideration.

Light responses to stimuli of constant light intensity and constant duration under the effects of URB597 and capsazepine

In our experiments, light intensity was kept constant and LE-PSP and action potentials were quantified and directly compared across drug conditions. Consistent with the input-output functions, application of URB597 did not have an obvious effect on LE-PSP or spike output. Different to the input-output function generated from increased stimulation time, no change in spike output was observed after co-application of URB597 and capsazepine, although a reduction in response was expected. This difference in light response could be due to the small sample size, which cause the statistical power to be weak. In fact, only five RGCs were

recorded successfully with the co-application of URB597 and capsazepine, which had a consistent light response. As previously mentioned, five minutes of perfusion time was allowed for drugs to fully penetrate through the retinal tissue. Moreover, a waiting time of two minutes was allowed at the beginning of each drug condition. During this period, spontaneous activity was recorded. If the recording was stable, there was good access to the cell body, and have a similar spontaneous activity to the previous control or drug condition, only then physiological recordings will follow. Some of the difficulties during recordings also involved the nucleus of RGC tending to move towards the pipette tip due to its position, or negative pressure inside the tip causing a great loss of cell access, or a dramatic increase in cell spontaneous activity. Such cells together with those that had more than 30% reduction in cell access and change in leak current of more than 200pA were eliminated. These were in total 27 RGCs.

In conclusion, in the TRPV1-/- mice, URB597 caused no change in RGC excitability, confirming the original hypothesis. Also, there was no change in RGC excitability after application of capsazepine, which differ to the input-output function. This potentially could be caused by the weak statistical power as the number of cells recorded was very small.

4.2.3 Anandamide and capsazepine modulate sodium and potassium channel kinetics in the absence of TRPV1 channel

Under voltage clamp configuration, application of URB597 significantly shifted the V-half value to the left. This finding indicates an increase in Na^+ entry into RGCs at lower membrane potentials, which leads to an increase in action potential output, and increased cell excitability. This does not support our proposed hypothesis and it is not consistent with the input-output function collected using current injection protocol under current clamp setup. The increase in cell excitability in the absence of TRPV1 channel could possibly be due to binding of anandamide to other ion channels such as CB1R mediated by NKCC1 channel. The mechanism of eCB action on NKCC1 transporter was explained by a reduction in intracellular Cl^- levels in RGCs, which in turn leads to their hyperpolarisation. This hyperpolarisation helps voltage gated sodium channels recover faster from their inactivation state. This all leads to the acute enhancement of intrinsic excitability of RGCs (Miraucourt et al., 2016). This mechanism also increases intrinsic cell excitability through interaction between glycinergic inhibition and eCB system involving Cl^- homeostasis, without the involvement of TRPV1 channels. On the contrary, the total number of Na^+ events and peak inward Na^+ current amplitude was significantly reduced. Because this is a direct comparison of the parameter values, although with relatively small sample size, the change in recording conditions such as cell access could have had an impact on individual cells responses. As a result, this has potentially contributed to the weak statistical difference between these groups. Co-application of URB597 and capsazepine produced no effect in V-half value or peak Na^+

inward current amplitude, but caused a reduction in the total number of Na^+ events. As for K^+, a significant reduction was observed in the I-V graph upon co-application of URB591 and capsazepine. It has been demonstrated by Mahmmoud et al. (2014) that capsazepine inhibits K^+ transport through Na^+, K^+-ATPase. As our I-V results indicate, this effect was seen in the TRPV1 knockout mice but not in wild type animals, suggesting a more prominent effect in the absence of TRPV1 channels. Furthermore, capsazepine did not reverse the effects produced by URB597 on V-half values. This is in alignment with our hypothesis and it also supports a non-reversal effect on input-output relationship as seen in current injections. Besides, this also suggests the shift of light response input-output relationship is likely to be caused by an upstream effect, rather than directly altering RGC excitability.

4.3 Experimental Limitations

The current study used patch clamping recordings in whole mount retina to target ganglion cells. This method allowed an overall output of the retina to be measured as ganglion cells are located at the last laminal layer of the retina before transmitting the final visual signals to the rest of the brain. Patch clamp recordings are technically challenging and small alterations in the external or internal environment can lead to dramatic changes in electrophysiological recordings. It was often noticed after careful analyses post experiments that several cells recorded would not meet our stringent inclusion criteria. These include a reduction in cell access, or fluctuation in membrane potential. In general, this limited the number of cells we could use to be included to the final sample. This is especially true for the TRPV1 knock out

animals, where two drugs were perfused requiring much longer recording time. Moreover, the patch clamp technique had limited us to test on specific targets in order to examine on the local effects. As retinal cells form highly complex neuronal circuits inside the eye, visual stimuli first activate photoreceptors, electrical signals travel through multiple synapses, then to the rest of the brain for further processing. In the case of light responses, drugs could bind to upstream cells and cause a much more complex effect such as on TRPM channels on ON-bipolar cells. To investigate whether the drug effects are actually due to presynaptic effects, blockers such as NBQX and SR95531 could be used to block glutamatergic and GABAergic currents, which isolates RGCs from its' presynaptic effects. Though, under such conditions, light response would no longer be able to be tested. But nevertheless, RGC local responses could be valuable and serve as complementary to the findings of our current results.

Another limitation arose from the methodology of the somatic voltage clamp technique itself. Most of the electrophysiological recordings are done by patching onto the soma/cell body, while most of the synaptic inputs take place at the dendrites. Due to the size of the cell body, space-clamp errors occur because of the holding voltage between the soma, dendrites and axon are different (Williams and Mitchell, 2008). As Williams and Mitchell (2008) pointed out, the somatic voltage clamp cannot control voltage at sites beyond the soma very precisely, which leads to inaccuracies in the recordings of synaptic responses. In the case of the eCB system it is located precisely in the synapses, with eCB being released from the postsynaptic terminal and binding to the CB1 receptors that are predominantly located on the

presynaptic terminal. This synaptic localisation of the eCB system, along with RGCs featured elaborate dendritic structures would make our results suffer from the space-clamp error as currents were injected directly into the soma rather than in the dendrites. Thus, the voltage-gated sodium channels located on the soma have a stronger influence on voltage clamp recordings due to its close proximity to the recording electrode compared to those on the dendrites. A solution was proposed by Castelfranco and Hartline (2004) by correcting the parameters of voltage-gated conductance.

5. Conclusion and Future Directions

5.1 Summary and Conclusions

This study contributes to the current understanding of endocannabinoid system and how it interacts with TRPV1 channels, as well as revealing the binding properties of TRPV1 channel agonist and antagonist. The present study demonstrated that TRPV1 channels play a crucial role in relation to the endocannabinoid system in RGCs. The endocannabinoid, anandamide partially acts on TRPV1 channels to increase cell excitability as application of TRPV1 agonist capsaicin produced an increase in cell excitability. Application of URB597, a blocker of the enzyme FAAH that hydrolyses anadamide, in the absence of TRPV1 channels, however, showed that anandamide also acts on other channels as RGCs were activated at a more hyperpolarised potential. Moreover, the originally postulated TRPV1 agonist and

antagonist, capsaicin and capsazepine were found to have non-specific binding as the application of capsazepine was able to reduce cell excitability in the TRPV knockout mice.

5.2 Future Directions

In addition to TRPV1 channels, recent studies point out to other targets of anandamide that may also play crucial roles in modulating RGC excitability, such as NKCC1 channels. Further investigations could be carried out to test the effects of anandamide on intracellular Cl^- levels by using the clomeleon sensor as described by Miraucourt et al. (2016) using TRPV1 knockout mice. Additionally, whether the effects produced by capsaicin, capsazepine and anandamide would still be present in TRPM knockout animals should be investigated. This would allow insights into how upstream TRPM receptor contributes to RGC excitability and retinal circuitry.

6. Reference List

AULD, V. J., GOLDIN, A. L., KRAFTE, D. S., MARSHALL, J., DUNN, J. M., CATTERALL, W. A., LESTER, H. A., DAVIDSON, N. & DUNN, R. J. 1988. A rat brain Na+ channel α subunit with novel gating properties. *Neuron,* 1**,** 449-461.

BADEN, T., BERENS, P., FRANKE, K., ROSÓN, M. R., BETHGE, M. & EULER, T. 2016. The functional diversity of retinal ganglion cells in the mouse. *Nature,* 529**,** 345-350.

BOYCOTT, B. B. & WASSLE, H. 1974. The morphological types of ganglion cells of the domestic cat's retina. *J Physiol,* 240**,** 397-419.

CASTELFRANCO, A. M. & HARTLINE, D. K. 2004. Corrections for space-clamp errors in measured parameters of voltage-dependent conductances in a cylindrical neurite. *Biological cybernetics,* 90**,** 280-290.

CATERINA, M. J., LEFFLER, A., MALMBERG, A. B., MARTIN, W. J., TRAFTON, J., PETERSEN-ZEITZ, K. R., KOLTZENBURG, M., BASBAUM, A. I. & JULIUS, D. 2000. Impaired Nociception and Pain Sensation in Mice Lacking the Capsaicin Receptor. *Science,* 288**,** 306-313.

CATERINA, M. J., SCHUMACHER, M. A., TOMINAGA, M., ROSEN, T. A., LEVINE, J. D. & JULIUS, D. 1997. The capsaicin receptor: a heat-activated ion channel in the pain pathway. *Nature,* 389**,** 816-824.

CECYRE, B., ZABOURI, N., HUPPE-GOURGUES, F., BOUCHARD, J. F. & CASANOVA, C. 2013. Roles of cannabinoid receptors type 1 and 2 on the retinal function of adult mice. *Invest Ophthalmol Vis Sci,* 54**,** 8079-90.

CHAVEZ, A. E., CHIU, C. Q. & CASTILLO, P. E. 2010. TRPV1 activation by endogenous anandamide triggers postsynaptic long-term depression in dentate gyrus. *Nature Neuroscience,* 13**,** 1511-U99.

CHÁVEZ, A. E., HERNÁNDEZ, V. M., RODENAS-RUANO, A., CHAN, C. S. & CASTILLO, P. E. 2014. Compartment-specific modulation of GABAergic synaptic transmission by TRPV1 channels in the dentate gyrus. *Journal of Neuroscience,* 34**,** 16621-16629.

COSENS, D. & MANNING, A. 1969. Abnormal electroretinogram from a Drosophila mutant. *Nature,* 224**,** 285-287.

CRAVATT, B. F., DEMAREST, K., PATRICELLI, M. P., BRACEY, M. H., GIANG, D. K., MARTIN, B. R. & LICHTMAN, A. H. 2001. Supersensitivity to anandamide and enhanced endogenous cannabinoid signaling in mice lacking fatty acid amide hydrolase. *Proc Natl Acad Sci U S A,* 98**,** 9371-6.

CRISTINO, L., DE PETROCELLIS, L., PRYCE, G., BAKER, D., GUGLIELMOTTI, V. & DI MARZO, V. 2006. Immunohistochemical localization of cannabinoid type 1 and

vanilloid transient receptor potential vanilloid type 1 receptors in the mouse brain. *Neuroscience,* 139**,** 1405-1415.

DI MARCO, S., NGUYEN, V. A., BISTI, S. & PROTTI, D. A. 2009. Permanent functional reorganization of retinal circuits induced by early long-term visual deprivation. *Journal of Neuroscience,* 29**,** 13691-13701.

DI MARZO, V., DE PETROCELLIS, L., FEZZA, F., LIGRESTI, A. & BISOGNO, T. 2002. Anandamide receptors. *Prostaglandins, Leukotrienes and Essential Fatty Acids (PLEFA),* 66**,** 377-391.

DI MARZO, V., GOPARAJU, S. K., WANG, L., LIU, J., BATKAI, S., JARAI, Z., FEZZA, F., MIURA, G. I., PALMITER, R. D., SUGIURA, T. & KUNOS, G. 2001. Leptin-regulated endocannabinoids are involved in maintaining food intake. *Nature,* 410**,** 822-5.

DIANA, M. A. & MARTY, A. 2004. Endocannabinoid-mediated short-term synaptic plasticity: Depolarization-induced suppression of inhibition (DSI) and depolarization-induced suppression of excitation (DSE). *British journal of pharmacology,* 142**,** 9-19.

DOCHERTY, R., YEATS, J. & PIPER, A. 1997. Capsazepine block of voltage-activated calcium channels in adult rat dorsal root ganglion neurones in culture. *British journal of pharmacology,* 121**,** 1461-1467.

ELPHICK, M. R. & EGERTOVA, M. 2001. The neurobiology and evolution of cannabinoid signalling. *Philos Trans R Soc Lond B Biol Sci,* 356**,** 381-408.

GOOD, C. H. 2007. Endocannabinoid-dependent regulation of feedforward inhibition in cerebellar Purkinje cells. *J Neurosci,* 27**,** 1-3.

GUZMAN, M. 2003. Cannabinoids: potential anticancer agents. *Nat Rev Cancer,* 3**,** 745-55.

HARTLINE, H. K. 1938. The response of single optic nerve fibers of the vertebrate eye to illumination of the retina. *American Journal of Physiology--Legacy Content,* 121**,** 400-415.

HASHIMOTODANI, Y., OHNO-SHOSAKU, T. & KANO, M. 2007. Presynaptic monoacylglycerol lipase activity determines basal endocannabinoid tone and terminates retrograde endocannabinoid signaling in the hippocampus. *J Neurosci,* 27**,** 1211-9.

HAVERKAMP, S., WASSLE, H., DUEBEL, J., KUNER, T., AUGUSTINE, G. J., FENG, G. & EULER, T. 2005. The primordial, blue-cone color system of the mouse retina. *J Neurosci,* 25**,** 5438-45.

HOCKING, M. B. P. S. 2016. RACGP - Prescription drug abuse – A timely update.

HUANG, J., STIEFE, L. K. & PROTTI, D. A. 2013. Implementing dynamic clamp with synaptic and artificial conductances in mouse retinal ganglion cells. . *J Vis Exp,* e50400.

JO, A. O., NOEL, J. M., LAKK, M., YARISHKIN, O., RYSKAMP, D. A., SHIBASAKI, K., MCCALL, M. A. & KRIŽAJ, D. 2017. Mouse retinal ganglion cell signalling is dynamically modulated through parallel anterograde activation of cannabinoid and vanilloid pathways. *The Journal of Physiology*.

KISHIMOTO, Y. & KANO, M. 2006. Endogenous cannabinoid signaling through the CB1 receptor is essential for cerebellum-dependent discrete motor learning. *J Neurosci,* 26**,** 8829-37.

KRIEGER, B., QIAO, M., ROUSSO, D. L., SANES, J. R. & MEISTER, M. 2017. Four alpha ganglion cell types in mouse retina: Function, structure, and molecular signatures. *PloS one,* 12**,** e0180091.

KUFFLER, S. W. 1953. Discharge patterns and functional organization of mammalian retina. *Journal of neurophysiology,* 16**,** 37-68.

LAFON, B., RAHMAN, A., BIKSON, M. & PARRA, L. C. 2017. Direct current stimulation alters neuronal input/output function. *Brain stimulation,* 10**,** 36-45.

LEE, S. H., LEDRI, M., TOTH, B., MARCHIONNI, I., HENSTRIDGE, C. M., DUDOK, B., KENESEI, K., BARNA, L., SZABO, S. I., RENKECZ, T., OBEROI, M., WATANABE, M., LIMOLI, C. L., HORVAI, G., SOLTESZ, I. & KATONA, I. 2015. Multiple Forms of Endocannabinoid and Endovanilloid Signaling Regulate the Tonic Control of GABA Release. *J Neurosci,* 35**,** 10039-57.

LEONELLI, M., MARTINS, D. O., KIHARA, A. H. & BRITTO, L. R. 2009. Ontogenetic expression of the vanilloid receptors TRPV1 and TRPV2 in the rat retina. *Int J Dev Neurosci,* 27**,** 709-18.

LEUNG, K. 2016. *Modulation of retinal light responses by the endocannabinoid system and the involvement of TRPV1 channels,* Sydney, Faculty of Science, University of Sydney.

LIU, L. & SIMON, S. 1997. Capsazepine, a vanilloid receptor antagonist, inhibits nicotinic acetylcholine receptors in rat trigeminal ganglia. *Neuroscience letters,* 228**,** 29-32.

MAHMMOUD, Y. A., SHATTOCK, M., CORNELIUS, F. & PAVLOVIC, D. 2014. Inhibition of K+ transport through Na+, K+-ATPase by capsazepine: role of membrane span 10 of the α-subunit in the modulation of ion gating. *PLoS one,* 9**,** e96909.

MASLAND, R. H. 2012. The neuronal organization of the retina. *Neuron,* 76**,** 266-80.

MIDDLETON, T. P. & PROTTI, D. A. 2011. Cannabinoids modulate spontaneous synaptic activity in retinal ganglion cells. *Vis Neurosci,* 28**,** 393-402.

MIDDLETON, T. P. & PROTTI, D. A. 2018. Cannabinoids modulate light signaling in ON-sustained retinal ganglion cells, Manuscript submitted for publication.

MIRAUCOURT, L. S., TSUI, J., GOBERT, D., DESJARDINS, J. F., SCHOHL, A., SILD, M., SPRATT, P., CASTONGUAY, A., DE KONINCK, Y., MARSH-ARMSTRONG, N., WISEMAN, P. W. & RUTHAZER, E. S. 2016. Endocannabinoid signaling enhances visual responses through modulation of intracellular chloride levels in retinal ganglion cells. *Elife,* 5.

MORGANS, C. W., ZHANG, J., JEFFREY, B. G., NELSON, S. M., BURKE, N. S., DUVOISIN, R. M. & BROWN, R. L. 2009. TRPM1 is required for the depolarizing light response in retinal ON-bipolar cells. *Proceedings of the National Academy of Sciences,* 106**,** 19174-19178.

MUSTAFI, D., ENGEL, A. H. & PALCZEWSKI, K. 2009. Structure of cone photoreceptors. *Progress in retinal and eye research,* 28**,** 289-302.

NELSON, R. 2007. Visual responses of Ganglion cells.

NUCCI, C., GASPERI, V., TARTAGLIONE, R., CERULLI, A., TERRINONI, A., BARI, M., DE SIMONE, C., AGRO, A. F., MORRONE, L. A., CORASANITI, M. T., BAGETTA, G. & MACCARRONE, M. 2007. Involvement of the endocannabinoid system in retinal damage after high intraocular pressure-induced ischemia in rats. *Invest Ophthalmol Vis Sci,* 48**,** 2997-3004.

PENZO, M. A. & PENA, J. L. 2009. Endocannabinoid-mediated long-term depression in the avian midbrain expressed presynaptically and postsynaptically. *J Neurosci,* 29**,** 4131-9.

PROTTI, D., DARWISH, I., J.Y., H. & YATES, C. F. 2015. The endocannabinoid system exerts a paradoxical effect on visually-evoked responses of mouse retinal ganglion cells. *Society for Neuroscience*.

PROTTI D.A., D., I, J.Y. HUANG AND YATES 2015. The endocannabinoid system exerts a paradoxical effect on visually-evoked responses of mouse retinal ganglion cells. *Society for Neuroscience*.

RAY, A. M., BENHAM, C. D., ROBERTS, J. C., GILL, C. H., LANNEAU, C., GITTERMAN, D. P., HARRIES, M., DAVIS, J. B. & DAVIES, C. H. 2003. Capsazepine protects against neuronal injury caused by oxygen glucose deprivation by inhibiting Ih. *Journal of Neuroscience,* 23**,** 10146-10153.

RUDOLPH, M. & DESTEXHE, A. 2006. Analytical integrate-and-fire neuron models with conductance-based dynamics for event-driven simulation strategies. *Neural computation,* 18**,** 2146-2210.

RYSKAMP, D. A., REDMON, S., JO, A. O. & KRIŽAJ, D. 2014. TRPV1 and endocannabinoids: emerging molecular signals that modulate mammalian vision. *Cells,* 3**,** 914-938.

SANES, J. R. & MASLAND, R. H. 2015. The types of retinal ganglion cells: current status and implications for neuronal classification. *Annu Rev Neurosci,* 38**,** 221-46.

SAPPINGTON, R. M., SIDOROVA, T., LONG, D. J. & CALKINS, D. J. 2009. TRPV1: contribution to retinal ganglion cell apoptosis and increased intracellular Ca2+ with exposure to hydrostatic pressure. *Invest Ophthalmol Vis Sci,* 50**,** 717-28.

SCHMIDT, T. M. 2009. Role of melastatin-related transient receptor potential channel TRPM1 in the retina: Clues from horses and mice. *Journal of Neuroscience,* 29**,** 11720-11722.

SCHWITZER, T., SCHWAN, R., ANGIOI-DUPREZ, K., GIERSCH, A. & LAPREVOTE, V. 2016. The Endocannabinoid System in the Retina: From Physiology to Practical and Therapeutic Applications. *Neural Plast,* 2016**,** 2916732.

SHEN, Y., HEIMEL, J. A., KAMERMANS, M., PEACHEY, N. S., GREGG, R. G. & NAWY, S. 2009. A transient receptor potential-like channel mediates synaptic transmission in rod bipolar cells. *Journal of Neuroscience,* 29**,** 6088-6093.

SILVERTHORN, D. U. 2013. *Human Physiology-An Integrated Approach,,* United States of America.

SONG, M. Y. & YUAN, J. X.-J. 2010. Introduction to TRP channels: structure, function, and regulation. *Membrane Receptors, Channels and Transporters in Pulmonary Circulation.* Springer.

STAROWICZ, K., NIGAM, S. & DI MARZO, V. 2007. Biochemistry and pharmacology of endovanilloids. *Pharmacology & therapeutics,* 114**,** 13-33.

STRAIKER, A. J., MAGUIRE, G., MACKIE, K. & LINDSEY, J. 1999. Localization of cannabinoid CB1 receptors in the human anterior eye and retina. *Invest Ophthalmol Vis Sci,* 40**,** 2442-8.

SUN, W., LI, N. & HE, S. 2002. Large‐scale morphological survey of mouse retinal ganglion cells. *Journal of Comparative Neurology,* 451**,** 115-126.

TURNER, H., FLEIG, A., STOKES, A., KINET, J.-P. & PENNER, R. 2003. Discrimination of intracellular calcium store subcompartments using TRPV1 (transient receptor potential channel, vanilloid subfamily member 1) release channel activity. *Biochemical Journal,* 371**,** 341-350.

VAN DER STELT, M. & DI MARZO, V. 2003. The endocannabinoid system in the basal ganglia and in the mesolimbic reward system: implications for neurological and psychiatric disorders. *Eur J Pharmacol,* 480**,** 133-50.

VAN DER STELT, M., TREVISANI, M., VELLANI, V., DE PETROCELLIS, L., MORIELLO, A. S., CAMPI, B., MCNAUGHTON, P., GEPPETTI, P. & DI MARZO, V. 2005. Anandamide acts as an intracellular messenger amplifying Ca 2+ influx via TRPV1 channels. *The EMBO journal,* 24**,** 3026-3037.

VARDI, N., ZHANG, L. L., PAYNE, J. A. & STERLING, P. 2000. Evidence that different cation chloride cotransporters in retinal neurons allow opposite responses to GABA. *J Neurosci,* 20**,** 7657-63.

VENKATACHALAM, K. & MONTELL, C. 2007. TRP channels. *Annu. Rev. Biochem.,* 76**,** 387-417.

WASSLE, H. 2004. Parallel processing in the mammalian retina. *Nat Rev Neurosci,* 5**,** 747-757.

WERNER, J. C., L 2014. *The new visual neurosciences*, The MIT Press.

WILLIAMS, S. R. & MITCHELL, S. J. 2008. Direct measurement of somatic voltage clamp errors in central neurons. *Nature neuroscience,* 11**,** 790-798.

YAMAMURA, H., UGAWA, S., UEDA, T., NAGAO, M. & SHIMADA, S. 2004. Capsazepine is a novel activator of the δ subunit of the human epithelial Na+ channel. *Journal of Biological Chemistry,* 279**,** 44483-44489.

YATES, C. 2014. *THE ENDOCANNABINOID SYSTEM: A FUNCTIONALLY KEY COMPONENT OF RETINAL SIGNALLING,* Sydney, Faculty of Science, University of Sydney.

YONG, A. 2016. *Effects of the High on Low-level Visual Processing:*

Investigating the Role of Cannabinoids using Optogenetics, Sydney, Faculty of Science, University of Sydney.

ZYGMUNT, P. M., PETERSSON, J., ANDERSSON, D. A., CHUANG, H.-H., SØRGÅRD, M., DI MARZO, V., JULIUS, D. & HÖGESTÄTT, E. D. 1999. Vanilloid receptors on sensory nerves mediate the vasodilator action of anandamide. *Nature,* 400**,** 452-457.